PLASTIC DEFORMATION OF NIOBIUM

Thesis submitted for the

Degree of Doctor of Philosophy

by

HO CHUL KIM

January 1969

Metallurgy Department
Imperial College
London S.W.7.

ABSTRACT

The influence of interstitial impurities, temperature, orientation and the sense of the applied stress on the low temperature deformation behaviour of single crystals of electron beam-melted niobium, of controlled orientation, has been investigated between 20.4° and 473°K.

The effect of various parameters on the electron beam zone melting process has been evaluated by their effect on certain physical and mechanical properties of the resulting crystals. The most important was found to be the vacuum pressure of the furnace during melting which suggests that the removal of the products of volatilization and degassing is a major part of the purification.

The amount of the yield drop depends on the level of impurity in the crystal and by increasing the overall purity the temperature dependence of the yield stress was significantly decreased. A model for yielding based on the multiplication and velocity characteristics of dislocations provided the best unified treatment of the yielding behaviour. The strain ageing kinetics were strongly influenced by the initial and relative concentration of interstitial impurities.

At low temperatures the yield stress depends on the orientation and on the sense of the applied stress, whereas at high temperatures it is independent of both of these factors. Catastrophic flow behaviour was observed in the crystals with ⟨111⟩ tensile axis and this may be caused by a combination of the localized adiabatic heating at severely necked regions and geometrical softening.

TABLE OF CONTENTS

CHAPTER 1

CHAPTER 1

1.1 Introduction

Deformation behaviour of the b.c.c. metals is known to be strongly influenced by impurity type and content, temperature, strain rate and the sense of the applied stress. These parameters affect the yielding and plastic flow behaviour, however, a precise knowledge of the dislocation mechanisms which are controlling these phenomena and unified models in terms of the basic parameters of dislocation generation and velocity are not available at present.

In the past, most of the work has been devoted to the investitation of polycrystalline materials of commercial purity and much useful information has been obtained on the effect of impurity, grain size, strain rate and temperature on the yielding and flow behaviour of the b.c.c. metals.

The growing demand for new and improved materials has stimulated the fundamental study of single crystals with a high degree of perfection in an attempt to obtain a better understanding of the actual atomic mechanism which governs the deformation behaviour. The recent development in the technique of preparing highly perfect single crystals of controlled orientation has removed some of the difficulties, however, at the present time, the available information on the mechanical properties of b.c.c. single crystals is still sparse and sometimes contradictory.

The present work is an attempt to understand some of the aspects of the apparent discrepancies which have arisen recently. The work consisted of a detailed investigation of orientation, temperature, and interstitial impurity dependence of the yielding and plastic flow behaviour in both tension and compression. Electron beam zone melted single crystals with a symmetrical orientation were used; mechanical tests were made between 20.4 and 473°K.

1.2 Yielding behaviour

The main characteristics of the yielding behaviour of the

b.c.c. metals containing small amounts of interstitial impurities is the pronounced drop in load on discontinuous yielding. Two highly significant contributions have been made to our understanding of this phenomenon.

The two contributions were made by Cottrell (1948) and Cottrell and Bilby (1948) who showed that solute may hold dislocations in place, and Johnston and Gilman (1959), Johnston (1962) who demonstrated that the yield drop may develop from the dynamic properties of dislocations.

1.2.1 Dislocation unlocking theory

According to the early theory of Cottrell (1948) and Cottrell and Bilby (1948), the discontinuous yielding is ascribed to the locking of dislocations by interstitial solute atoms which have migrated to the site of the dislocations. If the dislocations are locked, plastic deformation can occur when the stress acting on them is sufficient to free them from their impurity atmosphere. In principle a yield point occurs at a high stress by nearly simultaneous unpinning of dislocations followed by their motion at a lower stress. Hence, the lower stress is the stress at which unpinned dislocations continue to move and produce plastic deformation.

The important feature of this model is that it provides an explanation of the temperature and strain rate dependence of the yield stress (Cottrell 1957; Yokobori 1952; Fisher 1955). Since the unlocking process is considered to be a thermally activated one, the higher the temperature, the greater the thermal energy available, with the result the the applied stress for yielding decreases rapidly with increasing temperature.

The Cottrell concept of dislocation locking is undisputed in view of (1) the dependence of the yield drop and discontinuous yielding on impurities, (2) the kinetics of the yield point return and (3) direct observation in transmission electron micrographs of particles segregated along dislocation lines. One of the inadequ- of this model is that it does not explain the pre-yield microstrain

before the upper yield stress is reached (Bilby 1950; Cottrell 1950).

1.2.2 Dislocation multiplication theory

Another important contribution on the model of yielding was originally put forward by Johnston and Gilman (1959), Gilman and Johnston (1959) and Johnston (1962) to explain the behaviour of their lithium fluoride single crystals and later confirmed by Stein and Low (1960) for silicon iron single crystals. Subsequently the same idea was applied to the b.c.c. metals by Hahn (1962). The yield point was accounted for in terms of the rapid multiplication of dislocations and the stress dependence of their velocity. The essential features of the Hahn's model are as follows:

The total strain rate $\dot{\varepsilon}$, imposed by a testing machine in a undirectional test has two components, the elastic rate, $\dot{\varepsilon}_e$, of the machine and specimen, and the plastic rate $\dot{\varepsilon}_p$, of the specimen. Thus:

$$\dot{\varepsilon} = \dot{\varepsilon}_e + \dot{\varepsilon}_p \qquad (1.1)$$

The plastic strain rate is maintained by the motion of L lines per unit volume of mobile dislocations of Burgers vector b at a velocity, v, so that

$$\dot{\varepsilon}_p = b L v \qquad (1.2)$$

To establish an analytical relation for the stress-strain curve one must express L and v in terms of stress and strain.

Etch studies (Johnston and Gilman 1959; Hahn 1962) and electron microscopy (Keh and Weissman 1963) have shown that at small strain ($10^{-3} < \dot{\varepsilon}_p < 10^{-1}$) the total dislocation density , increases with strain in the manner:

$$\rho = \rho_o + C\dot{\varepsilon}_p^{a} \qquad (1.3)$$

where c and a are constants. It is assumed to hold at smaller strains to a first approximation. In the absence of dislocation locking. ρ_o is regarded

by Hahn as the average density of unlocked dislocations which are created heterogeneously at a stress level below that associated with significant mobility. Since there is no measured relation between the mobile dislocation density, L, and ρ, it is further assumed that

$$L = f\rho \qquad (1.4)$$

with f = 0.1 for the case of mobile dislocations produced by deformation. Initially, L_o must correspond to ρ_o independent of which of the above interpretations hold for ρ_o.

The stress dependence of the dislocation velocity in silicon iron was found by Stein and Low (1960) to be given by the expression:

$$v = (\tau/\tau_o)^m \qquad (1.5)$$

where τ is the applied resolved shear stress and τ_o is the shear stress for unit velocity, and m a constant. Several investigators (Chaudhuri and Patel 1962; Schadler 1964; Stein and Low 1960) have shown that this equation describes the dependence of the average velocity of an individual dislocation at the resolved shear stress only for velocities which were small relative to the shear wave velocity in the crystal. However, at present no other equation is available.

Johnston (1962) found that the work hardening in lithium fluoride closely approximates to the stress increment $\Delta\tau$, needed to maintain a given velocity. Hahn accepts this as conditionally applicable to metals in order to include work hardening. This gives a simple linear work hardening law:

$$\Delta\tau = q\varepsilon_p \qquad (1.6)$$

where q is the work hardening coefficient. Therefore it follows:

$$v = (\tau_o)^{-m} \quad (\tau - q\varepsilon_p)^m \qquad (1.7)$$

By combining equations (1.2) (1.3) and (1.4), the relation between flow stress, strain, strain rate can be written as:

$$\tau = q\dot{\varepsilon}_p + \tau_o \left(\frac{\dot{\varepsilon}_p}{bf(\rho_o + C\varepsilon_p^2)} \right)^{1/m} \qquad (1.8)$$

According to this model, the abrupt yield drop is a consequence of a small number of initial mobile dislocations (small L_0), a rapid multiplication rate (large a), and a low sensitivity of dislocation velocity to stress (small m).

More recently, Cottrell (1963) has shown an agreement with this basic concept of dislocation multiplication but also emphasised the importance of the role played by pinning. He re-wrote equation (1.8) in a slightly different form:

$$\tau = q\,\varepsilon_p + \tau_0 \left(\frac{\dot{\varepsilon}_p}{b(L_0 + f\,C\varepsilon_p^{\omega})}\right)^{1/m} \qquad (1.9)$$

Hereby, introducing the possibility that the mobile dislocation density need not be related initially to ρ_0 by the fixed factor of 0.1, and suggested that a sharp yield point can occur if one of the following three conditions is satisfied:

(1) $\rho_0 = 0$ and stress concentrations are not important. Yielding takes place when the stress is able to create dislocations in the dislocation free lattice. The stress then drops to the level necessary to move and multiply these dislocations.

(2) $L_0 = 0$, $\rho_0 > 0$ and stress concentrations are not severe. It does not require a total absence of initial dislocations but only that they should be locked by impurities or solute. Yielding begins when existing dislocations become unpinned (weak pinning), or when dislocations are created (strong pinning) at the upper yield point, depending on which is the easier process.

(3) $L_0 > 0$ and the necessary multiplication and velocity conditions are met, then the yield drop develops by multiplication.

None of the above models deals with the orientation dependence of the yielding behaviour. Jaoul and Gonzalez (1961) have investigated the uniform and non-uniform discontinuous yielding and showed that non-discontinuous yielding in iron and vanadium

is related to orientation effects in single crystal and strongly textured polycrystals. Jaoul's results qualitatively indicated that non-uniform discontinuous yielding occurs in single and polycrystals of the certain orientation when they have high elastic limits and low strain hardening rates.

1.3 Yield and flow stress

The low temperature strength of b.c.c. metals has been studied extensively and much discussion has led to considerable clarification in recent years. However, there is a disagreement on the major source of this strength whether it arises from the inherent lattice hardening or whether it arises from the interaction of dislocations with interstitial impurities in the b.c.c. lattice. Furthermore, this problem has become more complicated by the discovery of new variables, such as dependence of yield stress and its temperature dependence on the orientation of the stress axis and the sense of applied stress, in the deformation behaviour.

1.3.1 Orientation dependence

In the past the strain rate, and temperature dependence of the yield stress in b.c.c. single crystals have been studied without paying any serious attention to the orientation of the deformation axis (Lawley et al 1962; Mordike and Haasen 1962; Mordike 1962; Christian and Masters 1964). However, Rose et al (1962) have shown that when the orientation of the deformation axis is suitably chosen the yield stress and work hardening rate of a tungsten crystal can exhibit a strong orientation dependence. This effect was later confirmed in other b.c.c. single crystals; molybdenum (Guiu and Pratt 1966; Stein 1967), tantalum (Sherwood, private communication), niobium (Kim and Pratt 1966; Bowen et al 1967), iron (Stein and Low 1966; Keh 1966). In addition the three stages of work hardening were observed for an orientation near the centre of stereographic triangles in molybdenum (Guiu and Pratt 1966), tantalum (Mitchel and Spitzig 1965; Sherwood, private communication) iron (Keh 1966) and niobium (Mitchel et al 1963; Votava 1964).

Rose et al (1962) proposed the movement of jogs on screw dislocations to explain this effect. This view is supported by Guiu and Pratt (1966). This is based on the fact that the intersection of [111] and [$\bar{1}$11] slip dislocations will form jogs on screw dislocations on the [011] - [111] great circle. Since this plane is unstressed conservative motion of the jogs is difficult, but for orientations near ⟨100⟩ it is quite highly stressed and conservative motion should be possible.

1.3.2. The Effect of Impurities

It is well-established that the mechanical properties of metals are strongly influenced by the number and distribution of atomic defects, such as interstitial and substitutional impurity atoms and vacancies. It follows that the nature of the interaction between these defects and dislocations is important in understanding the deformation process in metals. Much of the published work is complicated by the presence of a sharp yield point and anisotropic yielding behaviour. However, fewer experiments have been performed on b.c.c. single crystals, with the addition of substitutional solute atoms than with the addition of interstitial atoms. It is generally recognised that interstitial impurity atoms distort the b.c.c. lattice tetragonally and thus interact more strongly with edge and screw dislocations. In the case of polycrystalline niobium a hardening rate per atomic percent of G/10 for substitutional atoms and 2G for interstitial nitrogen was reported (Evans 1962), where G is the shear modulus.

The major effects of impurity atoms on the mechanical properties are:

(1) An increase in the yield stress and a shifting of the whole stress-strain curve toward higher stress.

(2) The appearance of a yield point which depends on the concentration of impurities.

(3) A decrease in ductility with increasing impurity content.

Most observations revealed that b.c.c. metals have a large

temperature dependence of yield and flow stress. This is frequently attributed to the large Peierls-Nabarro stress inherent in the b.c.c. lattice at low temperatures (Basinski and Christian 1960. COnrad 1963; Dorn and Rajnak 1964; Christian and Masters 1964). Two models are currently given for the Peierls-Nabarro force, involving thermally activated motion of a double kink (Dorn and Rajnak 1964) and constriction of a sessile screw dislocation into a glissile cobfiguration (Mitchel, Foxall and Hirsch 1963). However, this view of hardening has been challenged seriously by recent experiments by Stein and his associates (1963, 1966, 1966) who, on lowering the carbon content from 200 ppm to less than 0.025 ppm in iron, found that the flow stress at all temperatures was reduced to less than 40% of its original value and found markedly decreased temperature dependence with increasing purity. Later this observation has also been confirmed in other b.c.c. metals single crystals by Koo (1963) on tungsten, Lawley et al (1962) on molybdenum, and Kim and Pratt (1966) on niobium. This effect and observation does allow us to conclude unambiguously that the Peierls-Nabarro force is not the sole hardening mechanism.

In the following, the quantitative theoriesof the magnitude of solute hardening will be reviewed.

A. Cottrell's model

The locking due to the elastic interactions between solute atom atmospheres and dislocations is important at low temperatures, but on raising the temperature thermal fluctuation would assist the applied stress in forcing the dislocations away from their atmospheres. Cottrell (1957) estimated that for iron containing carbon, the yield stress should vary as the cube root of the testing temperature:

$$\sigma = \sigma_0 - C (T)^{1/3} \qquad (1.10)$$

where C is constant, T, the absolute temperature and $\sigma_0 = V_m/3$ awab, the yield stress at $0^\circ K$, V_m the binding energy of the impurity atoms to a dislocation which increases with increasing narrowness of the dislocation, and a is the mean spacing between impurity atoms along the dislocation line. Break-away occurs when the dislocation has moved forward a distance aw, where w is the width.

Substituting V_m = 0.8 eV, a = b3/2, and aw = b, gives $\sigma_o = G/45$. Experimental values extrapolate to about one-fifth of this value at 0°K. Cottrell attributed this deviation to an under-estimation of a, since some of the sites along a dislocation line may not be filled with impurity atoms (Louat 1956).

Compared with other strengthening mechanisms, the thermally activated unlocking of dislocations from Cottrell atmospheres is more sensitive to the presence of interstitials. Lawley et al (1962) found a good agreement with this model for their zone-melted single crystals of molybdenum.

B. Cochardt, Schoeck and Wiedersich (1955)

The interaction energy of an interstitial solute atom with a screw dislocation in a b.c.c. lattice is given by

$$U = A \frac{\cos\phi}{r} \qquad (1.11)$$

where A is the interaction constant ϕ = 60, 180 and 360° are the three equivalent positions of lowest energy, and given by

$$A = \frac{\sqrt{2}\, b\, G\, a^3}{3\pi} (\varepsilon_1 - \varepsilon_2)$$

r is the distance from the dislocation line to the solute atom, b is the Burgers vector = $\frac{1}{2}\sqrt{3}\, a$, a is the lattice parameter, ε_1 and ε_2 are the principle strains of the unit cell caused by the solute atom, G is the anisotropic shear modulus = $\frac{1}{2}(C_{11}-C_{12})$.

C. Cracknell and Petch (1955)

In this model an edge dislocation line is considered to be pinned by long range stresses from interstitial atoms, the equation for the tensile stress due to the interaction of dislocations with random interstitial solute atoms is

$$\sigma_o = \frac{N^{11/9}}{(\alpha G)^{1/3} b^{5/3}} \left[\frac{16A}{\pi} \log \left(\frac{1}{2rN^{1/3}}\right)\right]^{4/3} \qquad (1.12)$$

where N is the number of interstitial solute atoms/cm^3, α the constant in the expression for the force to bend a dislocation

to a radius r

$$\tau = \frac{\alpha G b}{r}$$

A is the interaction constant for the particular metal and interstitial. Thus, the hardening rate is almost temperature-independent and approximately linear with concentration.

D. Schoeck and Seeger (1959)

This model is analogous to the Snoek effect for damping. Here they consider the interaction of interstitials with screw dislocations caused by the tetragonal distortion of interstitial atoms in the b.c.c. lattice. This causes a decrease in the energy of the system and thus the dislocations become locked. As a consequence, before the dislocation can be moved, the state of order must be destroyed, and this leads to a higher yield stress. Whereas locking due to atmosphere formation requires long range diffusion of interstitials, locking due to Snoek effect is achieved merely by rearrangement between neighbouring lattice sites, and takes place in times orders of magnitude smaller. Considering a screw dislocation in the ⟨111⟩ direction and carbon atoms in iron in the centre of the cube edge of the unit cell or in equivalent position, Schoeck and Seeger (1959) derived an expression for the yield stress using the same approach as Cochardt et al (1955):

$$\tau = 20.5 \frac{A}{b\, a^3} P \qquad (1.13)$$

where a denotes the lattice constant and $P = \frac{1}{2} C_o a^3$ the atomic fraction of interstitials, b the Burgers vector, A the interaction constant previously mentioned in Cracknell and Petch's model. It can be seen, from this equation, that the yield stress is linearly proportional to the atomic concentration of interstitials and independent of the temperature. They suggested that the temperature independence of the yield stress in regions above room temperature can be attributed to the Snoek ordering during dislocation movement and found a good agreement in iron.

E. Fleischer (1962a; 1962b; 1964)

This model also assumed the tetragonal lattice distortion.

The dislocation motion is supposed to be a series of thermally activated jumps through the stress fields produced by individual solute atoms, and the interaction energy of defects and the dislocations is calculated by the method described by Cochardt et al (1955). The resultant maximum force (which gives the flow stress at $0^{o}K$) was obtained by maximizing the rate of change of the energy with respect to motion along the slip plane. Using such a model, the activation energy for motion of edge dislocation is found to be

$$U = F_o\, b \left[1 - (\tau/\tau_o)^{\frac{1}{2}} \right]^2 \qquad (1.14)$$

The flow stress at $0^{o}K$

$$\tau_o = G\, \Delta\varepsilon\, (C)^{\frac{1}{2}}/3.3$$

The logarithm differential of dislocation velocity ($d \log v$) with respect to stress ($d \log \tau$) is given by

$$d \log v/d (\log \tau) = F_o\, b/kT \left(\sqrt{\tau/\tau_o} - \tau/\tau_o \right)$$

where F_o = the force acting on the dislocation at $0^{o}K$.

G = shear modulus

$\Delta\varepsilon$ = the difference between longitudinal and transverse strain of the tetragonal lattice distortion

C = the concentration of tetragonal defects.

This result was successfully applied to the temperature variation of the flow stressof f.c.c. ionic crystals provided screw dislocations determine this flow stress, since screw dislocations move at higher stresses than edges for the same velocity and that screws are impeded by the presence of jogs. The relationship between the flow stress and temperature is of the form $\tau^{\frac{1}{2}} - T^{\frac{1}{2}}$ and as seen in the equation the yield stress varies with the square root of concentration of defects. There is evidence for iron by Stein and Low (1966) who found a good agreement with Fleischer's theory for temperature dependence of hardening by carbon.

1.4 Peierls-Nabarro force

The force which opposes the movement of dislocations through an other wise perfect lattice from one equilibrium position to

the next, was considered by Peierls (1940) and Nabarro (1947). When a straight dislocation is moved from one valley towards the next, the atoms in the vicinity of the core of the dislocation change their positions and bond angles, causing the energy of the dislocation to increase, Midway between two adjacent valleys, the dislocation energy reaches a maximum value and any additional small displacement will cause the dislocation to fall down the hill into the next valley. The maximum shear stress necessary to promote such forward motion of the dislocation is known as the Peierls Nabarro force.

There are three major problems in the calculation of the Peierls Nabarro force associated with plastic deformation of a metal crystal. The first is concerned with the calculation of saddle point free energy for the successful nucleation of a pair of kinks as a function of the applied stress, so as to enable the determination of the frequency of formation of kink pairs along a dislocation; the second is associated with an estimation of the macrospic strain rate in terms of kinetics of nucleation and migration of kink pairs ; and the third problem is associated with the effect of interstitial impurities on the above two factors.

The overcoming of the Peierls Nabarro barrier by a dislocation segment is believed to be a thermally activated process. According to Seeger (1956) and Seeger et al (1957) the pairs of kinks can be formed under the combined action of the applied stress and thermal fluctuation, and the energy of a kink is given by:

$$U_K = (2a/\pi)\,(2E_0 ab\,\tau_0/\pi)^{\frac{1}{2}} \qquad (1.15)$$

where a is the distance between the position of minima of potential energy E_0 is the line energy of the dislocation, τ_0 the Peierls Nabarro force at $0^\circ K$. The activation energy of kink formation is given by:

$$H = U_K \left[1 + \tfrac{1}{4} \log (16\,\tau_0/\pi\tau)\right] \qquad (1.16)$$

Recently, Dorn and his co-workers (1964, a; 1964,b; 1965

1967) proposed a criterion for the Peierls Nabarro mechanism to estimate the saddle point activation energy. They found that $U_n/2\,U_K$ was a unique function of τ/τ_p, where U_n is the activation energy for the nucleation of a pair of kinks, $2U_K$ is the excess energy of kink pairs, τ is the effective stress and τ_o is the Peierls Nabarro stress at 0^oK. The relationship found between $U_n/2U_K$ and τ/τ_o is expressed in terms of temperature T (testing) and the athermal temperature T_c,

$$U_{n/2U_K} = T/T_c \qquad (1.17)$$

By analysing the existing experimental data in this manner they found a good agreement to the expected universal curve and they emphasise that this agreement provides the evidence in favour of the Peierls Nabarro mechanism as a controlling mechanism of the low temperature deformation behaviour of b.c.c. metals.

However, there is substantial evidence to show the influence of interstitial impurities on the yield and flow stress (for example Fleischer 1962, a; 1962b; . Fleischer and Hibbard 1963; Johnston 1962; Stein et al 1963; Stein and Low 1966; Stein 1967; Koo 1963; Lawley et al 1962). Dorn and his co-workers, including Conrad (1961, 1963), neglected the possible effects of interstitial impurities on the thermally activated portion of the low temperature yield stress or flow stress, or assumed that the interstitials do not slow down the velocity of the kink. Although the low temperature strength of b.c.c. metals has been the subject of much attention and discussion, the fundamental differences in the view of the source of low temperature flow stress is not yet clarified. Whether this effect arises from direct thermal activation of dislocations past interstitial impurities, or whether it is simply a reflection of modifications of the Peierls Nabarro mechanism, has not been solved.

1.5 Strain ageing

When a specimen is strained beyond the yield point a large number of free dislocations are produced and propagate through the crystal until they are gradually immobilized by various obstacles (strain hardening). If the specimen is unloaded, a yield point is not obtained when it is immediately reloaded. However, if the time between the release of load and re-application is sufficient to allow interstitial atoms to migrate to the dislocations and lock a large fraction of them, the yield point will reappear. A greater applied stress is then required to initiate plastic deformation by moving existing dislocations.

A detailed treatment was given by Cottrell and Bilby (1949) assuming that the yield point would reappear when some fraction of the free dislocations produced by pre-strain had been pinned. The number n (t) atoms per unit volume of material that have migrated into dislocations at temperature T after time t is given by:

$$n(t) = 3 (\pi/2)^{1/3} n_o L \left(\frac{A D t}{k T} \right)^{2/3} \qquad (1.18)$$

where n_o is the solute concentration in the material at $t = 0$
D is the diffusion coefficient of solute
L is the total length of dislocation per unit volume
A is the constant depending on the strain introduced into the lattice by a solute atom.

This equation (1.18) is valid only for the early stages of strain ageing. Harper (1951) modified the above equation to fit later stages of ageing by assuming that the rate of migration of solute is decreased in proportion to the amount already segregated. Thus, considering $q (q = \frac{n(t)}{n_o})$ as the fraction of solute which has migrated to dislocation.

$$q = 1 - \exp \left[-\alpha L (A D t/kT)^{2/3} \right] \qquad (1.19)$$

$$\log (1 - q) = \alpha L \left(\frac{A D t}{kT} \right)^{2/3}$$

This reduces to Cottrell and Bilby's equation when the

exponent is small and their measurement showed that this is in good agreement with experimental observation over almost the whole range of ageing times.

The process of strain ageing involves not only the return of the yield point, and increase in yield and flow stress but also increases in fracture stress, hardness, and electrical resistivity and decreased ductility. These changes due to strain ageing follow a $t^{2/3}$ law closely and at later stages the rate diminishes rapidly (Cottrell and Bilby 1949; Cottrell and Churchman 1949; Cottrell and Leak 1952; Thomas and Leak 1955). To explain all of these changes the strain ageing processes proposed are:

1. atmosphere formation (Cottrell and Bilby 1949; Formby and Owen 1965)
2. stress-induced ordering (Schoeck 1956· Wilson, Russel and Eshelby 1956)
3. precipitation formation (Thomas and Leak 1955; Wilson and Russel 1960; Bullough and Newman, 1962; Hartley and Wilson 1963; Mclennan 1965).

Generally the technique of yield point return as a function of ageing time and temperature has been used for the determination of the kind of element which is responsible for the strain-ageing process (Begley 1958; Brittarin and Bronley 1958; Harris and Peacock 1965; Stanley and Szkopiak 1962), but the result is still unsatisfactory.

1.6 Previous work on plastic deformation of niobium and programme of investigation

In the past, most work has been with polycrystalline niobium. These studies have dealt with yielding and work hardening behaviour (Adams, Roberts and Smallman 1960; Fourdeux and Wronski 1964; Van Torn and Thomas 1963); the appearance and effect of substructure on mechanical properties (Berghezan and Fourdeux 1963); the dislocation structure in deformed crystals (Wronski and Fourdeux 1964); the effect of purity on yielding and flow behaviour (Mincher and Sheely 1961; Imgram, Bartlett and Ogden 1963; Evans 1962; Votava 1964); the effect of temperature (Harris 1964), strain rate (Johnson 1960), twinning (Stiegler and

MacHargue 1964) and dislocation etch pits study in the pre-yield region (Koppenaal and Evans 1963).

There are very few results available for the properties of single crystals: Mitchell, Foxall and Hirsch (1963) studied the work hardening properties of zone-melted niobium single crystal for certain orientations, and found for an orientation near the centre of the stereographic triangle that room temperature deformation resulted in three-stage work hardening in the same manner as in the f.c.c. metals. Decreasing the test temperature and increasing the strain rate caused an increase in the yield stress and a decrease in the first stage work hardening rate. Slip line observation indicated long slip distances, evidenced by long straight slip lines for edge dislocations, and short wavy slip for screw dislocations. They suggest that their results support the double cross slip dislocation multiplication mechanism proposed by Low and Guard (1959).

The orientation dependence of yielding and work hardening behaviour of zone-melted niobium single crystals at room temperature, was investigated by Votava (1964) for corner orientations of the stereographic triangle, where he observed a sharp yield drop for all corner orientations. His tensile specimen was prepared during zone-melting by varying the power supplied, and he ascribed the observed yield drops to the lower density of fresh dislocations due to this method of preparation. Geometrical softening phenomena were observed for the crystals with <111> tensile axis which he attributed to the intensification of stress due to the lattice rotation.

Taylor and Christian (1965) reported work on as-grown and vacuum annealed niobium single crystals. They observed the temperature dependence of the yield stress for both purities which was found to be insensitive to the purity of crystals, and their results were in good agreement with the previous work of Christian and Masters (1964) on less pure single and polycrystalline niobium. A thin film transmission study has been reported by some authors (Taylor and Christian 1967) for single crystals of niobium purified in ultra high vacuum. At room temperature the microstructures observed after single glide were very similar to those which

have been reported for f.c.c. copper crystals. In stage 1, braids in the primary slip plane consisted mainly of edge dislocation multipoles, but more complex tangles containing many secondary dislocations were formed in stage II, and were joined into walls of a cell structure. The crystals oriented for double slip showed the formation of high angle boundaries after large strains. They suggested that screw dislocations f from different sources cross-slip and mutually annihilate at room temperature, but are prevented from doing this by the friction stress at low temperature.

Reid et al (1966) found a highly anisotropic deformation behaviour at 77°K, in tension and compression of niobium single crystals. Crystals with ⟨110⟩ orientation deformed by twinning in compression, while these crystals deformed by slip at higher stress in tension. Crystals with ⟨100⟩ axis deformed by slip for both tension and compression. Crystals near ⟨111⟩ orientation underwent catastrophic localised flow in tension, the plane of shear was found to be near {110}, and the shear direction near ⟨100⟩ They suggested that this anomalous behaviour was caused by the motion of dislocations with a ⟨100⟩ Burgers vector, as a consequence of the low value of the anisotropy factor in niobium at this temperature.

Recently, Duesbery and Foxall (1965), Bowen et al (1967) Foxall et al (1967) investigated the orientation dependence of the operating slip systems in tension and compression for certain orientations. They found some evidence of an assymmetry in the critical resolved shear stress for slip on {112} plane, which increases with decreasing temperature. An attempt has been made to explain this effect in terms of the dissociation of a/2⟨111⟩ screw dislocation on {112} planes. However, Sherwood, Guiu, Kim and Pratt (1967), by examining the orientation dependence of yield stress in tension and compression for corner orientations of niobium and other b.c.c. crystals, demonstrated that the anisotropic behaviour in tension and compression cannot be accounted for simply in terms of an anisotropic Peierls stress due to dislocation core asymmetry.

It is seen from the preceding review and discussion of the present state of our knowledge of the relationship between the mechanical properties and crystal imperfection, that there are still many questions which need experimental investigation. In this thesis the work was designed to study the effect of impurity on the yielding and flow behaviour, and of orientation and temperature effects on the yielding and work-hardening behaviour in tension and compression for the single crystals of niobium of symmetric orientation.

The present work was divided into three parts:

1. The preparation of single crystals involving the evaluation of purity resulting from changing the various parameters during crystal growth.
2. The effect of the interstitial impurities on the yielding and strain ageing behaviour.
3. The effect of orientation and temperature on the deformation behaviour in tension and compression.

CHAPTER 2

GROWTH OF NIOBIUM SINGLE CRYSTALS

CHAPTER 2

2.1 Introduction

Since Andrade's success (1937) with grain growth at high temperature, this technique has been used widely to produce single crystals of high melting point materials. Tsien and Chow (1937) had obtained molybdenum single crystals of several centimetres in length from 0.25 mm dia. wire. Chen, Maddin and Pond (1951) modified Andrade's original method by applying a small tensile strainsduring annealing to grow a single crystal of several centimetres in length and 3 mm in diameter. Using the same technique, single crystals of niobium, 1 cm long and 3 mm in diameter, were also prepared by Maddin and Chen (1953).

Several disadvantages are associated with the use of the Andrade technique (1937) or the modified version of it (Chen, Maddin and Pond 1951. Tsien and Chow 1937). This technique is restricted to a material having high thermal and low electrical resistivity. There is no means of precise orientation control and the size and purity are limited. Nevertheless, this technique has some advantage, particularly in the case of materials having a phase change between the melting point and room temperature.

However, the increasing demand for single crystals of greater purity, high perfection, better quality and larger size has led to the development of the floating zone melting technique, which was first used by Keck and Golay (1953) to grow single crystals of silicon. In this technique no retaining crucible is required and extra purification is achieved as a result of zone refining and evaporation of impurities if the process is carried out in vacuum.

Growing of single crystals by the zone-melting technique and the factors pertaining to the technique of zone-melting and their evaluation are discussed overleaf.

2.2 Zone-melting

The term "zone-melting" denotes a group of methods for controlling the distribution of solube impurities or solute in crystalline materials. A narrow zone travels slowly along a polycrystalline rOd resulting in a single crystal and re-distribution of the solute. The final distribution of the solute, concentration profile, depends primarily on the effective segregation coefficient K and the starting composition.

The theory of this process has been thoroughly studied by Pfann (1952; 1958). He derived an equation for the concentration profile after single and multiple zone melting passes, assuming a two-phase system in which the melt is always homoggeneous, and that the diffusion of impurities in the solid is negligible, and the segregation coefficient K is constant. The solute concentration in the solid with distance from the starting end is given as:

$$\frac{C}{C_o} = 1 - (1 - K)\, e^{-Kx/\ell} \qquad (2.1)$$

where C_o is the initial concentration, ℓ is the zone length and K is effective segregation coefficient. The solute distribution for different values of K is predicted by equation (2.1) if C_o is known.

According to Burton et al (1953), the effective segregation coefficient, K, is related to the equilibrium coefficient K_o by the equation:

$$K = \frac{K_o}{K_o + (1 - K_o)e^{-f\delta/D}} \qquad (2.2)$$

where K_o is defined as the ratio of solute concentration in the freezing solid to that in the main body of the liquid. $f\delta/D$ may be regarded as normalized growth velocity.

The basic equations for the solute concentration profile

after multiple zone passes have been derived by Reiss and Halfand (1940), Burris et al (1955), and Lord (1961) as a function of distance in units of zone length. It is predicted that the purification in a specific solvent-solute system would depend upon the number of zone passes and the effective segregation coefficient which is, in turn, a function of zone speed. Hence, a greater degree of purification could be expected by the slower zoning speed and larger number of zone passes. There will be a gradual decline in the efficiency of purification with each repeated pass to a point where the limit of solute distribution may be reached (Burris, Stockman and Dillon, 1955).

This process of purification applies to the zone-melting proces only. However, in the present case electron beam floating zone-melting is carried out in a vacuum. Therefore, the purification is thought to be achieved by vacuum distillation of lower melting point elements and the volatilization of gases and impurity (Wulff 1959; Winkler 1960; Smith 1958; Votava 1964; Drangel and Murray 1964) elements as volatile compounds as well as by zone-melting.

Crystal growth takes place simultaneously with the zone melting process. The molten zone travelling along a polycrystalline rod leaves the solidified portion behind it in the form of single crystal, provided suitable conditions are maintained to avoid the formation of extraneous nuclei ahead of the growing crystals. These conditions are fulfilled by keeping the degree of supercooling of liquid near the interface to a minimum. In practice, this is achieved by imposing a steep temperature gradient in the molten solid and a slow cooling rate, i.e. a slow zone speed.

2.3 Electron beam floating zone melting

The usual method of heating by induction to obtain a molten zone (Buehler and Kunzler 1961; Vernick, Doris and Byrnes 1959; Buehler 1958) has been superseded by the electron bombardment technique since its development by Davis, Caverley and Lever (1956).

Fig. 2.1 General view of the electron beam zone melting apparatus

In this technique the electrons from a ring-shaped tungsten filament are accelerated towards the rod and focussed on a narrow region, and this is achieved by applying a high voltage across the filament as a cathode with the rod acting as an anode. The floating zone is supported by the surface tension of the molten liquid and its stability is discussed by Heywang. The melting process takes place in a vacuum chamber. By moving the cathode, the molten zone travels along the polycrystalline rod leaving a single crystal behind.

Single crystals of many refractory metals including W, Rh, Mo Va, Nb, Ni, Ta and Si are prepared in this way and their purity and perfection are superior to that obtained by any other method.

2.4 Description of Apparatus

Fig. 2.1 is a general view of the electron beam zone melting apparatus in which the single crystals of niobium were grown. The cylindrical furnace chamber is made from nickel plated mild steel cooled by running water. This chamber is evacuated through the bottom by a (6 inches diameter) oil diffusion pump with a pumping speed of 300 litre/sec. A liquid nitrogen cold trap between the diffusion pump and the chamber reduces the back-streaming of oil vapour into the chamber. On one side of the furnace wall there is an observation quartz window protected by a moveable radiation shield and silica glass plate which is easy to move and clean. The vacuum pressure is measured by an ionization gauge with its head connected to the side of the chamber.

All internal parts of the furnace, Fig. 2.2, can be lifted and lowered into the furnace by a hoist.

The liquid nitrogen-filled stainless steel "cold finger" attached to the lid, acts as a trap for vapours, thereby effectively improving the vacuum pressure inside the furnace.

The cathode is insulated by two pyrophylite blocks which are mounted on lead screws.

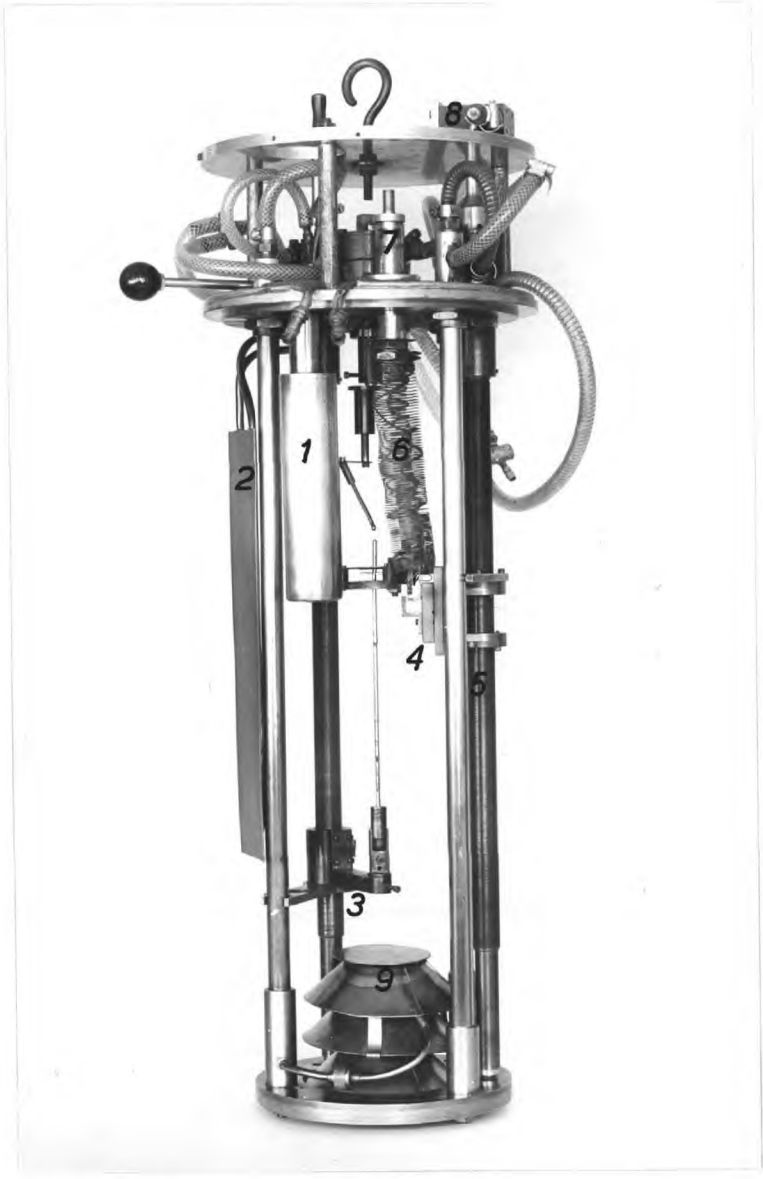

Fig. 2.2 Internal parts of the electron beam zone melting furnace

1. Liquid nitrogen trap
2. Movable window shield
3. Lower sample clamp, adjustable in height
4. Insulating pyrophilite block
5. Water-cooled lead screw
6. Extendible current leads
7. Vacuum sealed terminals
8. Reduction gear
9. Water-cooled baffle

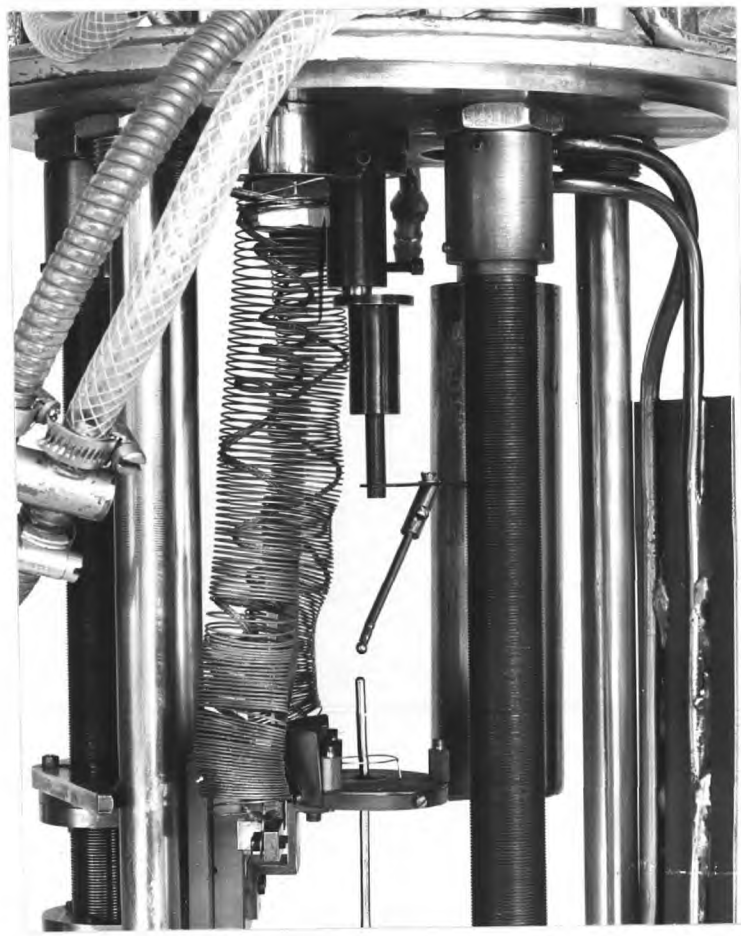

Fig. 2.3 Detail of the seed holder, the top focussing plate has been removed

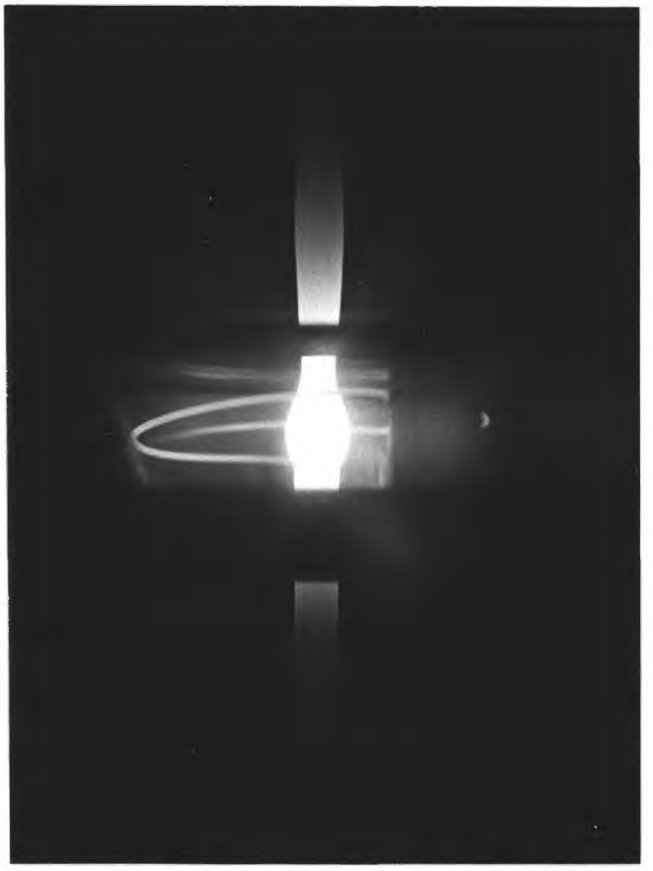

Fig. 2.4 Molten Zone

The cathode assembly used in the initial stages of this investigation is similar to the one developed by Cole et al (1961). In this, the filament is hidden from the molten zone to avoid contamination of the crystals by metallic elements emmitted from the filament, and to avoid coating of the filament with the metal ejected or evaporated from the molten zone. Because of the high impedance of this design, the emission current was very low, making power control difficult and resulting in a poorly shaped single crystal. In addition no sputtering from the molten zone was encountered when niobium crystals were grown, and so a direct focussing cathode of low impedance was constructed in collaboration with P.J. Sherwood. The top and bottom focussing plates are made of molybdenum, while a tungsten filament (0.5 mm in diameter) loop is supported horizontally by a leg resting on the bottom focussing plate. This ensures that the plates are at the same potential so that the electrons are focussed electrostatically.

The high voltage, 10 KV, 1 Amp, D.C. supply unit has a full wave rectifier, supplied by Miles Hivolt Ltd. It incorporates a trip circuit to prevent overloading and a power control circuit, operated by a thyratron, which regulates the temperature of the filament and therefore, the emmission current. The control circuit is similar to that used by Birbeck and Calverley (1959). It is necessary to operate the emitter in limited range to ensure effective regulation.

The filament heating current is supplied by a high voltage insulated transformer with a rating of 20 Amp. at 50 Volt.

2.5 Operating characteristics and Growing Procedure

With water cooling of the furnace chamber, the vacuum pressure of the furnace was about 6×10^{-6} torr. When the cold finger was filled with liquid nitrogen the pressure improved to 2.5×10^{-6} torr. On maintaining the rod at the melting point, the pressure rose to $8 - 9 \times 10^{-6}$ torr, but after several minutes decreased to about 4×10^{-6} torr.

A stable molten zone of 3 mm length, in a 3 mm diameter rod,

could be formed using a voltage of 2.5 - 2.6 KV and emission current of 77 - 80 mA during the first zone pass. This gives a melting power of 200 watt. The second pass required slightly less power, about 184 watts. A 6 mm diameter rod of the same material required 558 watts at 6.2 KV and 90 mA. Fig. 2.4 shows the cathode assembly and configuration of the molten zone of 3 mm diameter rod for the downward pass.

The starting polycrystalline rod of 3 mm diameter and 28 cm length was mounted in the furnace and subjected to zone-melting. After completing the first zone pass, the power was decreased taking the crystal below its melting temperature. For zone levelling, the crystal was re-melted at a distance of 7 zone lengths from the last freezing zone and the second pass resumed. This procedure was adopted to avoid disturbances in orientation and also to avoid contamination from heating of the chuck and from the accumulated solute at the end of the rod after the first zone pass.

The variation of vacuum pressure with time using the zone refining process (A), zone levelling process (B), and fast zone levelling (C) are shown in Fig. 2.5. In all three cases there is an appreciable fall in pressure after the first zone pass. Thereafter, the decrease is less with subsequent zone passes.

Uniformity in the distribution of impurity along the crystal was achieved by a "zone levelling" (Pfann 1958) technique with a number of zone passes alternatively in opposite directions.

To evaluate the influence of the variables controlling electron beam zone-melting, single crystals were grown as follows:

Type A Crystals

1. By a zone levelling technique at a zone speed of 2.5 mm/min with various numbers of zone passes on ⟨110⟩ and ⟨100⟩ orientation.

2. By a zone levelling technique at a zone speed of 2.5 mm/min with two zone passes for crystals oriented in ⟨100⟩, ⟨110⟩, ⟨111⟩, and the centre of a stereographic triangle.

Type B crystals

By a zone levelling technique at a zone speed of 5 mm/min with two zone passes for ⟨110⟩ orientation.

Type C crystals:

By a zone refining technique at a speed of 2.5 mm/min. with two zone passes for ⟨110⟩ orientation.

Type D crystals

By zone refining at a speed of 2.5 mm/min with one zone pass for ⟨110⟩ orientation at a vacuum pressure.

1. between $4.4 \rightarrow 3.9 \times 10^{-5}$ torr.
2. between $4.9 \rightarrow 3.0 \times 10^{-6}$ torr.

The starting polycrystalline material is in the form of electron beam melted rod and was supplied by Fansteel Hoboken, Belgium. A chemical analysis of the starting material and of crystals of one and four zone passes made by E. . Du Pont de Nemours & Co., U.S.A. is shown in Table 2.1.

2.6 Seeding of oriented crystals

A randomly oriented crystal was fixed to a 6 mm diameter stainless steel cap which was then sliced through a plane normal to the desired orientation. The cut surface was attached by a screw to the horizontal plane of the holder so that the seeding direction coincided with the vertical axis of the rod. See Fig. 2.3. Subsequent crystals of the same orientation were grown by using a length of crystals previously grown by this method and were less than 3° from the desired orientation.

Fig. 2.6 shows the orientation of crystals of one zone pass grown without seeding. There was no definite preferred orientation, however, it is noticeable that the crystals tended to grow with their axis closer to ⟨110⟩ than any other orientation. Similar results were reported on iron single crystals grown by a strain annealing technique using zone refined iron (Michalak 1965). It is possible that the ⟨110⟩ preferred orientation of the

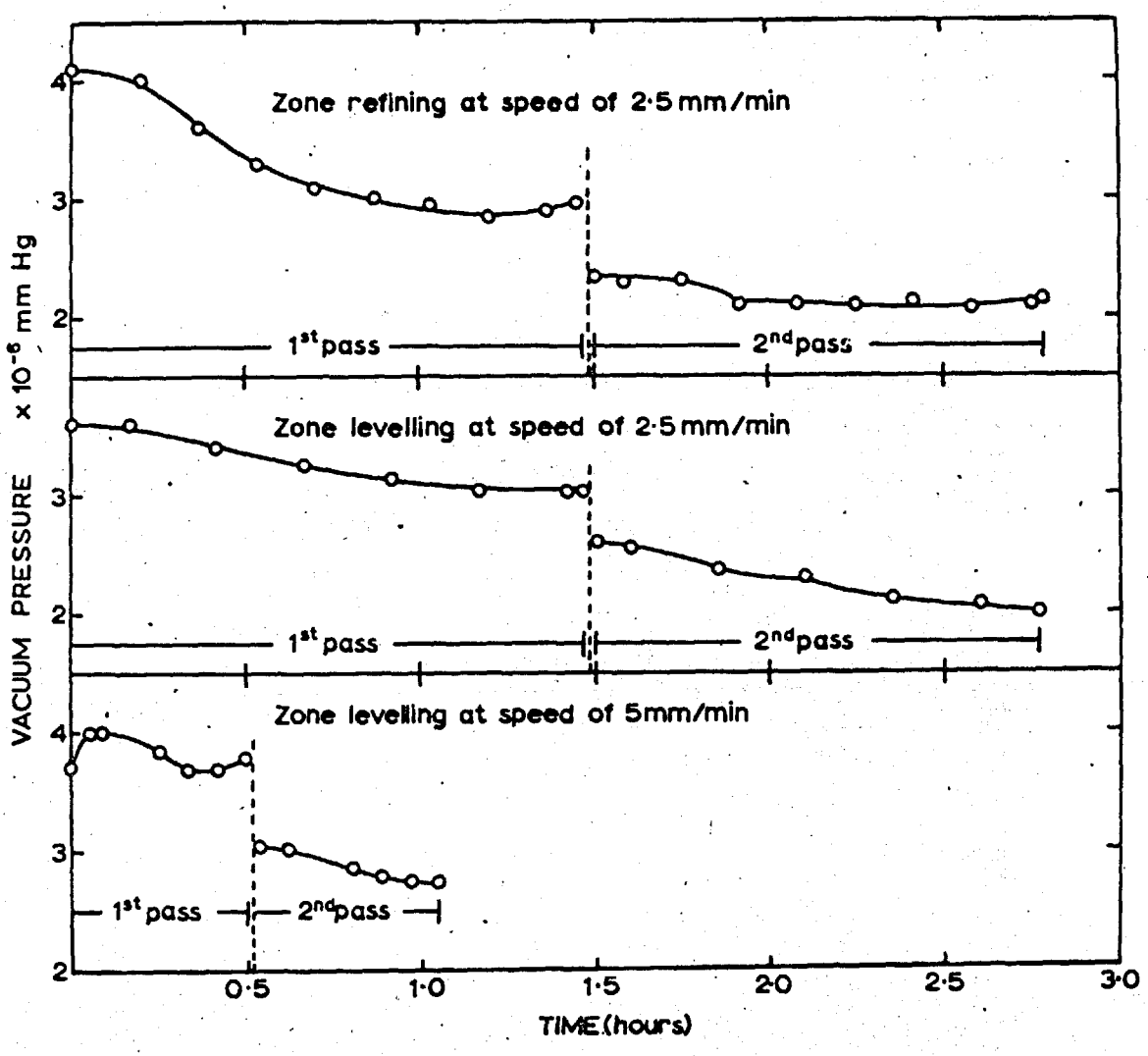

Fig.2-5. Variation of Vacuum Pressure with Time during the Zone Melting of Niobium Single Crystals.

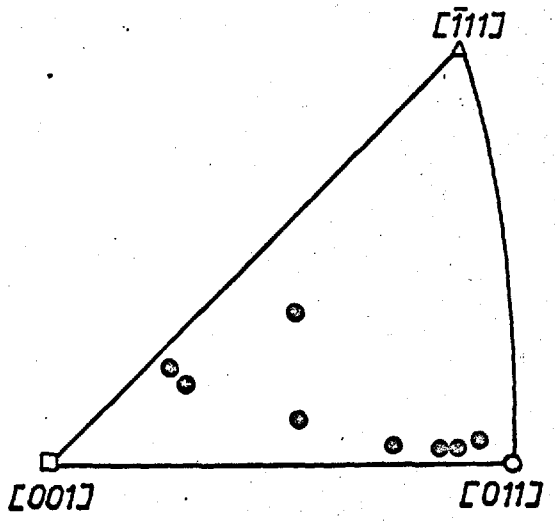

(A) Polycrystalline region at end of the final zone

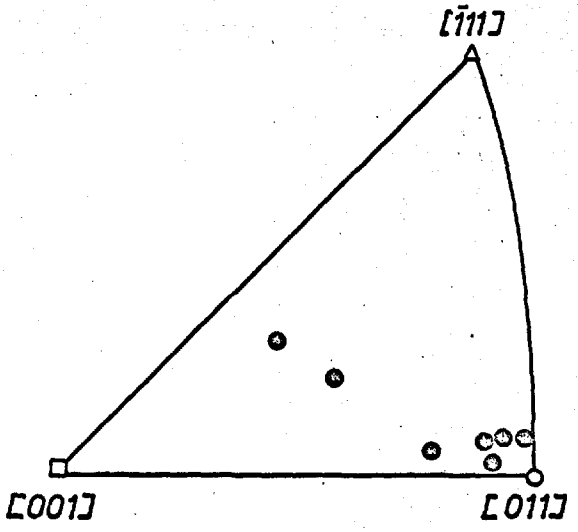

(B) Single crystal region

Fig.2-6. Stereographic representation of Crystals grown without seeding

recrystallization and wire deformation textures (Barrett 1943) may be responsible for such behaviour in b.c.c. metals.

2.7 Evaluation of the effect of zone melting

The electron beam zone melting technique has been used by many workers for preparing pure single crystals of the b.c.c. transition metals for mechanical tests. The purity of the crystals has been commonly evaluated by means of resistivity ratio measurements (Barrett 1943), hardness (Votava 1964, Drangel and Murray 1964), tensile tests (Mitchel, Foxall and Hirsch 1963) and chemical analysis (Reed 1966). However, in this investigation strain ageing experiments were also used for the purpose of evaluation

In order to avoid the complexity which may arise from crystallographic geometry all the tests were carried out on tensile specimens oriented in the ⟨110⟩ orientation. This orientation was chosen because preliminary experiments showed that the yielding behaviour was influenced by impurities to a greater extent than in any other orientation.

The resistivity ratio measurement has long been used as a measure of impurity content present in solid solution. This has been described in detail by Kunzler and Wernick (1958). In the present investigation resistances were determined at low temperature in a liquid nitrogen bath (77°K) and at the high temperature were measured in a mixture of ice and water (273°K) for varying numbers of zone passes.

Hardness measurements were made on a cross section at one end of the tensile specimens after preparation by spark planing and subsequent chemical polishing for 45 sec. in 7 parts of nitric acid and 3 parts of hydrofluoric acid. Since it is well-known that the microhardness value under low load is higher than the value obtained from macrohardness it was decided to carry out both types of hardness measurements. Indentations were made with a Reichert microhardness tester using a load of 24 grammes, and Vickers hardness tester using a load of 1 kilogramm.

Tensile tests were performed at a strain rate of 4.9 x 10^{-4} sec^{-1}. The stress at the first deviation from linearity in the stress strain curve was taken as the yield stress of each crystal, i.e, proportional limit. Each specimen was prepared according to a procedure described in 3.2

For the strain ageing experiments, two single zone pass crystals of identical orientation were grown at the same zone speed. However, crystal D1, was grown with the pressure between 4.4 → 3.9 x 10^{-5} torr, whereas crystal D2, was grown at a vacuum pressure of 4.9 → 3.0 x 10^{-6} torr. They were then pre-strained at room temperature at a strain rate of 4.9 x 10^{-4} sec^{-1}, unloaded and then given ageing treatments at 296°, 373° and 473°K for various time intervals.

2.7.1 Effect of number of zone passes

In the electron beam zone melting technique the degree of the purification depends firstly on the purity of the starting material as predicted in equation (2.1) Hence, under identical conditions of zone length, vacuum pressure during melting, zoning speed and direction, and starting material, the purification achieved should depend solely on the number of zone passes. This fact has been confirmed by previous workers on electron beam melted niobium (Mitchel et al 1963), on tungsten (Koo 1963) by means of yield stress, and on molybdenum (Lawley et al 1962) by means of hardness.

The present results of resistivity ratio $R_{273°K}/R_{77°K}$, micro-hardness and Vickers hardness, and yield stress, are presented in Fig. 2.7 as a function of the number of zone passes.

The value of resistivity ratio, $R_{273°K}/R_{77°K}$ of 5.3 - 5.46 for one to six zone passes are slightly higher than the values reported by Votava (1964) of 5.05, 5.15 and 5.10 for eight, sixteen and twenty-seven zone passes of niobium. This discrepancy may result either from different compositions of starting material, or zone speed or from both factors. Votava used the niobium supplied by Murex Co., and a zone speed of 14 mm/min, about 5.6 times faster than that used in this work.

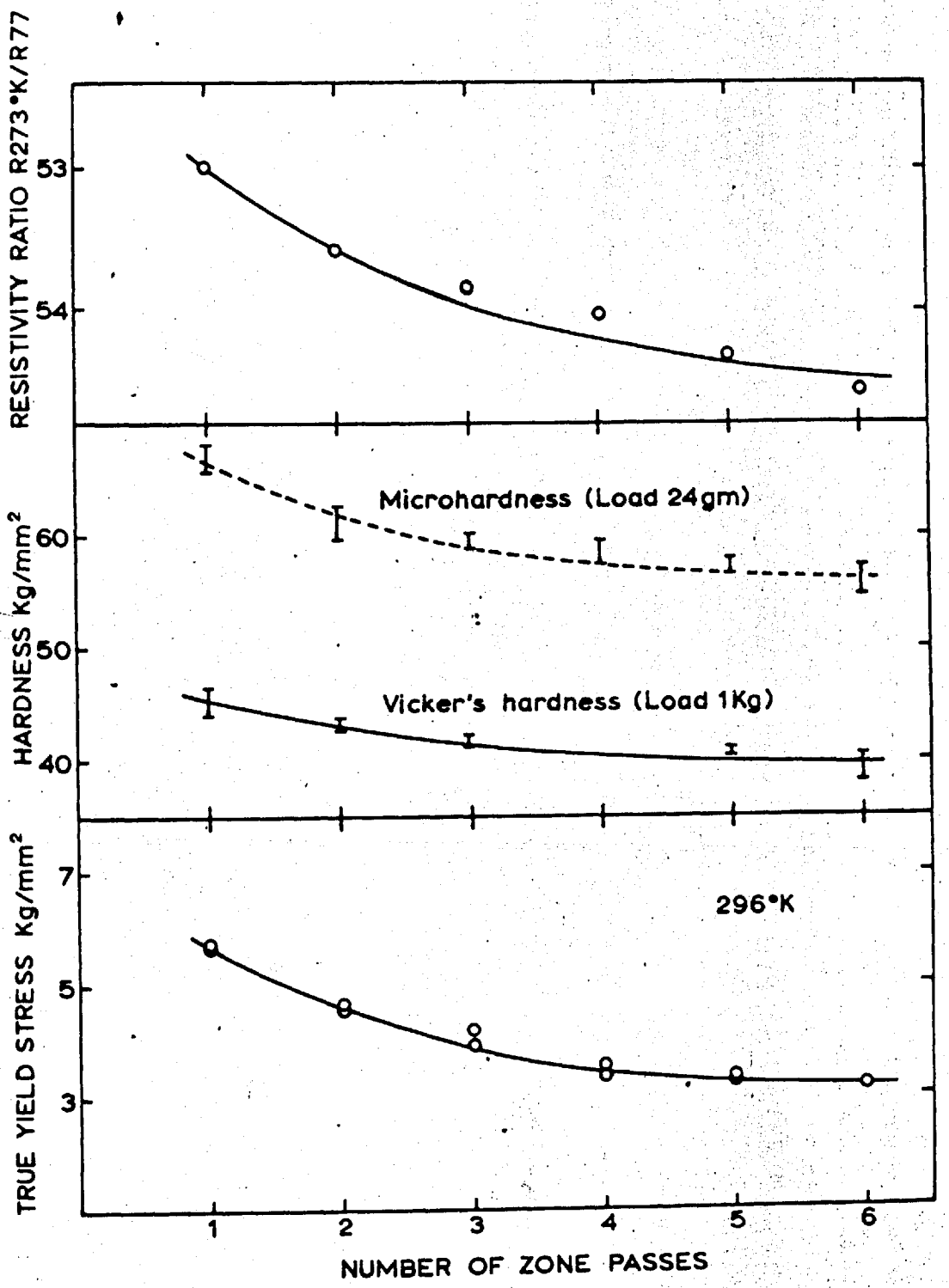

Fig.2-7. Variation of Resistivity Ratio, Hardness and Room Temperature Yield Stress with Number of Zone Passes

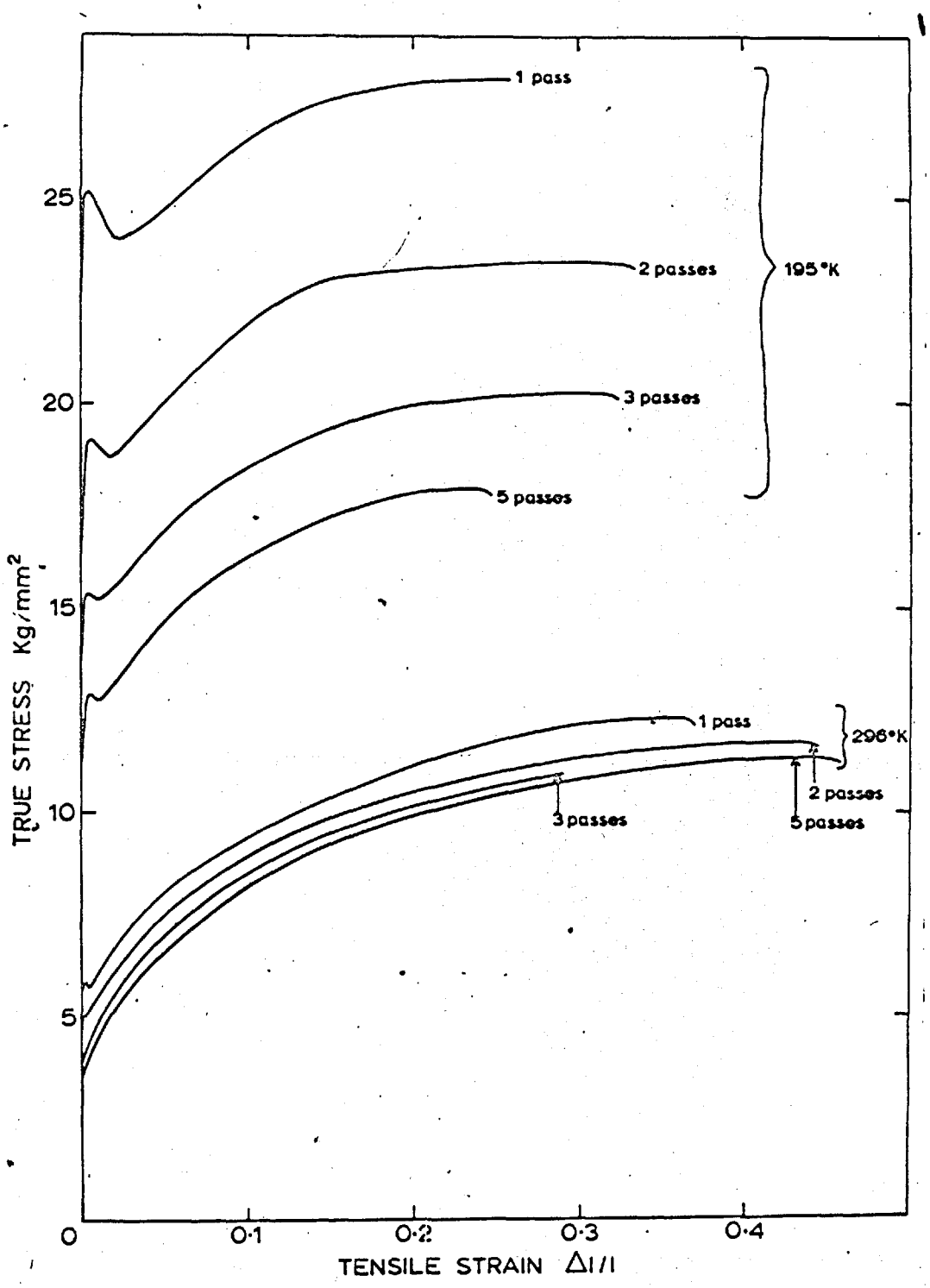

Fig.2-8. Tensile Stress Strain Curves of <110> oriented Crystals with Varying Number of Zone Passes.

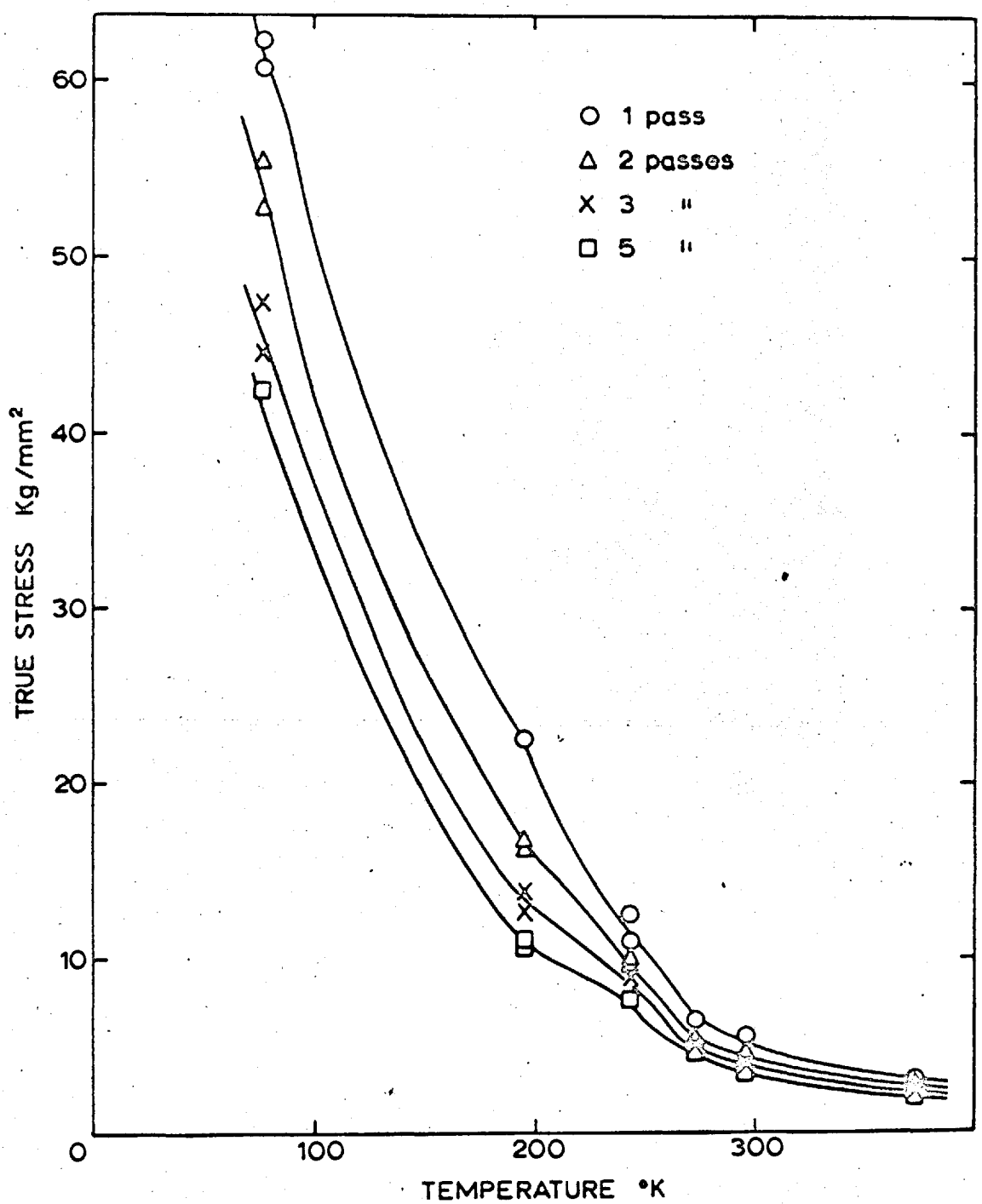

Fig.2-9. Temperature Dependence of the Yields Stress of Crystals of <110> Orientation with Varying Number of Zone Passes.

Variations of both microhardness and Vickers hardness were also apparent but became less marked as the number of zone passes increased. For one to six zone passes the microhardness varied from 67 to 56 Kg/mm^2, whereas the Vickers hardness varied from 45 to 40 Kg/mm^2. Votava's Vickers hardness varied from 44 to 48 Kg/mm^2.

The decrease in yield stress with increasing number of zone passes was more rapid than the variation observed using the above mentioned other methods. The yield drop, as in Fig. 2.8, and the temperature dependence of the yield stress, in Fig. 2.9, changed markedly with increasing number of zone passes. This will be discussed in detail in 4.7

2.7.2 Effect of zone levelling speed

As shown in Fig. 2.10, the variation of hardness along the crystal for both fast and slow zone levelling speed crystals was hardly detectable, whilst the yield stress was generally higher, and increased significantly with distance from the starting end in the case of fast zone speed crystals. In this work the zone speed differed by a factor of two, and this caused a significant change in the impurity distribution profile along the crystal, and in the overall purity. These changes may have arisen from differences in the time available for purification during zone melting. However, Drangler and Murray (1964) found that the slower zoning speed for electron beam melted tungsten and molybdenum improved the crystal near the starting end only, whereas the rest of the crystal did not vary.

2.7.3 Effect of zone refining and Zone levelling

The factors which may have an influence on the concentration profile along a crystal have previously been discussed in 2.2 A considerable impurity gradient is navoidable in the zone refining process, but in contrast a more uniform, or level, concentration profile could be expected in the zone-levelling process. The results of hardness measurements and of yield stresses along a zone-refined crystal and the other levelled crystal, after two zone passes at the same zone speed, are compared

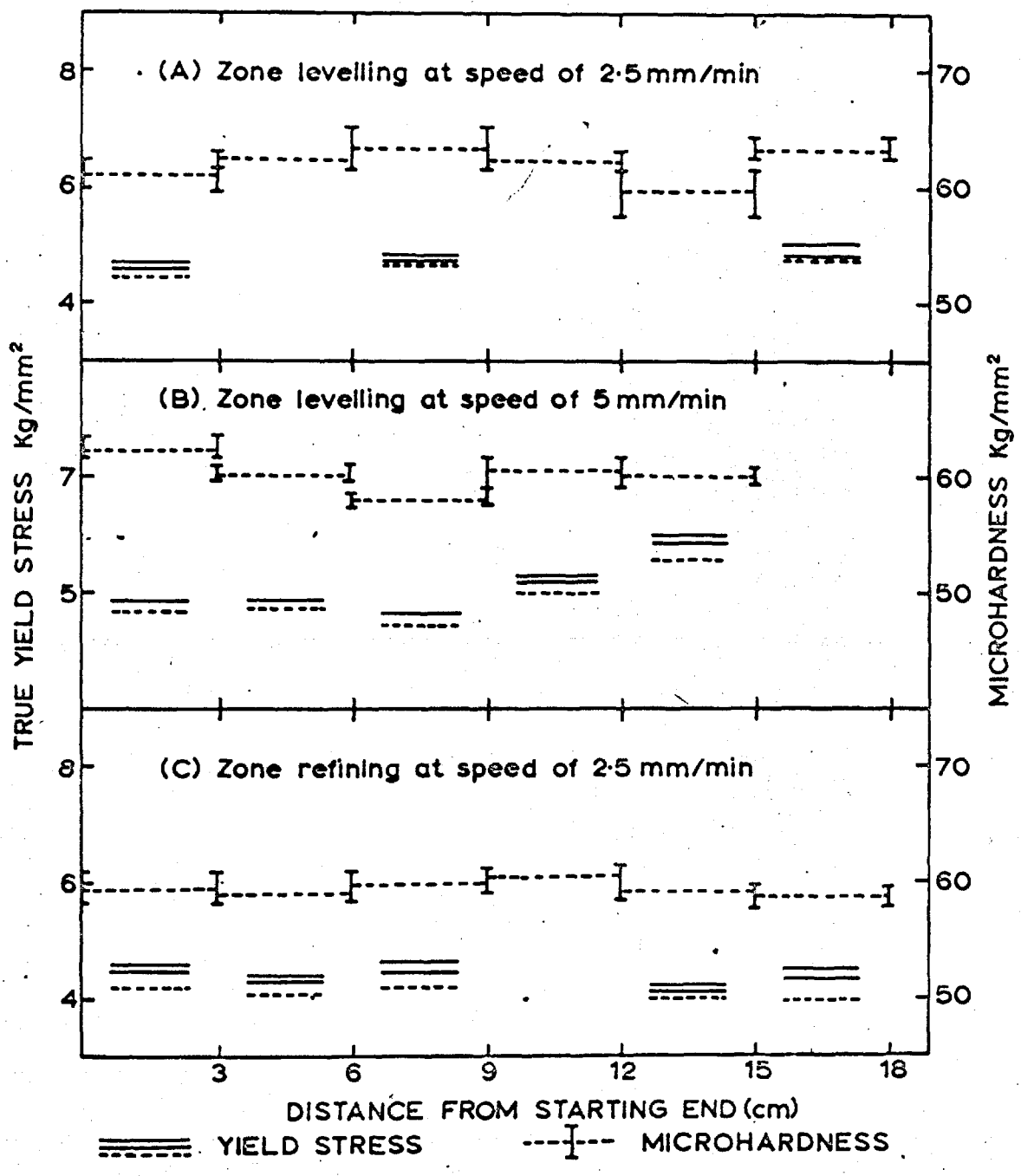

Fig.2-10 Variation of Hardness and Yield Stress at room temperature with distance from the Starting end of the Crystal.

in Fig. 2.10. No significant differences in hardness along and between the two differently prepared crystals were observed. However, the yield stress was slightly lower and decreased towards the finishing end in the case of the zone-refined crystals. Whether this slight difference is caused by the characteristics of the zone-refining process or by experimental scatter in the measurements is not clear. By contrast Koo (1963) has found that in zone-refined tungsten single crystals, the yield stress increased rather steeply up to 7.6 cm from the starting end and then remained constant up to the finishing end (22.9 cm from the starting end). The theoretically predicted "tail-up" concentration profile in the zone- refining process does not apply to the present observation. Theory suggests that, for the present case of niobium, K must be >1 for the impurity controlling the yield stress.

2.7.4 Effect of vacuum pressure during the zone melting

Previously it has been accepted that the purification mechanism involved in electron beam zone melting techniques entails the vacuum distillation of lower melting point elements and volatilization of oxides and nitrides as well as zone-refining. (Wulff 1957; Winkler 1960; Smith 1958; Votava 1964; Dragel and Murray 1964). Yet, in the present investigation the vacuum pressure was found to be the most influential parameter, being more important than the number of zone pass or zone speed in controlling the purity of single crystals.

In Fig. 2.11 crystal D 1, grown at poor vacuum pressure, shows a much higher proportional limit, larger yield drop and larger susceptibility to strain ageing than the crystal D 2, grown in a better vacuum pressure. This provides substantial evidence of the importance of interstitial impurities on the initial yielding and strain ageing behaviour.

The proposed purification mechanisms of "Vacuum distillation and volatilization of lower melting point elements" may be a contributing factor. The vapour pressures of many elements are sufficiently high to bring about distillation at, and near

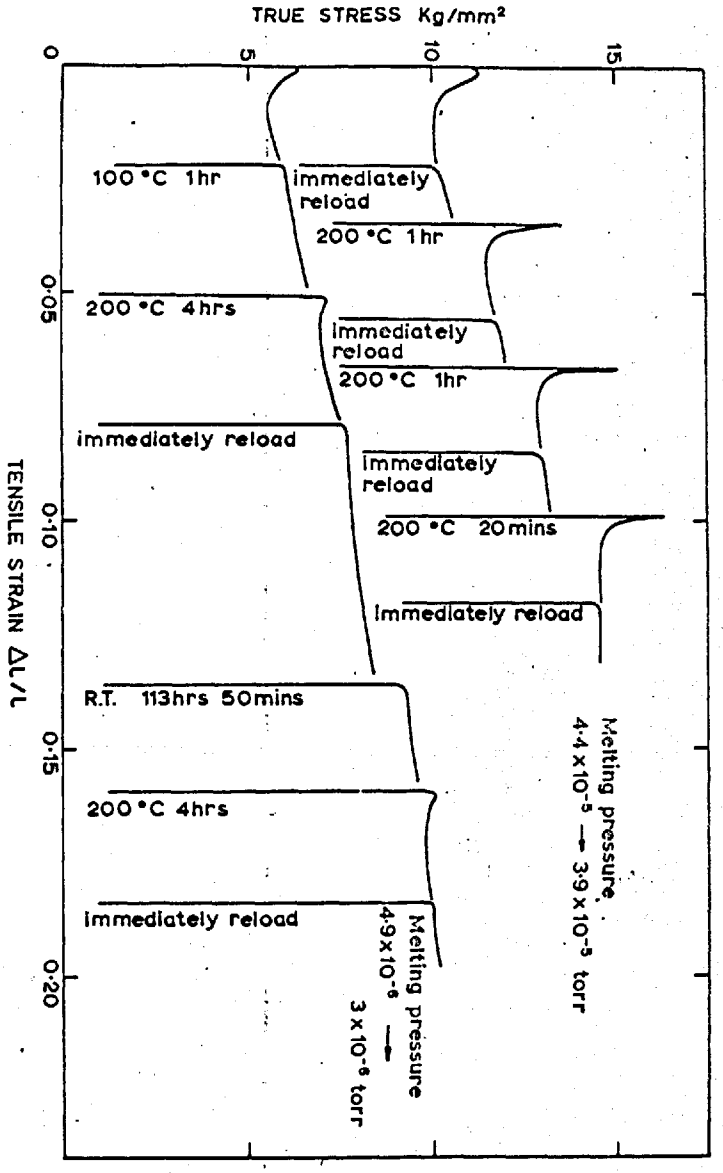

Fig.2-11. Strain Ageing Characteristics of Crystals with different Purity.

the zone melting temperature. They are transferred through the vapour phase to a cooler part of the furnace, such as the liquid nitrogen filled "cold finger" or the water-cooled furnace wall. However, in the case of dissolved gaseous elements such as nitrogen and oxygen, the solubility is proportional to their partial pressures. By improving the vacuum pressure in the furnace the solubility is correspondingly reduced and this leads to the higher purity crystal. This explains the above observed effect of vacuum pressure on the purity of crystals. Furthermore, the observed similarity between the improvement of vacuum pressure with time (also number of zone passes) and the improvement of purity achieved with increasing number of zone passes also provides substantial evidence to support this view of the purification mechanism.

2.7.5 Chemical analysis and purification mechanism

It is unfortunate that during the current work of investigation the chemical analysis of the metallic elements was not carried out. The extensive chemical analysis of Reed (1966) shows that the tantalum and tungsten contents have not been altered after 12 zone passes. This suggests that the considerable concern about contamination by tungsten from the filament of the cathode assembly is not so serious as has been suggested by previous workers. The vapour pressure of pure tungsten and tantalum are comparatively low at the zone melting temperature, and these values are further reduced due to their small concentrations in the niobium crystals. Even at the very low vacuum pressure which was employed in the current work, the removal by distillation of these elements cannot be expected. On the other hand, analysis of the interstitials showed that the carbon content increased with increasing number of zone passes, whilst the nitrogen content markedly decreased. The oxygen results were rather scattered.

In contrast to Reed (1966), the present chemical analysis indicates that the carbon content was reduced by half after four zone passes, and the nitrogen content reduced similarly after the first zone pass. The oxygen content decreased after the

Table 2.1 (Weight in .p.pm.)

Chemical Analysis of Starting Material

and of Single Crystals after

one and four zone passes

	O_2	H_2	C	N_2
Starting material:	29	1	7 - 8	63
One pass (1)	12	*	7 - 9	28
(3)	21	*	*	35
Four passes (1)	37	*	4	20
(3)	29	*	4	31

Precision of Method ; $O_2 \pm 3$ p.p.m.

$H_2 \pm 1$ p.p.m.

C ± 5 p.p.m.

$N_2 \pm 2$ p.p.m.

* = not determined

first zone pass and then increased to a level in excess of that found in the starting material.

A comparison between the report of Reed and the present analysis implies that carbon contamination due to back-streaming from the vacuum system took place in his case, which, due to the better cold trap this did not occur here. In the case of dissolved gaseous elements such as nitrogen and oxygen the solubility is found to be decreased by increasing the temperature and by decreasing the vacuum pressure. However, an increase in oxygen in the present case with further zone passes is not unreasonable. Consider the thermodynamics of oxide formation calculated from the free energy of formation of NbO, the equilibrium partial pressure of the Nb/NbO system at approximately 2,400°C is 10^{-10} torr. (Steele 1965). The oxygen partial pressure in the vacuum furnace is probably less than that, so it can be stipulated that no NbO is formed in the molten zone. However, as the temperature drops immediately behind the molten zone, the partial pressure of the oxygen will be sufficient to form NbO because the equilibrium partial pressure of oxygen in the Nb/NbO system decreases rapidly with temperature. This suggests that NbO is formed after the zone has passed over the crystal. The oxygen content could be further reduced only by further improvement in the vacuum pressure and by increasing the temperature gradient near the molten zone.

Based on the present chemical analysis the observed larger yield drop and higher yield stress occurred in the least number of zone passes, as shown in Fig. 2.8, and this effect is very likely due to the carbon or nitrogen interstitial impurities.

2.7.6 Summary

1. A good agreement was found between resistivity ratio, hardness and yield stress in the evaluation of purity caused by varying the zone melting parameters.

2. The improvement in overall purity achieved with increasing number of zone passes was found to be greater between one and two zone passes, then diminished between subsequent zone passes.

3. A fast zone speed resulted in poor purity of crystal and caused a considerable gradient in impurity distribution along a single crystal rod. This arose from an increase in the value of the effective distribution coefficient.

4. No significant difference in the impurity distribution profile was observed between zone-levelled and refined crystal when the same zone speed was used.

5. The vacuum pressure during the zone melting process was found to be the most influential parameter in controlling the purity of crystals.

6. Good agreement was found between the progress of purification and the improvement in the vacuum pressure with time. This implied that the removal of the products of volatilization and degassing by the vacuum system was a major part of the purification. Vacuum distillation of lower melting point elements would also be promoted by decreasing the furnace pressure.

7. Chemical analysis showed that the improvement in overall purity due to further zone passes was most likely due to the reduction of carbon or nitrogen contents. This may be associated with the observed higher yield stress and discontinuous yielding behaviour in the crystals with the least number of zone passes.

CHAPTER 3

PREPARATION OF SPECIMEN AND EXPERIMENTAL TECHNIQUES

CHAPTER 3

3.1 Introduction

It is well known that the stress-strain behaviour of single crystals is very sensitive to the surface damage introduced during preparation of the specimen. Therefore it is desirable to minimize any cold-worked layer.

The usual methods employed by previous workers to produce single crystal specimens are the following:

A. Chemical or electrolytic machining (Schadler and Low 1962; Lawley, van den Sype and Maddin 1963; Titchener and Davies 1963; Lawley and Gaigher 1964).

These methods are supposed to be strain-free from any possible damage due to machining effects. Thus their applicability in the case of niobium was investigated. The apparatus consisted of smooth rotating wheel of pyrophilite, partially submerged in a chemical solution of 7 parts HNO_3 and 3 parts of HF. Above this a specimen was mounted. The crystal was held in contact with an acid layer over the wheel and rotated more slowly than the wheel in the opposite direction. For electrolytic machining, the specimen was connected to a positive electrode and a Pt cathode was immersed into the electrolyte consisting of 9 parts of H_2SO_4 and one part of HF. This method was found to be only practical when the crystal rod was very uniform in diameter and the machining rate very slow. Usually, the as-grown single crystal rod was not uniform as a result of having been grown in a superheated condition. Therefore, it was neccessary to reduce the diameter quite markedly.

B. Mechanical machining and subsequent removal of deformed layer by chemical or electrolytic polishing.

Single crystals of tungsten machined by centreless grinding (Ferris et al 1962; Koo 1963) and of molybdenum by flat-surface grinding (Guiu 1965) were reported. However, the stress-strain

curves of comparable orientation of molybdenum by Guiu showed a significant difference in the work hardening rate from that of Lawley and Gaigher (1964), prepared by electrolytic machining. In spite of fast and accurate machining of specimens the detection of a damaged layer in the specimen and subsequent removal of the deformed layer present great difficulties.

C. Spark machining and subsequent removal of the damaged layer by chemical and electrolytic polishing.

Electric spark machining is a process in which material removal is achieved by spark erosion. The amount of removal from the surface is controlled by the intensity, and the time interval of the spark between the electrode and the work piece. The principle involved in this process is thought to be that the material removal occurs either by surface melting (Samuels 1962; Williams and Wade 1956) or by vaporization by the spark. It has been established that the resultant surface is plastically deformed (Samuels 1962; Williams and Wade 1956), in some cases cracks are present to a certain depth (Samuels 1962; Williams and Wade 1956; Beardmore and Hull 1966). It is generally believed that the damage is caused by thermal shock (due to the high temperature) or possibly by a cavitation effect in vapour pockets formed in the spark discharge. Since its development as a laboratory tool by Cole et al (1961) this technique is most widely used with a view to minimizing surface damage.

3.2 Machining of single crystal specimens

Fig. 3.1 shows an as-grown single crystal of niobium in a two-stage goniometer, used to align a seed crystal in the desired orientation.

The average length of all as-grown single crystals was about 25 cm long, and about 7 zone lengths were cut off from both ends of each single crystal to guarantee that all specimens would be of the same purity.

Tensile specimens were produced using a Servomet SMD spark

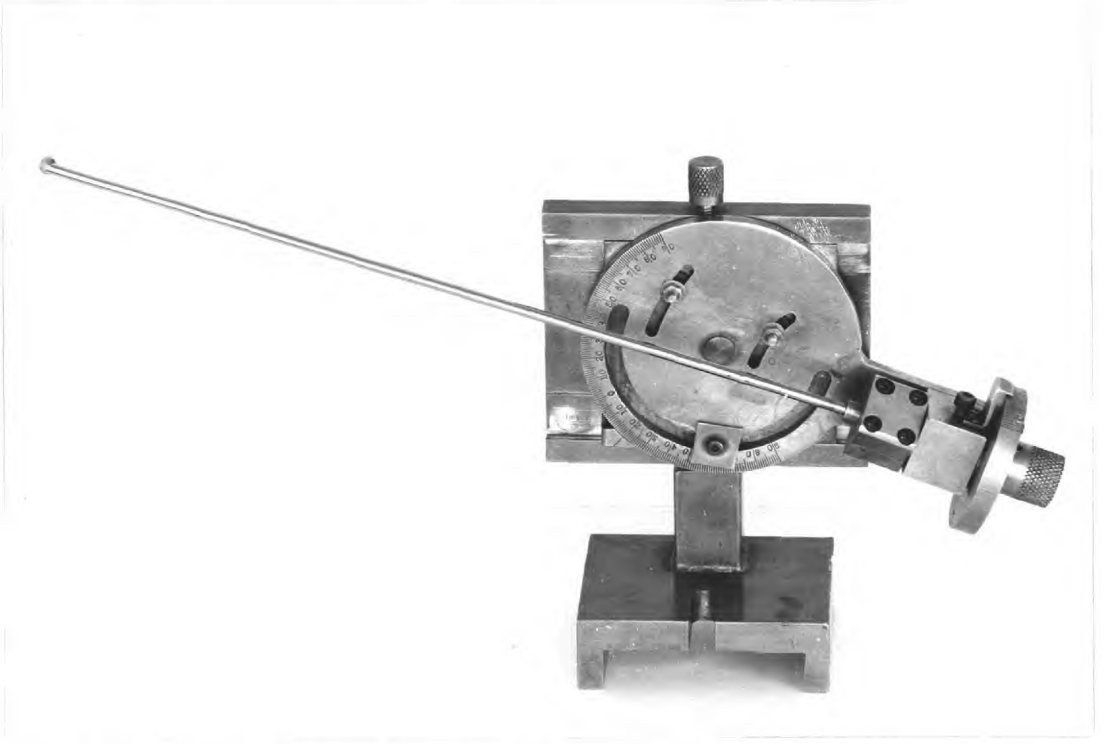

Fig. 3.1 Niobium single crystal rod in two stage goniometer

machine. As-grown single crystals of 3 mm dia. were cut into 3 cm length by the spark slicer. They were then spark-lathed, starting from range 4 and finishing at range 7, which is the finest range. In this way the tensile specimens were given a 16 mm gauge length with a shoulder radius of 3 mm. The final diameter of the specimens was 2.7 - 2.8 mm depending on the uniformity of the diameter of the as-grown crystal. The deformed layer of 100 microns due to the spark lathing was subsequently removed by electrolytic polishing for one hour at a voltage of 15 - 17 volt and 0.3 - 0.4 amp. Fig. 3.2 is the X-ray Laue picture of the as-machined surface which shows a split Debye ring on a background of faint spots. Due to the removal of 50 microns from the surface, the ring disappears and spots become as clear as those of an undeformed single crystal.

Cylindrical compression specimens were prepared by slicing previously spark lathed and electrolytically polished lengths of single crystal with a carborundom wheel. The compression faces were ground on 600 grade silicon carbide paper using a specially designed jig to ensure that the faces were accurately parallel. Gauge lengths were about 6 mm, and gauge diameters 2.5 mm except for specimens to be tested in the temperature range of 8 - 20.6°K. In the latter case, the gauge length was 2.46 - 2.5 mm and the gauge diameter 1.27 - 1.68 mm.

3.3 Effect of the damaged layer on the stress-strain behaviour

The effect of the damaged layer introduced during the spark machining on the stress-strain behaviour was investigated by testing two specimens from the same single crystal rod. These were cut consecutively to avoid the complexity of inhomogeneity of solute distribution along the rod and polished for different amounts after spark machining. Fig. 3.3 indicates that the specimen retaining the damaged layer has a steeper work-hardening at the beginning of plastic flow and a slightly higher yield stress.

This is very similar to the difference in the work-hardening rates at the early stages of deformation in molybdenum single

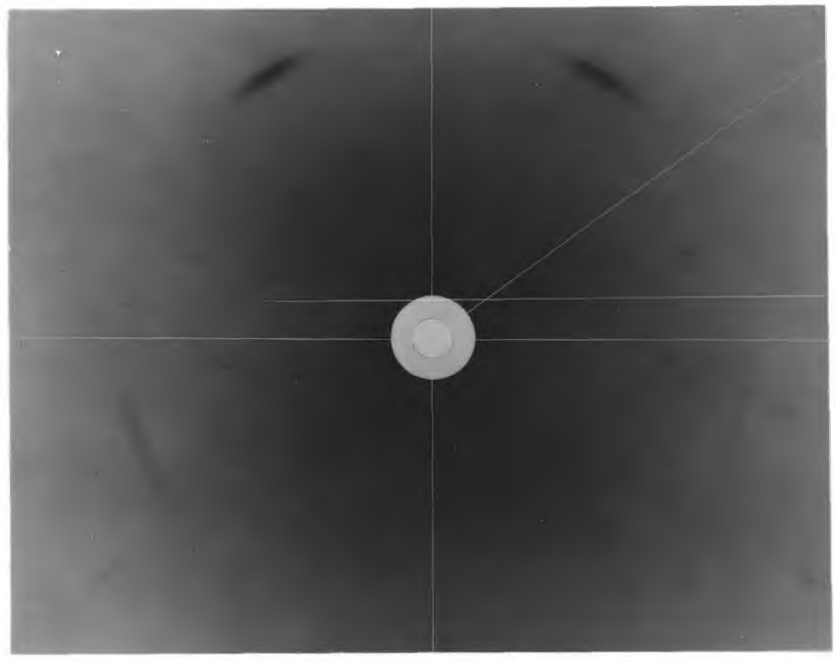

(a) as machined

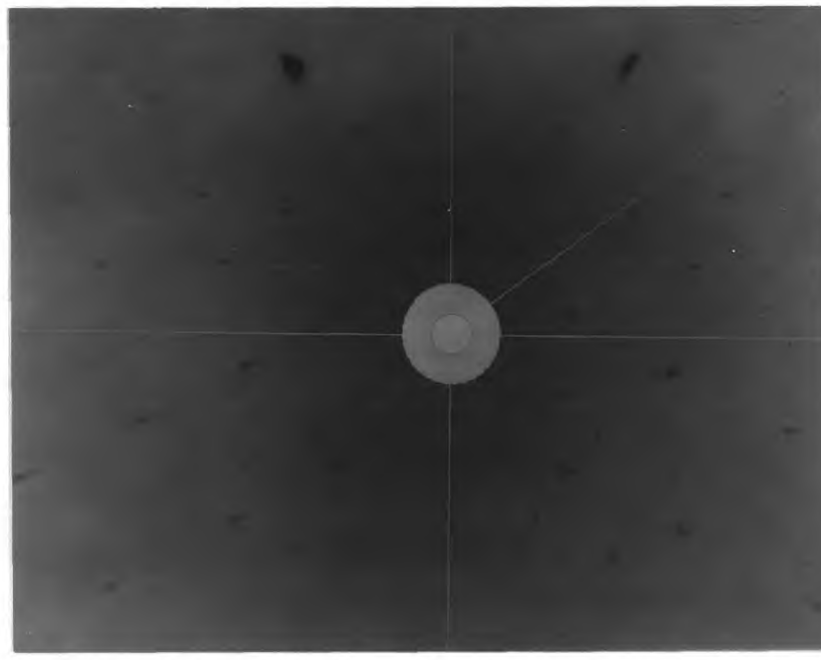

(b) after machining and subsequent removal by electrolytic polishing of 50 microns from the surface

Fig. 3.2 X-ray Laue photographs of a single crystal specimen of niobium

crystals prepared by electrolytic machining (Lawley and Gaigher 1964) and mechanical grinding (Guiu 1965). It is probable that fresh dislocations in the latter, which were introduced during mechanical grinding, were not removed completely by subsequent electrolytic polishing thus causing a steeper work hardening rate.

3.4 Testing machine and accessories

Tension and compression tests were conducted in an Instron Machine, model TT-CM, fitted with a load cell. The automatic load recorder has a 1/4 sec full scale response. A quick change push-button unit supplied with the instrument allowed a rapid change of cross head speed to be made before and during a test. With the insertion of a decade speed reducer into the drive gear system, the cross head speed could be varied in discrete steps from 0.005 to 50 cm/min.

For tests at other than room temperature a frame made of nickel plated mild steel, mounted on the bottom of the mobile cross head, was used. This frame could be submerged in a liquid during the tests.

Special split thread friction type grips were designed to fit the tensile specimen as shown in Fig. 3.4.

The compliance of the system composed of a testing machine, load cell, universal coupling and grip adapters, is 0.0011 mm/Kg at a load of 50 Kg and 0.00075 mm/Kg at a load of 500 Kg.

During this investigation, a standard cross head speed of 0.05 cm/min in tension and 0.02 cm/min in compression was used, corresponding to a strain rate of 4.9×10^{-4} sec^{-1} and 4.5×10^{-4} sec^{-1} respectively.

The various testing temperatures were obtained by immersing the frame and the specimen in a liquid contained in a Dewer flask;

Fig. 3.3 The effect of Damaged Layer due to Spark Machining on the Stress Strain Curves of 110 Oriented Niobium Single Crystals in tension.

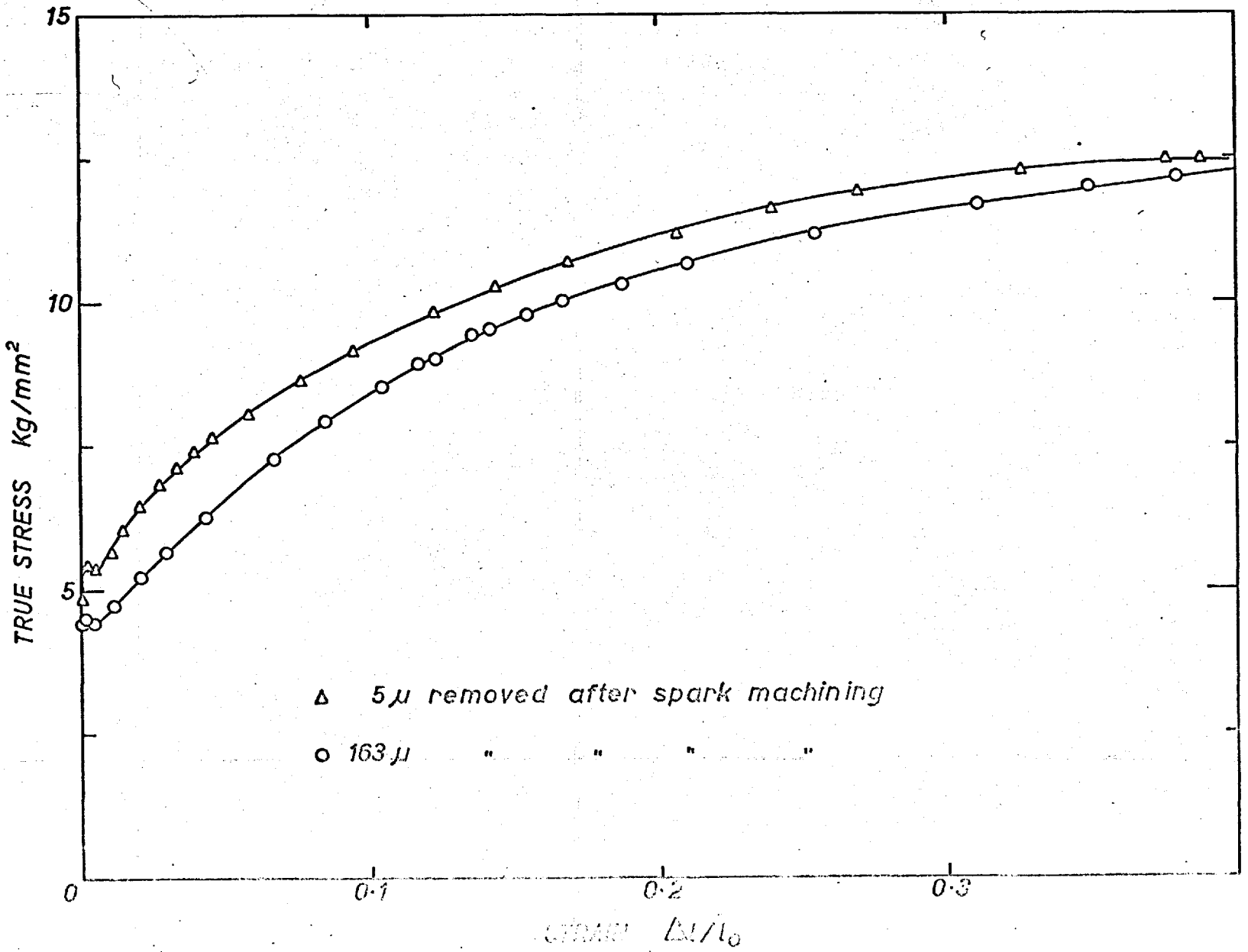

(a) Compression Rig

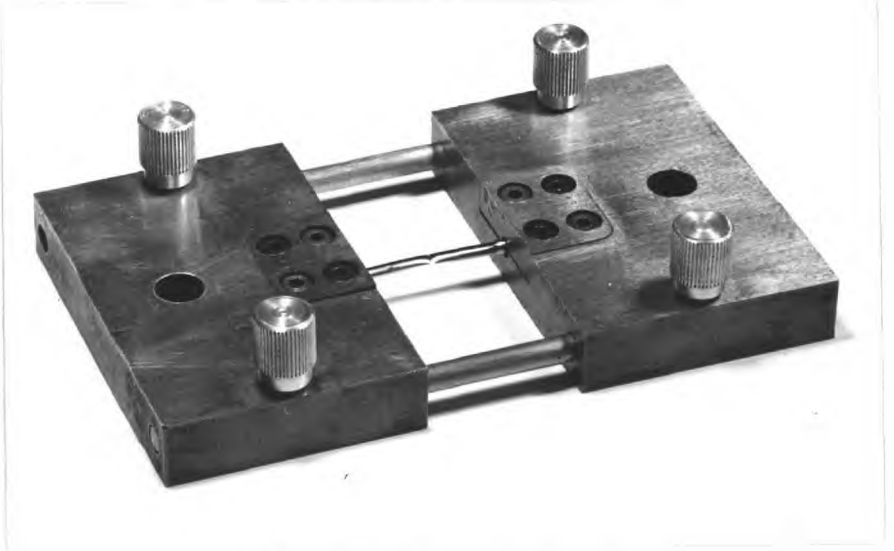

(b) Tension Rig

Fig. 3.4 View of a Specimen in the Instron Testing Machine

473°K	Silicone oil
373°K	Silicone oil
273°K	Mixture of water and ice
243°K	Boiling Iceon 12
195°K	Sublimation of solid CO_2 in acetone
163°K	Iceon 12 cooled with liquid nitrogen
77°K	Liquid nitrogen

To ensure long term stability of the testing temperature, fixed temperatures were obtained by heating the silicone oil with an electric resistance heater placed in the bottom of the Dewer flask. The temperature was stabilized within $\pm$ 3°C by adjusting the heating voltage with a variable transformer. Temperatures were then measured with pentane and mercury thermometers, and a Al-Chromel thermocouple placed close to the specimen.

3.5 Strain ageing

Strain ageing experiments were performed with tensile specimens of the previously described size in an Instron testing machine using a cross head speed of 0.05 cm/min (equivalent to a strain rate of 4.9×10^{-4} sec^{-1}). The specimens were pre-strained up to 2% at room temperature, then unloaded leaving a small amount of load to maintain axiality of specimens during placing and replacing in the temperature bath. The ageing temperature ranges from 403° to 473°K were measured by a Al-Chromel thermocouple placed near the middle of the specimen. The temperature of the bath fell when the grips and the frame entered the silicone oil bath, but quickly returned to the previous temperature. The ageing time was measured from the moment the specimen reached the desired ageing temperature. After the ageing treatment the specimens were cooled in air to room temperature, and tests were then continued.

3.6 Dislocation etch pits in niobium

The recent developments in the experimental technique for the direct observation of individual dislocations has made a great advancement in the understanding of fundamental

aspects of the plastic deformation of crystalline solids. Among numerous methods which include transmission electron microscopy, the Lang camera technique, and field ion microscopy, the dislocation etch pits method is used most widely on bulk specimens as a simple and non-destructive method.

In the case of niobium, Koppenaal and Evans (1965) first used the etch pits method to reveal the initiation and progress of plastic strain in the microstrain region in a recrystallized polycrystalline specimen. Electrolytic polishing was carried out at 15 - 20 volts, and 0.087 - 0.133 Amp/cm^2 in a solution of 9 parts of con H_2SO_4 and 1 part of HF, while maintaining a temperature of about 35 - 40°C, using Pt as a cathode. Electro-etching was carried out intthe same solution at 1 - 2 volts, and 0.004 Amp/cm^2 for the first stage, and 5 - 6 volts and 0.02 Amp/cm^2 for the second stage.

As a preliminary examination, the etching behaviour of electro-etching and chemical etching of recyrstallized polycrystalline specimens was investigated. The etchant, consisting 6 parts of H_2SO_4, 2 parts of HF and 2 parts of HNO_3 (Koo 1962) was used for chemical etching. As shown in Fig. 3.5A and 3.5B no significant difference was observed in either etching method. However, etch pits produced by the chemical etching method were of a more regular shape. Fig. 3.6A and B are typical etch pit configurations of recrystallized polycrystalline specimens. In general the shape and size of pits were found to depend on the grain orientation with respect to the specimen surface. Some grains showed no etching effects.

In order to reveal fresh dislocations due to plastic deformation a decoration treatment, at 573°K for 16 hours in the vacuum furnace, was necessary. When, however, the specimen was wrapped with niobium foil during this treatment, no fresh etch pits could be made. This implies that some contamination was necessary for this process. Fig 3.7 shows the dislocation etch pits for deformed polycrystalline niobium specimen which were not wrapped during the decoration treatment.

In the case of single crystals, no previous work

(a) Chemical etching x 250

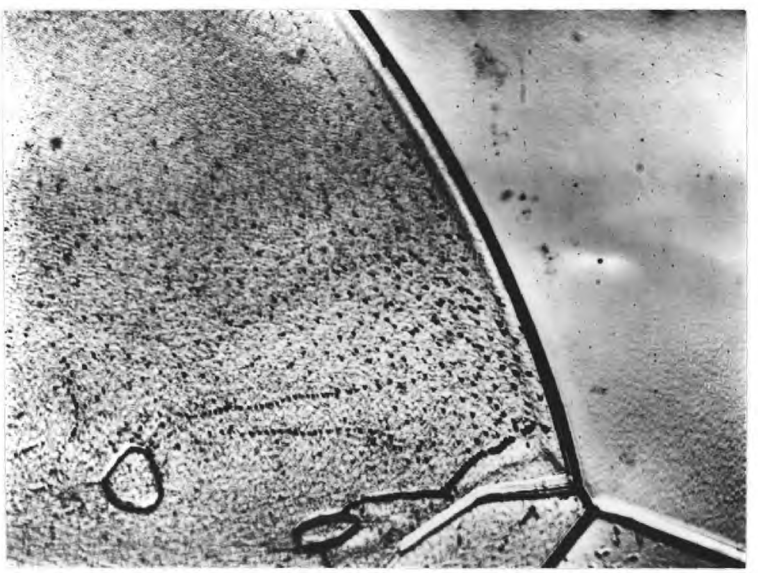

(b) Electrolytic etching x 250

Fig. 3.5 Etch pits on recrystallized polycrystalline niobium

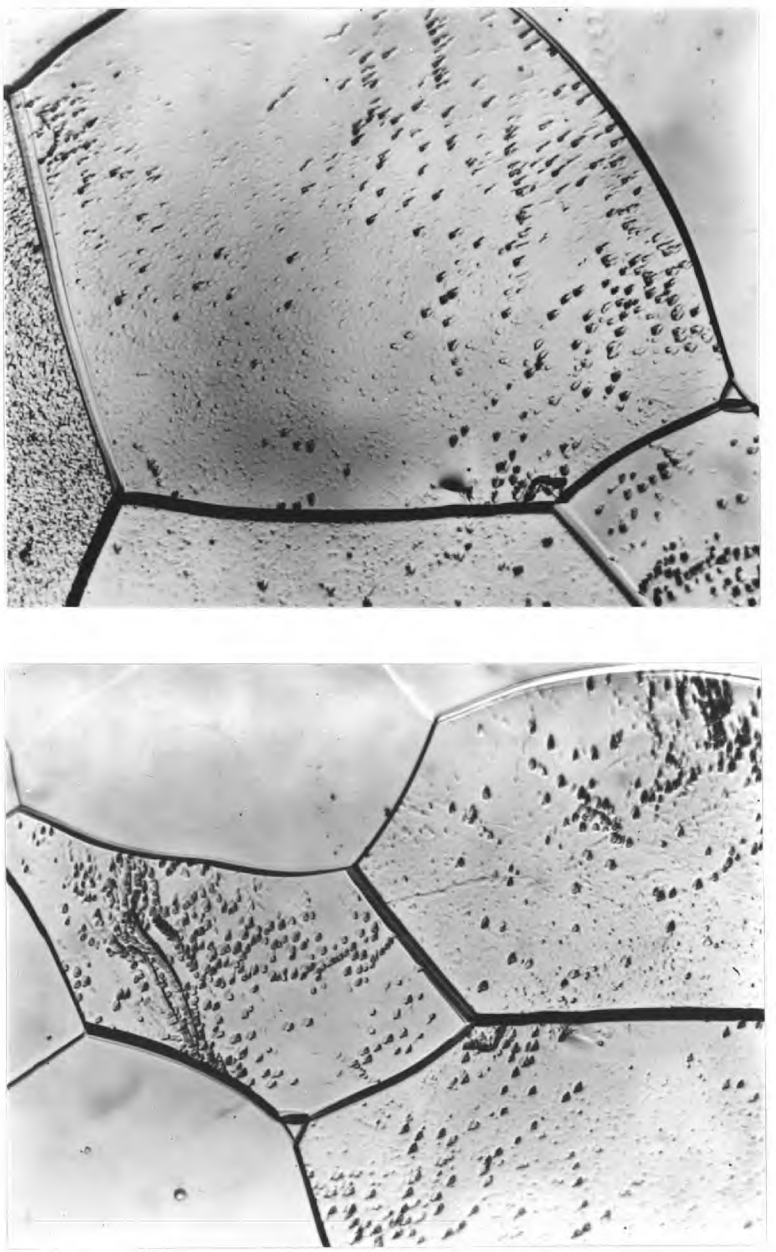

Fig. 3.6 Etch pits on recrystallized polycrystalline niobium x 250

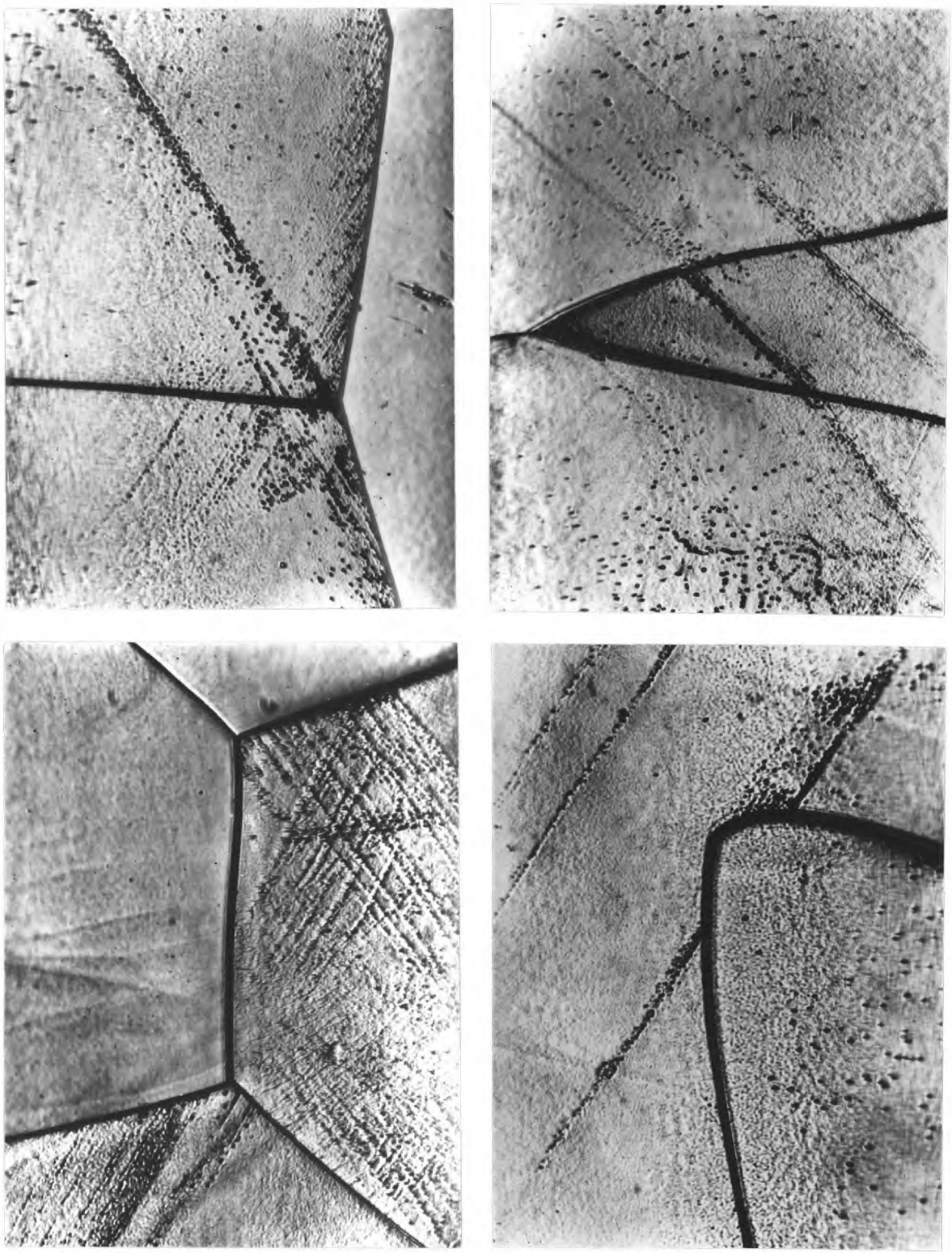

Fig. 3.7 Etch pits configuration on polycrystalline niobium strained up to the upper yield point
x 250

has been reported on the etching behaviour and its characteristics. In the present,investigation, the shape and density of pits were found to vary with the plane of observation. A specimen with its axis along ⟨110⟩ was etched electrolytically, the etch pits on the {111} plane have a pyramid shape while those on a plane progressing towards {112} are more elongated as shown in Fig. 3.8

It was felt that the variation of the etch pit density with crystallographic angle cannot be the result of preferential dislocation arrangment in the crystal, but was merely due to the characteristics of etching behaviour. Because of this obvious limitation, further effort towards the use of this technique has been dropped.

PIT DENSITY

$6{\cdot}0 \times 10^{5}$ cm^{-2}

{112}

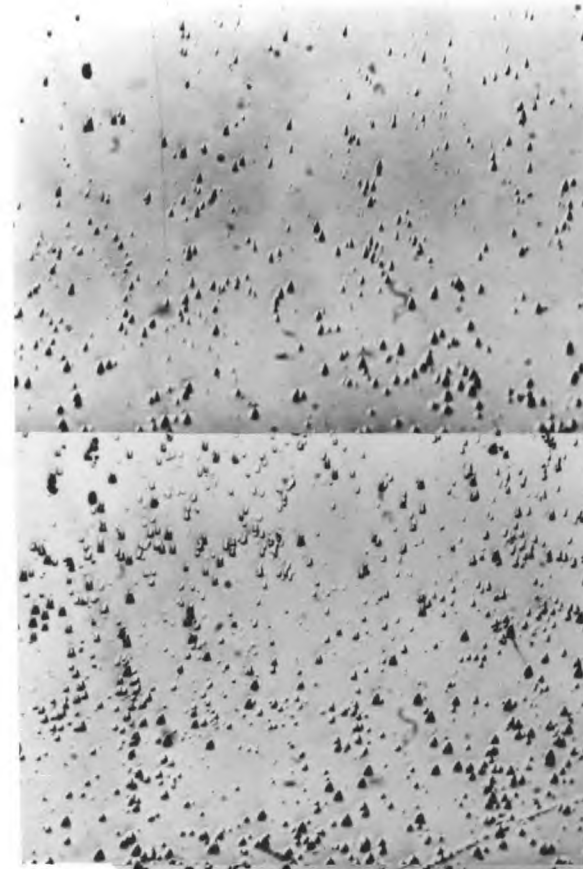

$1{\cdot}3 \times 10^{6}$ cm^{-2}

$1{\cdot}43 \times 10^{6}$ cm^{-2}

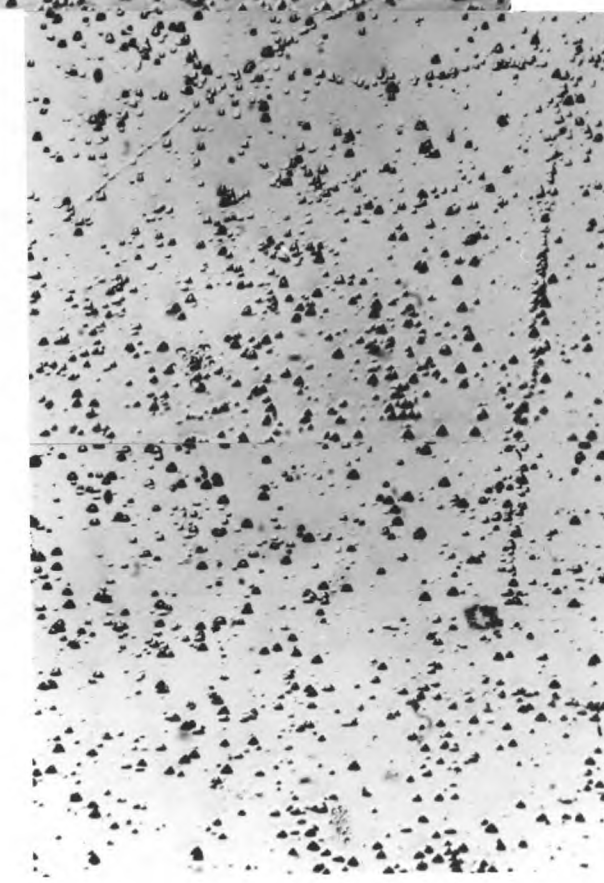

$1{\cdot}08 \times 10^{6}$ cm^{-2}

{111}

Fig. 3.8. Variation of the etch pit density with the plane of observation. Electrolytic etching. x150

CHAPTER 4

YIELDING AND STRAIN AGEING OF NIOBIUM SINGLE CRYSTALS

CHAPTER 4

4.1 Introduction

The majority of the previous work on the evaluation of purification effects has been carried out on commercial purity polycrystalline material. These types of studies might entail evaluating the effect of oxygen and carbon on the mechanical properties, but the base material of different workers would probably differ vastly in other impurity contents. Further confusion arose due to variation in strain rate, grain size and structural perfection within grains. Christian and Masters (1964) suggested that it was not sufficient to have the same grain size but that the same degree of lattice perfection was required in order to compare results.

Recently, however, very pure highly perfect single crystals have been grown using electron beam zone melting, and a subsequent heat treatment, and decarburization technique. This allowed a systematic study of the yielding and plastic flow behaviour of single crystals of controlled purity and orientation without involving the complicated problems of grain boundaries. The previous detailed studies on the effect of impurities on single crystals produced by electron beam zone melting, or subsequent hydrogen purification are due to Lawley et al (1962) on molybdenum, Koo (1963) on tungsten, Stein et al (1963), Stein and Low (1966) on iron and Stein (1967) on molybdenum. They have shown that increasing the number of zone passes which is effectively further purification, causes a large reduction in both the yield stress and its temperature dependence.

In the present work the variation of the yield drop, and the temperature dependence of the yield stress with increasing overall purity was investigated, and in addition, strain ageing experiments were carried out for identically orientated single crystals. The results are compared with the current theories of discontinuous yielding, solid solution hardening and strain ageing by interstitital impurities.

4.2 Effect of impurities on the yielding behaviour

4.2.1 Effect of impurities on the stress-strain behaviour

A pronounced effect of overall purity was observed on the stress-strain curves. The purer crystal which received a greater number of zone passes had appreciably lower proportional limit, upper and lower yield stress and flow stress than the less pure crystal.

Typical stress-strain curves of ⟨110⟩ oriented single crystals after various numbers of zone passes at 195° and 296°K are shown in Fig. 4.1 to illustrate common yield point phenomen. Generally, a pre-yield microstrain followed by a smooth yield drop at and below room temperature was observed and the subsequent work hardening was rather low and almost insensitive to the temperature. The onset of necking occurs at smaller strains with decreasing temperature. However, above room temperature, the yield point disappeared for all crystals and as the temperature was further increased the crystals showed a large uniform elongation. No twinning was observed for any of the crystals in this range of temperature between 77° to 373°K.

The most interesting observation is that the existence and magnitude of the yield drop and pre-yield microstrain are dependent on the number of zone passes which reflect the lowering of interstitial impurities by successive passes.

The values of the proportional limit are summarized in Table 4.1. This limit is defined as the value of the stress at which the first departure from linearity is observed.

4.2.2 Effect of impurities on the temperature dependence of proportional limit

The temperature dependence of the proportional limit of ⟨110⟩ and ⟨100⟩ oriented single crystals was determined from 77° to 373°K for various numbers of zone passes. These are plotted in Fig. 4.2 for ⟨110⟩ and Fig. 4.3 for ⟨100⟩ orientations. Increasing the number of zone passes, i.e. overall purity, causes

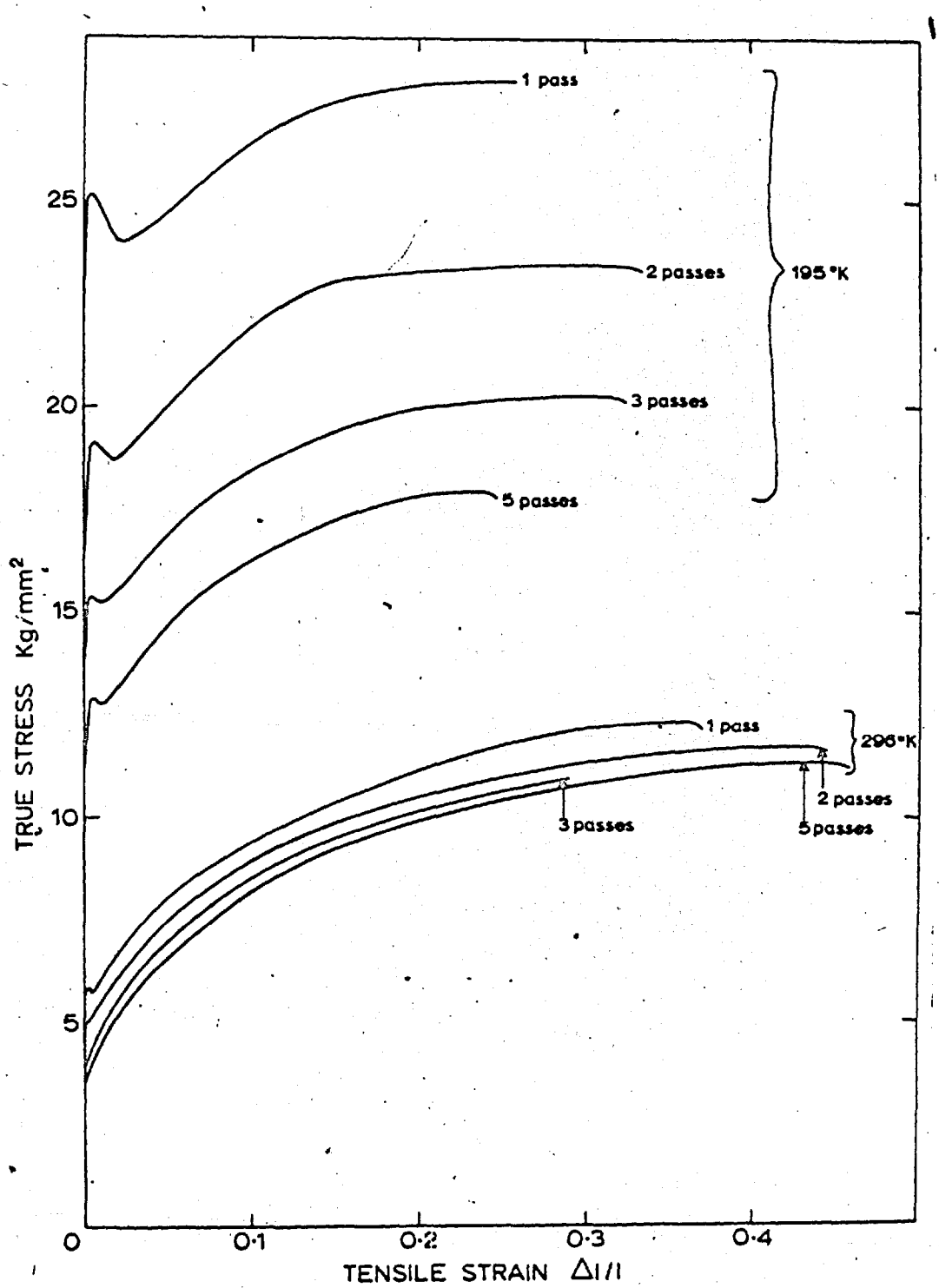

Fig.4-1. Tensile Stress Strain Curves of <110> Oriented Single Crystals with Varying Number of Zone Passes.

Table 4.1

Proportional limit of single crystals of ⟨110⟩ Orientation with various Numbers of Zone Passes

Temperature ^{o}K	Numbers of Zone passes	Proportional limit ($Kg\ mm^{2}$)	
373	1	3.18	2.95
	2	2.72	2.65
	3	2.63	2.59
	5	2.01	2.00
296	1	5.65	5.80
	2	4.57	4.66
	3	3.91	4.10
	5	3.24	3.55
273	1	6.44	6.10
	2	5.37	5.55
	3	5.16	5.00
	5	4.65	4.61
243	1	10.75	11.25
	2	9.50	8.70
	3	8.20	8.51
	5	7.50	7.30
195	1	22.0	17.62
	2	15.1	16.18
	3	13.3	13.70
	5	10.7	11.0
152	2	23.4	23.0
77	1	60.5	62.2
	2	52.5	55.2
	3	44.1	47.3
	5	42.25	42.0

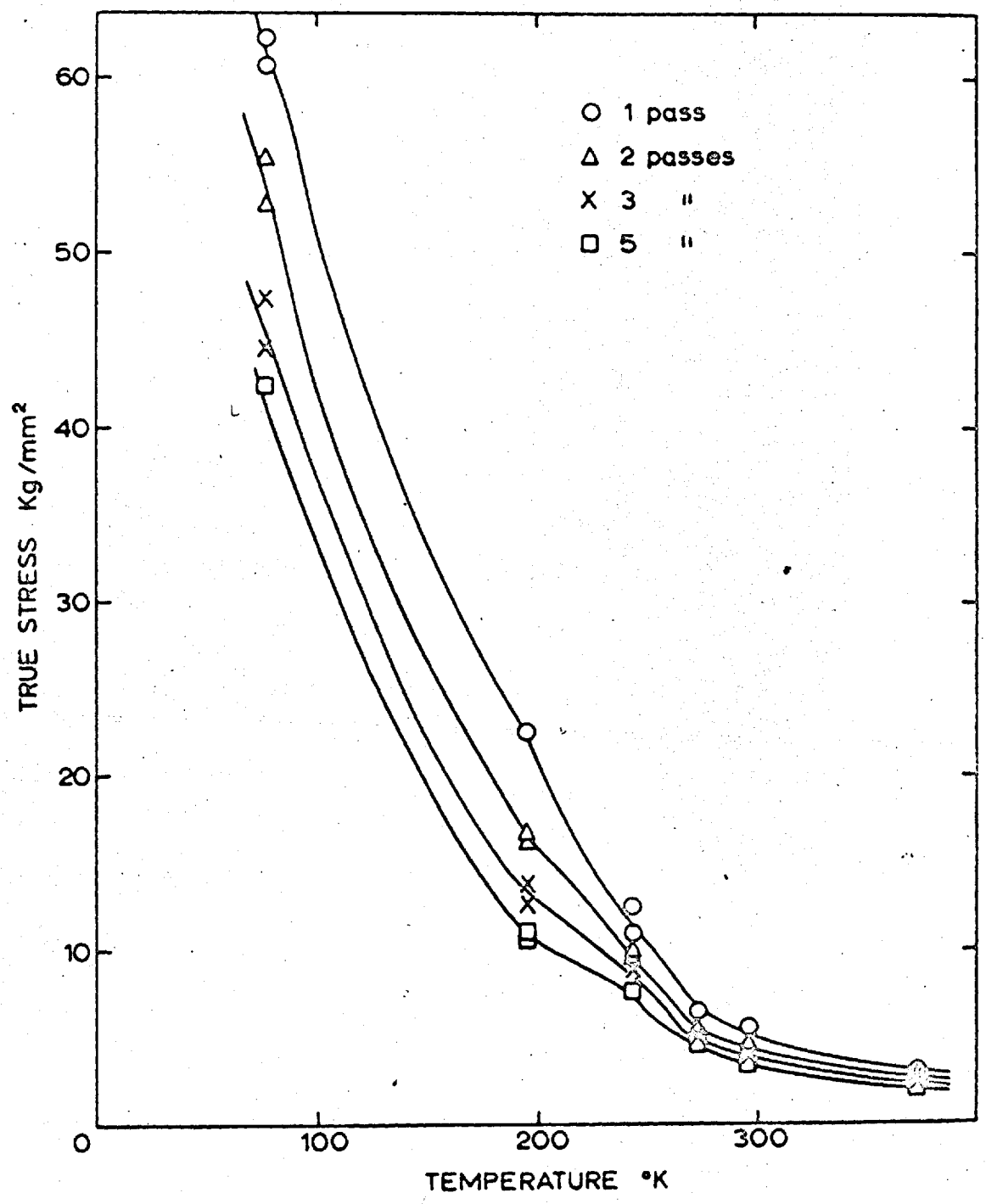

Fig.4-2. Temperature Dependence of the Yield Stress for Crystals with <110> Orientation with Varying Number of Zone Passes.

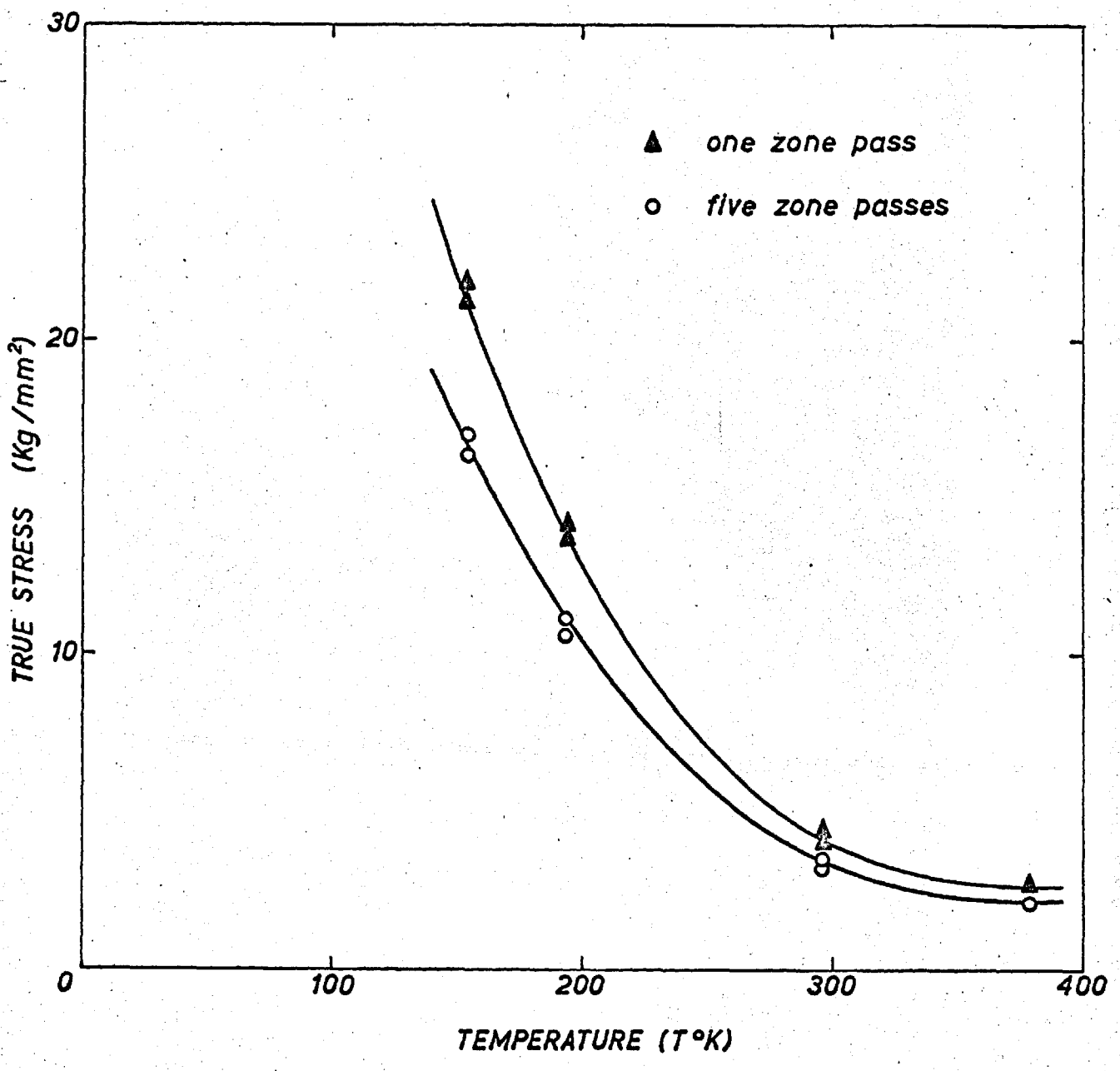

Fig.4-3. Temperature Dependence of the Yield Stress of Crystals with <100> Orientation with Varying Number of Zone Passes.

a significant decrease in the proportional limit and also the temperature dependence markedly below a transition temperature of 300°K.

This observation agrees with recent work of Lawley et al (1962) and Koo (1963) on electron beam melted single crystals of molybdenum and tungsten respectively. Similar results were also reported by Stein et al (1963) on iron crystals containing 0.005, 44, and 100-300 ppm carbon, and Stein (1967) on molybdenum single crystals prepared by electron beam melting and subsequent purification.

4.3 Discussion

4.3.1 Effect of impurity on the yielding behaviour

The yield point in polycrystalline b.c.c. metals is a well known effect which involves impurity atoms and is generally observed in metals containing traces of interstitial impurities such as carbon and nitrogen. It has been demonstrated by Low and Gensamer (1944) that the discontinuous yielding of polycrystalline iron occurs if it contains either of these elements. Schawartzbart and Low (1949) have shown that the presence of carbon in a single crystal of iron produces a yield point. However, a recent systematic study of orientation effects on the plastic deformation behaviour of electron beam melted tungsten (Argon and Maloof 1966, Carlick and Probst 1964, Rose et al 1962), molybdenum (Guiu and Pratt 1966), niobium (Votava 1964) and tantalum (Ferris et al 1961, Sherwood, private communication) has shown that the crystals yield discontinuously when the tensile axis is chosen along the <110> orientation. This observation suggests that the yield drop cannot be attributed merely to the presence of an impurity but that a crystallographic or geometric nature must also be considered because this phenomenon is observed in crystals with specific orientations. This orientation dependence of yielding behaviour will be presented in 5.3 and here we shall limit our discussion to the interstitial impurity effect on the discontinuous yielding.

As discussed in 1.2.1 and 1.2.2 three models have been

proposed to account for the presence of yield drop; by Cottrell(1963), Cottrell and Bilby (1949) who showed that solute atoms may lock dislocations in place, and by Johnston (1962) who demonstrated how yield drops may develop from the properties of moving dislocations. In Cottrell and Bilby's theory of yielding it is assumed that there is no dislocation motion until the upper yield point is reached and that there, some dislocations can break away from the impurity atmosphere and can continue to move at a lower stress, resulting in a sudden yield drop. In the present case of zone melted single crystals of niobium, there is, undoubtedly a sufficient number of impurity atoms to form an impurity atmosphere in spite of single or multiple zone passes. In crystals containing one atomic ppm of impurity in solid solution, and a dislocation density of 10^6 lines cm^{-2} which is common in zone melted single crystals, approximately 10^3 impurity atoms are available for each atom plane of dislocation. Shadler (1960) has found some evidence which suggests the unlocking of dislocations in zone melted tungsten single crystals.

Phenomenologically, the yielding behaviour and strain ageing experiments in the present work, agree with Cottrell and Bilby's prediction. The existence of a yield drop at low temperature, and the dependence of the magnitude of the yield drop on the overall purity are in agreement with the theory. In addition, Fig. 4.4 shows stronger temperature dependence of upper yield stress than lower yield stress and flow stress (because of low work-hardening, some of the flow stress data are not included). Similarly, a stronger temperature dependence of initial yielding (upper yield stress) than for the flow stress, is reported by Conrad and Schoeck (1960) for electrolytic iron and by Lawley et al (1962) for multiple zone passes molybdenum single crystals. Here, the initial yield stress is attributed to the Cottrell atmosphere phenomenon.

However, the large amounts of plastic strain which precede the upper yield point certainly indicate that many dislocations move prior to the upper yield point. The assumption which Cottrell and Bilby made that the number of mobile dislocations in the crystal is zero, cannot be correct because most of the crystals are handled and machined prior to testing. It is

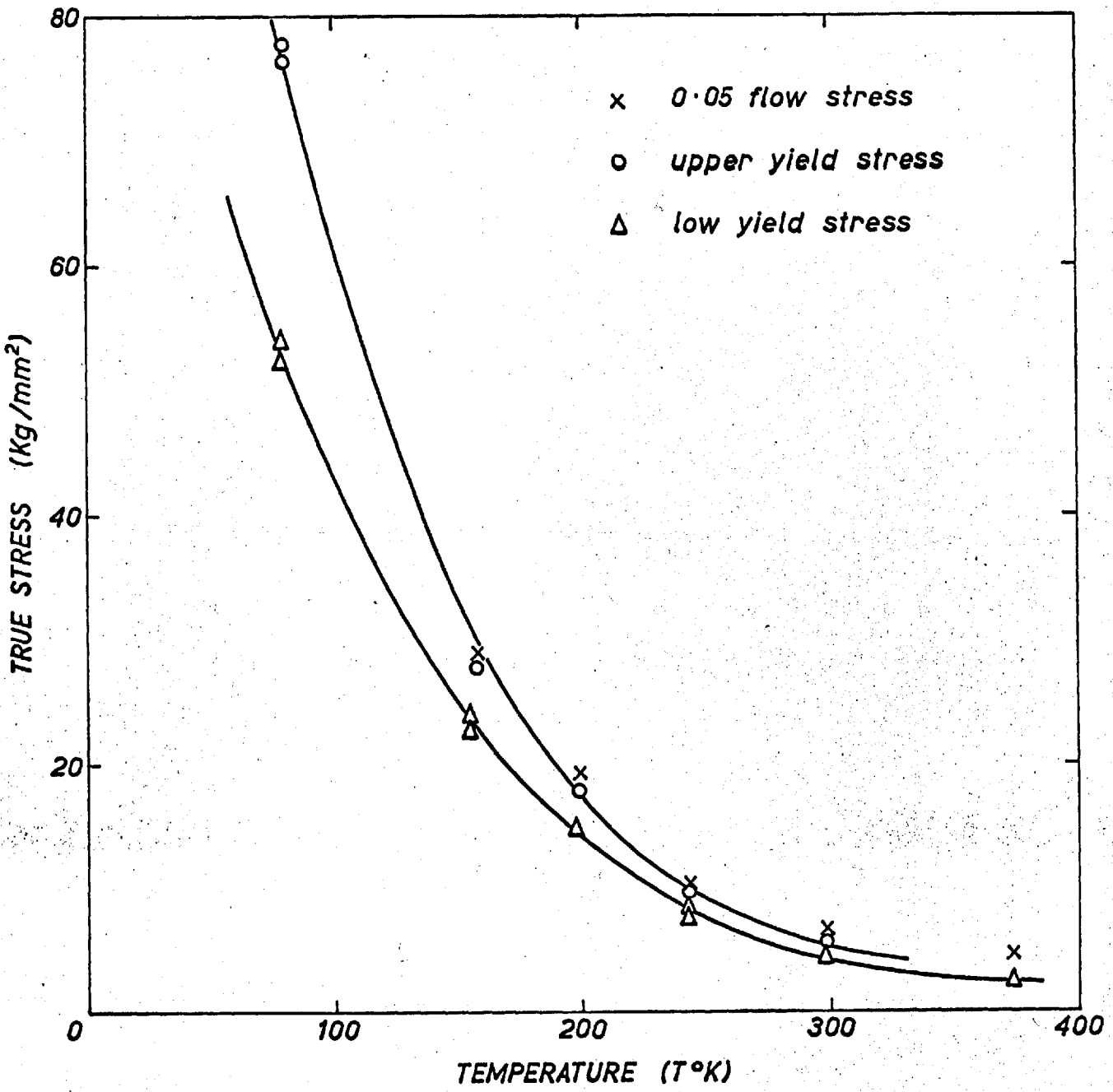

Fig.4-4. Temperature Dependence of the Low, Upper Yield Stress and 0.05% Flow Stress for <110> Oriented Single Crystals.

extremely difficult to handle most materials without introducing any dislocations. This assumption may be reasonable for the crystal after strain ageing treatment because all the dislocations have received the same ageing treatment and pinning may be either permanent or temporary, i.e. unpinning may occur at attainable stress or it may not. For further support, the current microstrain experiments by Brown and co-workers and Lawley and Meakin (1966a, 1966b) at the region of 10^{-6} plastic strain, provides sufficient evidence for dislocation motion well below the proportional limit.

The model of Johnston (1962), Johnston and Gilman (1959) which was later extended by Hahn (1962) for many b.c.c. metals, is based on the dynamic properties of the dislocations and their rate of work hardening. Equation (1.8) is able to account for many features of the deformation behaviour of b.c.c. metals. At the moment, we can deal conveniently with one of these features, namely the yield point itself.

On Hahn's model, a sudden yield drop is a consequence of (a) the small number of mobile dislocations initially present (b) large a, (c) small m in equation 1.8. This treatment also suffers some difficulties. In view of the large number of grown-in dislocations usually present in b.c.c. metals, 10^6 - 10^8 cm^{-2}, it is suggested that impurity locking immobilizes them in order to satisfy the first requirement. To be consistent ρ_o, by definition of ρ equation 1.3, would immediately fix L_o as in a tenth of ρ_o normally a high value. If grown-in dislocations are locked, the L_o would be too high.

In his revised theory, Cottrell (1963) suggested that a yield drop could occur if one of three conditions was satisfied: the first condition $\rho_o = 0$ is not relevant to the present case, and the second condition $L_o = 0$, $\rho_o > 0$ is the same requirement which Hahn made. The third condition, namely that $L_o > 0$ is relevant to the present case, and in this requirement it is not necessary to have a total absence of dislocations initially, but it is required for them to be either weakly or strongly pinned. Yielding takes place when the initial dislocation

becomes unpinned, or in the case of strong pinning, when dislocations are created at the upper yield point. Thus, Cottrell distinguishes, as do Gilman and Johnston, between yielding by creation and yielding by multiplication of dislocations with the reservation that unpinning in the creation process need not occur if locking is strong. This phenomenon, in which dislocations begin to move at the upper yield stress, is not likely to occur often unless all dislocations are pinned in a strain aged crystal. However, the present observations cannot be explained using either of the proposed models.

The experiment in which the yield drop at low temperatures becomes more pronounced as the overall purity is decreased, suggests a possible difference in the initial dislocation density in the crystals of differing purities. If we assume that the stress dependence of the dislocation velocity is unaffected by impurity, then conceivably this could affect the proportional limit, The major role of an impurity can be proposed as a pinning obstacle reducing the number of mobile dislocations. Therefore, the present observations suggest that thermal unpinning must take place at a stress below the upper yield point, and then the further behaviour of the crystals is controlled by a multiplication mechanism. However, both models fail to explain the orientation dependence of the yielding behaviour. While still in a speculative mood, we shall present further evidence in the next paragraph on the temperature dependence of the yield stress.

4.3.2 Effect of impurity on the temperature dependence of the yield stress

In order to compare the observed magnitude of strengthening by impurity with theoretical predictions, it is essential to know the amount and kind of impurities in the crystals. Currently, vacuum diffusion, a spectrography, electrical resistivity and resistivity ratio measurements have been widely used as analysis techniques. These techniques still do not give a reliable analysis, for instance, Lawley et al (1962), starting from 99.95% purity of molybdenum, found an increase in purity to 99.995% after single zone pass but no further increase after six

zone passes. This is most likely due to a lack of sensitivity of the analysis techniques since six zone pass crystals showed significantly different mechanical properties. Bowen et al (1967) reported the increase in the resistivity ratio $\frac{R_{273^oK}}{R_{4.2^oK}}$ from 200 to 1400 between zone melted and subsequent heat treatment. This method has a definite advantage over the other methods, because it is non-destructive, and one can eliminate a possibility of introducing a specimen shape factor that might enter into resistivity measurements. However, this method does not tell which solute contributes most effectively to the temperature independent part of the resistivity and neglects any contribution from lattice imperfections. Because of the difficulty and uncertainty in the estimation of amount and kind of impurities in the crystal it is extremely difficult to make a quantitative discussion and comparison with various proposed solid solution hardening theories.

Koo (1963) has estimated the difference in the amount of interstitial impurities in solid solution of tungsten single crystals of one and five zone passes as 4 ppm of carbon from electrical resistivity measurements and this estimate was used to calculate the magnitude of strengthening predicted by various solution hardening theories.

TABLE 4.2

Cracknell and Petch	(1955)	0.011 Kg/mm^2
Schoeck and Seeger	(1959)	0.047 Kg/mm^2
Fleischer	(1962)	1.846 Kg/mm^2

Fleischer's theory gives the highest magnitude of strengthening but even this indicated value is at least one order of magnitude smaller than the observed value of strengthening of 28.4 Kg/mm^2. Stein et al (1963) and Stein and Low (1966) have used radioactive tracer techniques to analyse the carbon content in radioactively carburized and then decarburized iron and once again the strengthening was substantially higher than indicated

by any of the proposed theories. Although strengthening is usually attributed to the interstitial impurities in a solid solution for all b.c.c. metals, the above discrepanc shows that the real observed strengthening cannot be accounted for by the current theories of strengthening based on the elastic interaction of dislocations with interstitial impurities.

With regard to the temperature dependence of the yield stress, as shown in Fig. 4.2 and 4.3, there exists a very large difference in the value of yield stress and its temperature dependence between pure and less pure niobium single crystals of identical orientations in the temperature range 77^{o} - 300^{o}K. It appears to be a general trend in b.c.c. metals that the decrease in the temperature dependence of the yield stress may result upon decreasing the impurity level beyond a certain level. This effect was found by Lawley et al (1962) and Koo (1963) on electron beam melted molybdenum and tungsten, and Stein et al (1963) and Stein and Low (1966) on decarburized iron, and Stein (1967) on zone melted and hydrogen-purified molybdenum. All these results agree with the present observation down to 77^{o}K. However, there is a contradictory observation. Keh and Nakada (1967) found that by adding interstitials (C + N) to purified iron, the athermal part of the yield stress of iron is raised but its temperature dependence is not altered, but they found the same reduced temperature dependence when they plotted their results for proportional limit against temperature.

Christian and Masters (1964) and Christian and Taylor (1965) also report the same temperature dependence for commercial purity polycrystalline niobium of 115 HV and 150 HV, and zone melted and subsequently heat-treated niobium. In the case of Keh and Nakada it was considered that orientation effects on the yield stress and yield stress criterion may be the reasons for this discrepancy. There is no reason to believe that the orientation effect should be dependent on the interstitial contents. In the present work Fig. 4.3 shows an apparently decreased temperature dependence for purer crystals in the $\langle 100 \rangle$ oriented single crystal and this decreased temperature dependence is common to all orientations. With respect to the yield stress criterion they believe

that, in order to measure the true effect of interstitials on the lattice friction stress; the lower yield stress is a better criterion, Schadler (1964) however has demonstrated that the temperature dependence of the proportional limit yield stress most accurately represents the temperature dependence of the dislocation mobility in tungsten. In fact, Lawley et al (1962) found the same effect for the flow stress at 2% plastic flow stress and Stein and Low (1966) found a more pronounced effect when they plotted the yield stress instead of proportional limit.

The results of Lawley et al (1962) at least down to 77°K, indicate that Cottrell-Bilby's locking may give an important temperature dependent contribution to the yield stress. However, the steep increase in the yield stress actually exceeds that for the less pure crystal, indicate a more complex situation. Lawley et al suggested the more rapid fall-off in yield stress with temperature for the purer crystal may be due to differences in factors in the rate equation:

$$\dot{\varepsilon} = N A b \nu e^{-U/kT} \qquad (4.1)$$

where $\dot{\varepsilon}$ is the strain rate, N is the number of active sites per unit volume, A is the area swept out by a dislocation per successful fluctuation, b is the Burgers vector, ν is the frequency factor, and U is the activation energy. Re-writing and noting that U is the difference in the total energy to overcome the barrier U_o and the work done by applied stress W in overcoming the barrier,

$$W = U_o - kT \log N A b \nu_o/\dot{\varepsilon} \qquad (4.2)$$

It is clear from the above equation that the pure and less pure crystal will have the same stress at 0°K if the U_o values are the same. Similarly, if the number of active sites or the strain per fluctuation Ab is larger for the purer crystal, this would also result in a more rapid increase in yield stress with decreasing temperature. This latter requirement is included in the overcoming of the Peierls-Nabarro barrier. The preceding situation is not anticipated on the simple basis of Cottrell-Bilby's atmosphere dilution on purification which Lawley et al were in

favour of, since here we expect a lowering of U_o and consequently of the yield stressat 0^oK.

So far five models have been proposed to describe the interaction of dislocations with randomly distributed stress centres due to solute atoms and other defects. The separation of these models should be possible through the effect of solute concentration on flow stress with temperature.

The models of Mott and Nabarro (1948), Seeger (1958) and Friedel (1963) lead to a proportionality between flow stress and conentration c, whereas Fleischer (1962) and Gilman's model (1965) requires a proportionality between τ and $c^{\frac{1}{2}}$

With regard to the temperature dependence of flow stress, Friedel's model leads to a linear decrease of τ with T, Mott and Nabarro's model gives a linear decrease of τ with $T^{2/3}$. Seeger's model predicts a linearity between $\tau^{2/3}$ and $T^{2/3}$. However, these predictions have never been reported as applicable to the b.c.c. metals. As an example of lack of applicability of Mott and Nabarro's model (1948), as used by Seeger (1958), Fig. 4.5 plots $\tau^{2/3}$ against $T^{2/3}$ for one and five zone passes niobium single crystals of ⟨110⟩ orientation in tension. The lack of linearity in this plot indicates that the parabolic force distance relationship which was assumed by Mott and Nabarro (1948), and Seeger (1958), does not apply in the present case.

In the following section, the other two models, Fleischer (1962) and Gilman (1965), will be discussed in detail.

The distinctive feature of the interstitial impurities in b.c.c. metals is the large lattice distortion which causes rapid hardening. Fleischer (1962a, 1962b) assumed that a dislocation moving on a slip plane interacted strongly only with those defects lying within one atom spacing of the glide plane. The interaction energy of the defect at the dislocations was calculated by the method described by Cochardt et al (1955). The stress to move a dislocation an appreciable distance at 0^oK corresponds to the stress required to overcome the maximum retarding

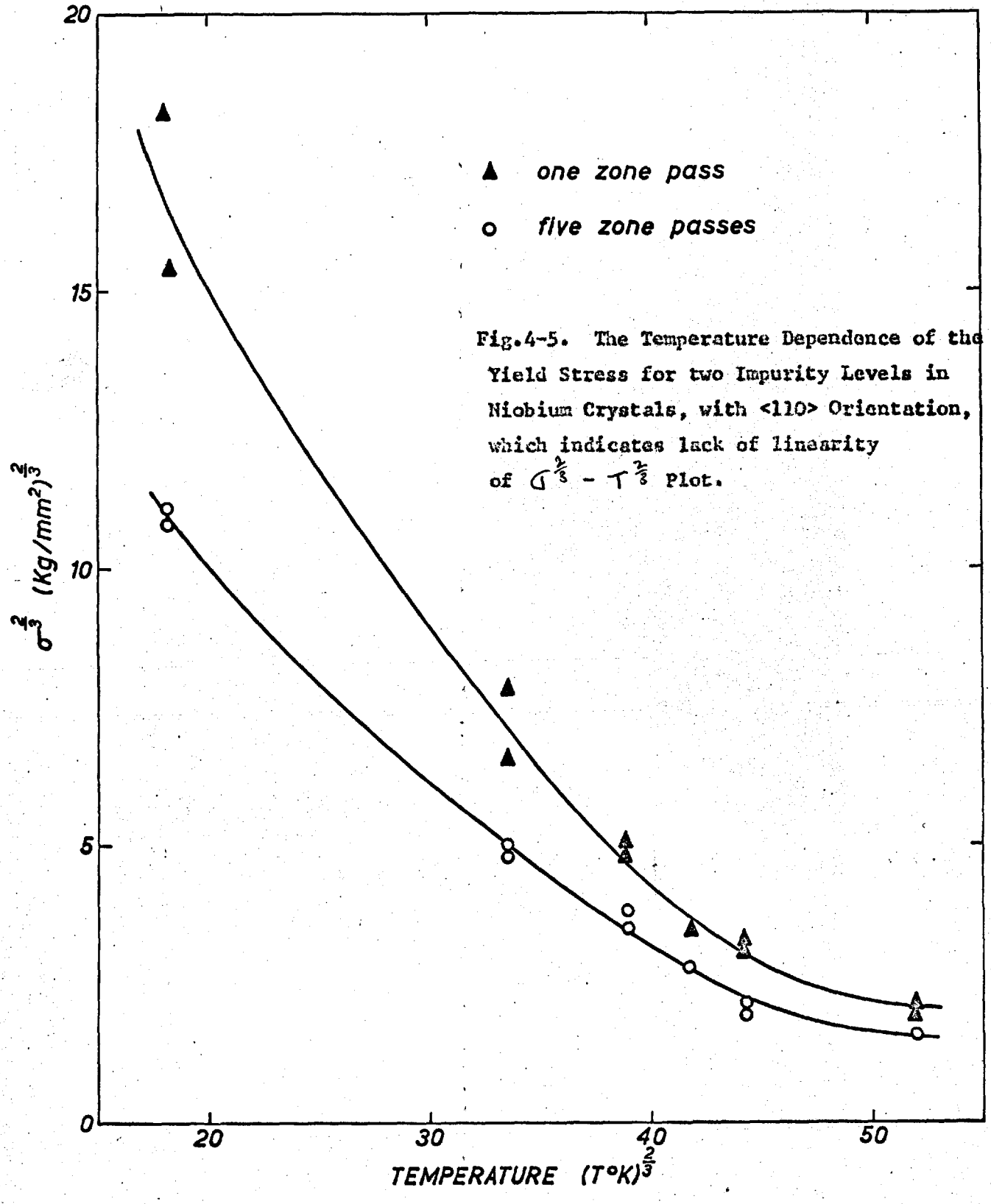

Fig.4-5. The Temperature Dependence of the Yield Stress for two Impurity Levels in Niobium Crystals, with <110> Orientation, which indicates lack of linearity of $\sigma^{\frac{2}{3}} - T^{\frac{2}{3}}$ Plot.

force exerted on the moving dislocations by the defects. At a finite temperature the dislocations can move at lower stress because the motion is thermally activated. He used an approximate force-distance relationship for tetragonal lattice distortion to calculate that the impurity hardening depends on the temperature according to the relation:

$$(\tau/\tau_o)^{\frac{1}{2}} = 1 - (T/T_o)^{\frac{1}{2}} \qquad (4.3)$$

where $\tau_o = F_o/bL = G\,\Delta\varepsilon\, c^{\frac{1}{2}}/3.3$ is the yield stress at T_o (0^oK), τ is the yield stress at T^oK.

This equation predicts a linear relationship between $\sigma^{\frac{1}{2}}$ and $T^{\frac{1}{2}}$ but this prediction does not hold in the present case, as shown in Fig. 4.6, where $\sigma^{\frac{1}{2}}$ is plotted against $T^{\frac{1}{2}}$ for one and five zone passes single crystals of niobium of $\langle 110 \rangle$ orientation. The experimental observation fails to fall on a straight line and therefore his assumption is inappropriate for the present case. However, Stein and Low (1966) found a reasonably good agreement between this theory concerning the role of carbon impurity on the yield stress, the temperature dependence of the yield stress and interaction strength of dislocations with carbon contents in their decarburized ultra pure iron single crystals.

Fig. 4.7 illustrates that the present results were found to be a best fit to the straight line when logarithm yield stress was plotted against temperature and within the accuracy of the data the points can be fitted with an expression of the form:

$$\sigma = A\, e^{-BT} \qquad (4.4)$$

The difference between the yield stress of the one and five zone passes crystal should reflect the impurity contribution to the yield stress. This difference is plotted in Fig. 4.8 and also can be fitted with the form:

$$\Delta\sigma \sim e^{-BT} \qquad (4.5)$$

This expression has been used previously by Johnston and

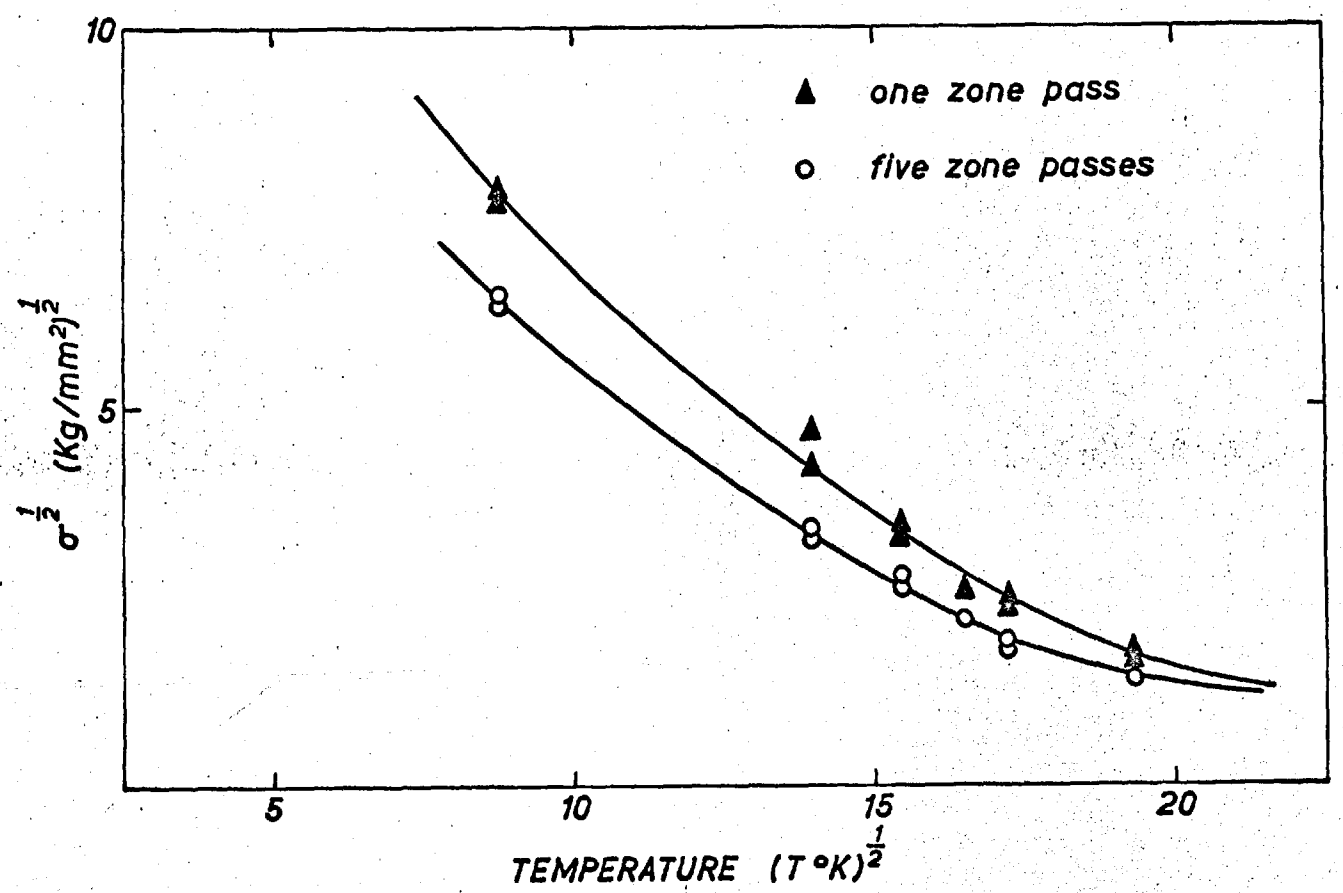

Fig.4-6. The Temperature Dependence of the Yield Stress for two Impurity Levels in Niobium Crystals with <110> Orientation, which indicates lack of Linearity of $\sigma^{\frac{1}{2}} - T^{\frac{1}{2}}$ plot.

Gilman (1957) and Johnston (1962) to fit the flow stress of pure and impure lithium fluoride single crystal. Later, Gilman (1965) clarified the pre-exponential A in equation 4.4 by applying reaction rate theory to dislocation mobility, where the activation energy is inversely proportional to the applied stress, so the dislocation velocity is related to the applied stress. The probability of a successful nucleation event is proportional to:

$$e^{-U^*/KT} \qquad (4.6)$$

where $U^* = W X C^{\frac{1}{2}}/b\tau$ is the activation energy including interaction between dislocation with defect (C) and the applied stress and Burgers' vector b is in the denominator. k is Boltzman's constant, and T is the temperature.

The glide nucleation rate $\dot{g}$ is given

$$\dot{g} = \left(\frac{KT}{h}\right) e^{-f^*/KT} \left[\exp\left(-\frac{WXC^{\frac{1}{2}}}{b\tau KT}\right)\right] \qquad (4.7)$$

where h is Planck's constant, and f^* is the vibrational free energy minus the energy of the translational mode that carries it across the saddle point. At constant temperature equation 4.7 takes the form

$$\dot{g} \sim e^{-D/\tau} \qquad (4.8)$$

where D is the characteristic drag stress. This form is consistent with the observed stress dependence of dislocation velocities. When $\dot{g}$ is constant, the flow rate is constant for a fixed dislocation density and this determines the flow stress in a constant strain rate test. Gilman stated that constancy of $\dot{g}$ means $\log T - KT\,(WXC^{\frac{1}{2}}/b - f^*)$ has a fixed value of $\log \phi$ However, this is incorrect, this should be corrected to $\log T - \frac{1}{KT}\left(\frac{WXC^{\frac{1}{2}}}{b\tau} - f^*\right)$. He gives the final form:

$$\tau_y = \left[\frac{A_o}{f^* + KT \log (T/\phi)}\right] e^{-BT} \qquad (4.9)$$

where $A_o = (WX)_o C^{\frac{1}{2}}/b$ which indicate the interaction between dislocations and defects at 0^oK.

The dominant term in equation 4.9 is the expondential one,

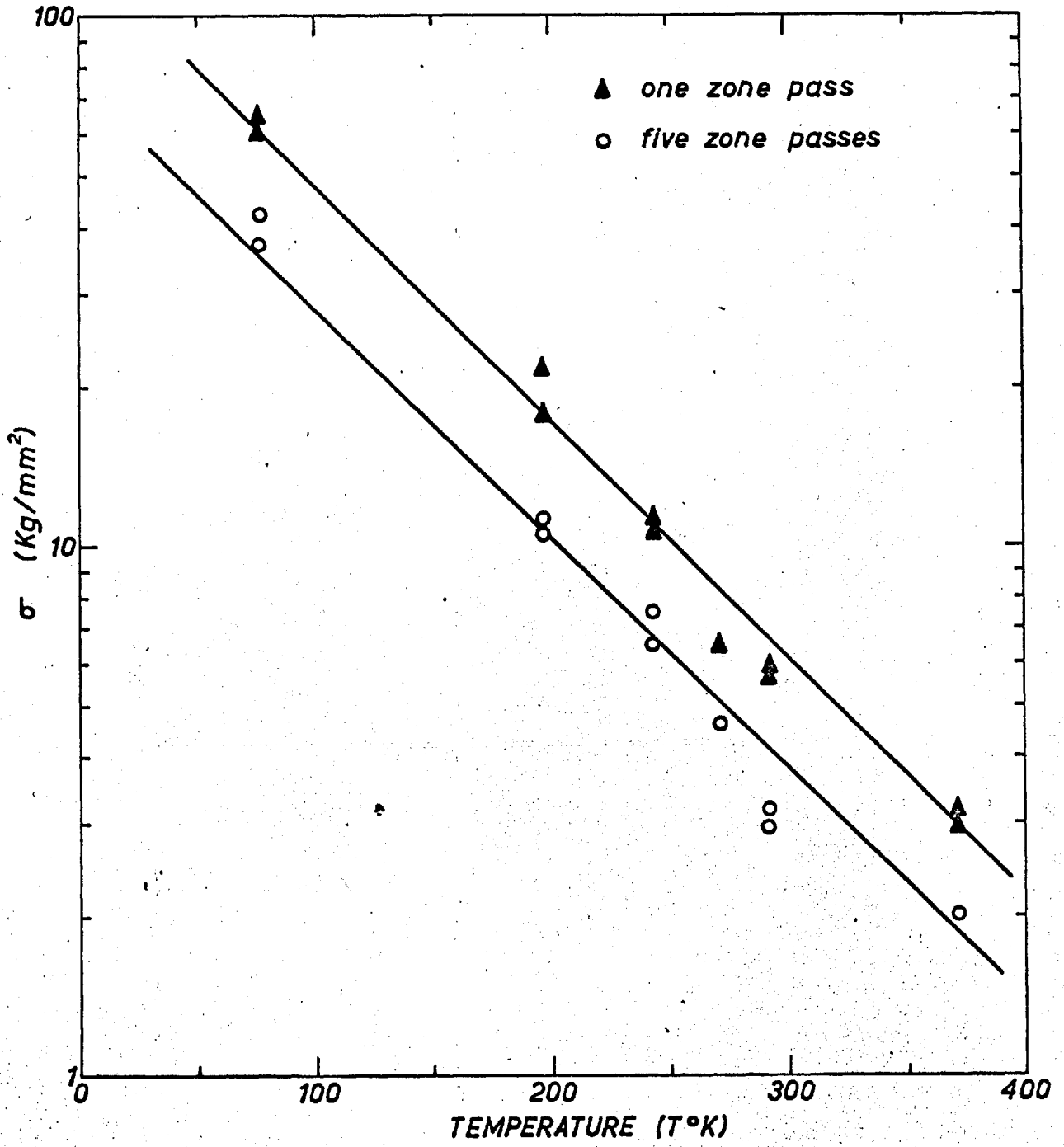

Fig.4-7. Exponential Temperature Dependence of the Yield Stress for two Impurity Levels in Niobium Crystals with <110> Orientation.

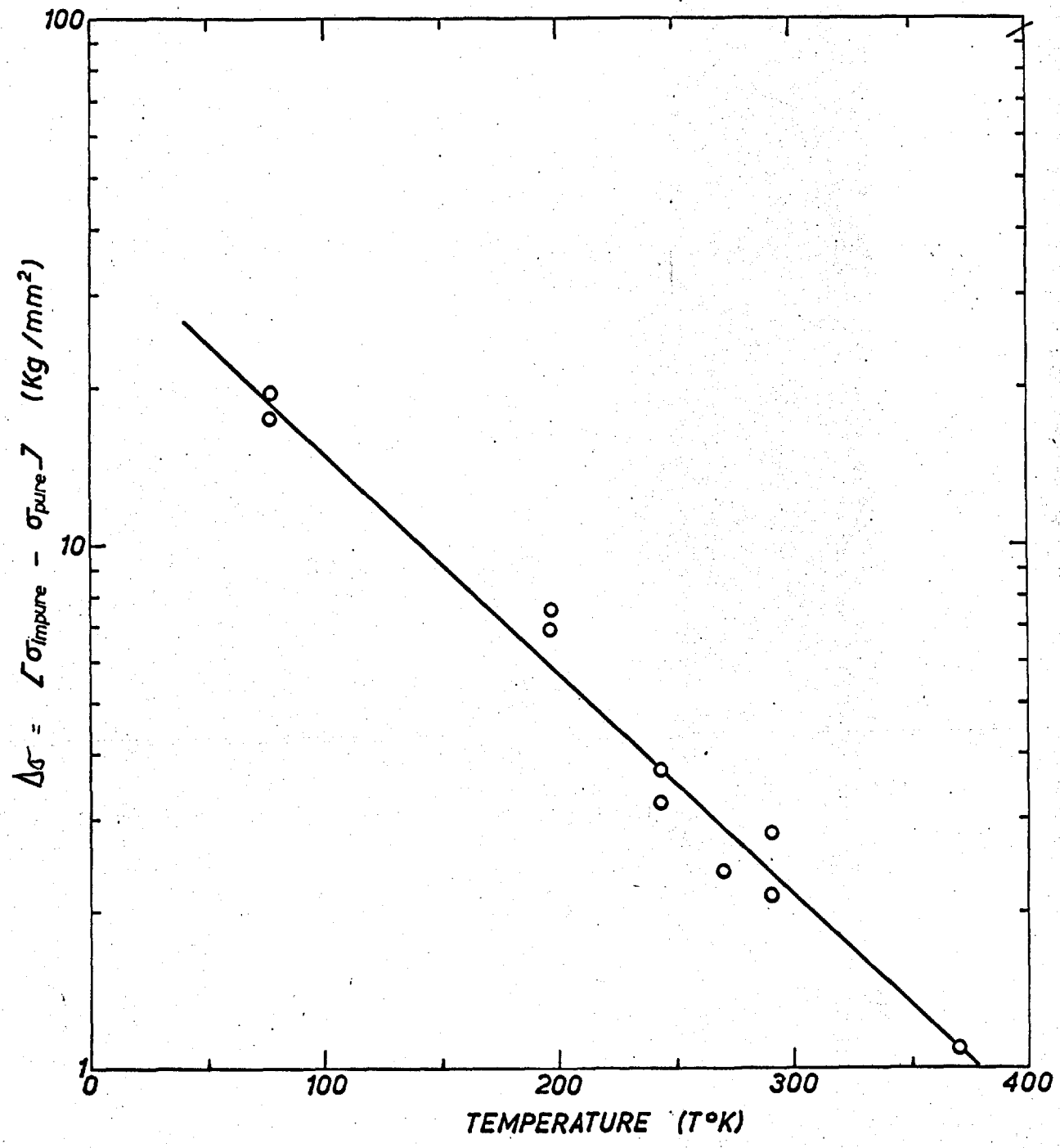

Fig.4-8. Exponential Temperature Dependence of the Impurity Contribution to the Yield Stress. $\Delta\sigma$ is the Difference between that for pure and less pure Crystals with <110> Orientation.

as $T \rightarrow 0^{\circ}K$, $\tau_y \rightarrow A_0/f$ and depends on the defect-dislocation interaction. This is an analogous expression to the equation of stress to produce a constant dislocation velocity $V = Ae^{-BT}$, which was found experimentally in lithium fluoride (Johnston and Gilman 1957). A similar linear dependence of log flow stress on the temperature was observed by Gilman and Johnston (1957), Johnston (1962) and Westbrook (1953) on lithium fluoride single crystals.

This equation is based on two basic assumptions: firstly that the yield stress is proportional to the square root of defect concentration. There is a considerable amount of experimental data to justify this assumption. Fleischer (1962) and Fleischer and Hibbard (1963) and Fleischer (1967) have evaluated the effect of varying the concentration of the interstitial impurities in b.c.c. metals. They found that in Wert's data (1950) for iron with 0.025 up to 2500 ppm carbon, Stein and Low's data (1966) for iron with 0.0025 up to 250 ppm and Evan's data (1962) for nitrogen in niobium with 400 up to 2200 ppm the yield stress monotonically increases as the square root of the concentration.

Secondly, the main effect of point defects is to increase the quasi-viscous drag on moving dislocations, which means a change in D in equation 4.8. This equation is not theoretically based, but gives a good representation of experimental results in which the velocity of dislocations are measured by etch pit techniques (Johnston and Gilman 1959, Stein and Low 1960, Chaudhuri et al 1962, Schadler 1960). There is a certain criticism about the use of Arrhenius type of rate equation (Christian 1964) because the temperature dependence was less well described than the stress dependence in this kind of equation. There is also a limitation in this equation. For example, Stein and Low (1960) plotted $\log v$ against $\frac{1}{T}$ at constant stress. These plots were straight lines at low stress but were curved at high stresses. Christian (1964) considered two possibilities for this discrepancy, one is that the actual rate-equation would be more complex than the present one, the other is that the use of equation $v = \left(\frac{\tau}{\tau_0}\right)^m$ the velocity is a function of stress. He was inclined to believe

in the second possibility. In the expression of the form of $\sigma = Ae^{-BT}$ both A and B are adjustable parameters, therefore there is a large range of possible adjustment. In fact Conrad (1961) and Conrad and Prekel (1967) have shown that the dislocation velocity measurement in silicon iron (Stein and Low 1960) and their measurement in molybdenum, agrees reasonably with the usual interpretation of the Peierls Nabarro mechanism for the temperature dependence of flow stress using

$$\dot{\varepsilon} = N A b \nu e^{-U/KT}$$

However, the main and most important difference between Gilman's model and the Peierls Nabarro mechanism is that in the former the limiting value $A_o = (WX)_o C^{\frac{1}{2}}/b$ is dependent on the concentration of impurities. C, W and X are interaction energies with impurities per unit length of dislocation, whereas the latter model is essentially impurity independent.

As discussed in the preceding paragraph, the yielding behaviour and yield stress are dependant on such parameters as density of initial mobile dislocations, the mobility of dislocations and the rate of work hardening. The measured yield stress will reflect the behaviour if we understand precisely how these parameters come into play or if we can make some empirical relationship between the measured yield stress and the fundamental properties of dislocation behaviour. In this sense, this model has an advantage over any other existing model for both yielding behaviour and temperature dependence of the yield stress.

4.3.3 Activation parameters

Many previous workers came to the conclusion that a Peierls Nabarro mechanism controls the thermally activated deformation process in b.c.c. metals. This conclusion was reached through the analysis of the parameters of the rate controlling process, such as activation energy H, activation volume V, and pre-exponential factor $\dot{\varepsilon}_o$ in the following equation

$$\dot{\varepsilon} = \dot{\varepsilon}_o \exp\left(-\frac{\Delta G}{KT}\right) \qquad (4.10)$$

$\dot{\varepsilon}_o = \rho b S \nu$

ρ = mobile dislocation density

b = Burgers vector

S = Average distance of dislocation after every successful fluctuation

G = Change of free energy

The activation energy H and volume V can be calculated using the following equation (Conrad 1961, Conrad and Hayes 1963):

$$-\frac{\Delta H}{KT} = \left(\frac{\delta \log \dot{\varepsilon}}{\delta \tau}\right)_T \left(\frac{\delta \tau}{\delta T}\right)_{\dot{\varepsilon}} \qquad (4.11)$$

Where $\left(\frac{\delta \log \dot{\varepsilon}}{\delta \tau^*}\right)_T$ is the strain rate sensitivity which can be determined by either stress relaxation (Guiu and Pratt 1964, Sargent 1965) strain rate cycling or strain rate dependence of the yield stress (Conrad 1961, 1963, Conrad and Hayes 1963) and τ^* is effective stress on dislocation.

From comprehensive analysis of the existing experimental data Conrad (1961) and Conrad and Hayes (1963) have found that the value of activation energy and volume with stress and strain for many b.c.c. metals is virtually independent of the purity, dislocation structure and of whether yielding or flow was considered. A similar conclusion was reached by Basinski and Christian (1960) and Christian and Masters (1964) after an analysis of their results on iron, niobium, tantalum and vanadium.

However, some of the evidence that Conrad (1963) has collected against other specific mechanisms is not substantiated by other results. For example, the work of Mordike and Haasen (1962) on iron single crystals showed that both activation energy and volume were structure sensitive. Morkike's work on tantalum (1962) and Rose et al (1962) on tungsten favours the conservative motion of jogs in screw dislocation. On the other hand, the work of Gregory (1963), Gregory et al (1963) and Guiu and Pratt (1966) on niobium and molybdenum favour a non-conservative movement of jogs as the rate-controlling mechanism.

One of the main features for the Peierls Nabarro mechanism is a very large value of activation volume at low stress and its independence of impurity contents and dislocation structure. The present work on niobium and the recent work of Stein et al (1963), Stein and Low (1966) on iron, Stein (1967) on molybdenum, and Koo (1963) on tungsten, Lawley et al (1962) on molybdenum suggest that temperature dependence of the yield stress has indicated a strong function of impurity content. These observations leave substantial doubt as to the conclusion reached previously that impurity has no effect on the activation parameters for low temperature deformation of b.c.c. metals.

Here, the strain rate cycling experiment was performed with an Instron Testing machine by altering the strain rate by a factor of 10. All experiments were conducted using a cross head speed of 0.05 at slow strain rate and 0.5 cm/min at fast strain rate. In Fig.4.9 the true stress changes due to strain rate change are plotted against true stress for niobium single crystals of ⟨110⟩ oriented, one and three zone passes at 243° and 296°K. The shear stress is resolved on the system with the largest Schmid factor, which in this case is 0.471. It was observed that $\Delta\tau$ was decreased with increasing stress and the difference between these two crystals was hardly detectable at 296°K, however, at 243°K the impure crystal exhibited a larger strain rate sensitivity than the purer crystal. Christian (1964) suggested that the better way of presenting strain rate cycling data was to plot $\Delta\tau$ as a function of stress. In this way, one would effectively remove the work hardening contribution and would be more clearly representative of the sensitivity of dislocation velocity to stress as a function of strain. He reported many examples of b.c.c. metals that exhibit a constant value of $\Delta\tau$ as a function of stress or strain. This effect was taken to support the position that yielding and flow behaviour in b.c.c. metals is controlled by a single thermally activated process. However, as in Fig. 4.9, in the present work it was found that $\Delta\tau$ was decreased with strain, and the impure crystal had a larger strain rate sensitivity at the same stress. This suggests that the prediction based on a single thermally activated process is not valid, and reaffirms the importance of impurity content in the yielding and flow behaviour.

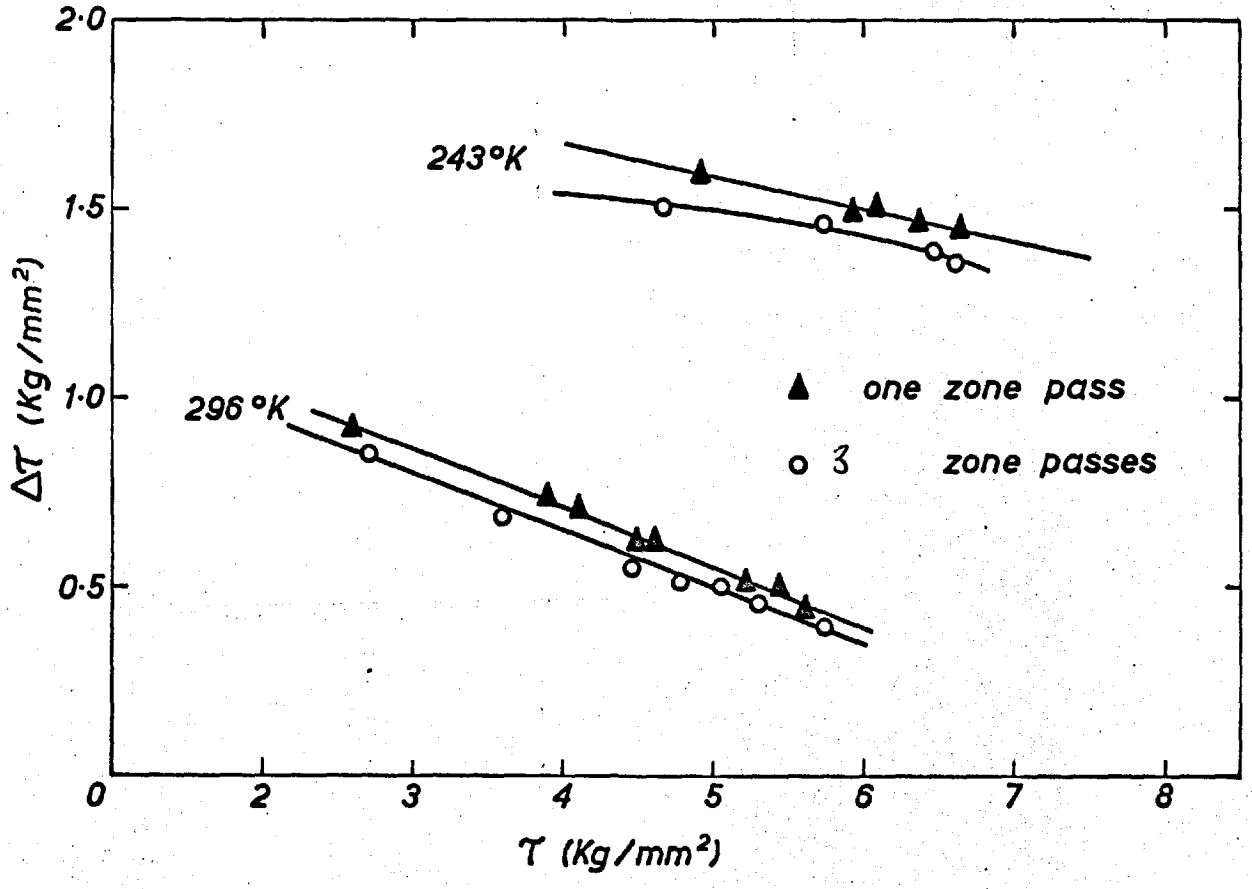

Fig.4-9. Shear Stress Change for a Factor of 10 in Strain Rate as a Function of Shear Stress.

The activation volume and energy for yielding at 296°K are summarized in Table 4.3.

TABLE 4.3

Activation volume of yielding at 296°K

Number of zone passes	Activation volume
1	41.02 b^3
2	48.3 b^3
6	74.1 b^3

Table 4.3 shows that the purer crystal has a larger activation volume and this is in agreement with the results of Mordike and Haasen (1962) on iron, and Stein and Low (1966 at 195°K on iron. Mordike and Haasen studied iron single crystals containing 30 ppm carbon and 50 ppm nitrogen, and found the variation of activation volume with imprutiy is consistent with a mechanism in which small carbide particles determine the activation volume for yielding and flow. Stein (1966) observed an unusual behaviour at 298°K, where the impure crystal has less strain sensitivity, corresponding to a larger activation volume than the pure crystal. They suggested that either more than one mechanism was controlling the deformation process or that a single mechanism, purity dependent, such as solid solution hardening or dispersion hardening was occurring. However, they failed to observe any kind of precipitate formation by electron microscopy for their ultra pure iron crystal. In contrast, Keh and Nakada (1967) recently reported that in iron single crystals the value of the activation volume for various contents of (C + N) impurities deformed at 77°K was nearly constant and independent of nitrogen content. This discrepancy between the present observation and that of Keh and Nakada may be attributed to the sensitivity of the activation volume in the high stress (or low temperature) region.

Another strong argument for the Peierls Nabarro mechanism is the yield stress at 0°K. If a Peierls Nabarro mechanism is

indeed a single thermally activated controlling mechanism, all the yield stresses of the various impurity level of crystal should merge at $0^{\circ}K$. In the present case the tensile tests have been conducted down to $77^{\circ}K$ so the trend is not clear, however, the work of Stein and Low (1966) on iron and Stein (1967) on molybdenum apparently shows that there exists a large daviation between pure and less pure crystals, at $20^{\circ}K$. It is unlikely that these curves can extrapolate to the same value at $0^{\circ}K$. Conrad (1963) and Nabarro et al (1964) have argued from the result of Lawley et al (1962) on molybdenum that at $4.2^{\circ}K$ the yield stress is independent of impurity contents and this is consistent with Peierls Nabarro mechanism. Accepting this view then the observed steeper increase in the yield stress for purer crystal between $77^{\circ}K$ to $4.2^{\circ}K$, and reduced temperature dependence than impure crystal between $77^{\circ}K$ to $300^{\circ}K$, suggests that more than one mechanism is controlling the temperature dependence of yield and flow stress in b.c.c. metals. This is contradictory to the idea of a single thermally activated process. Above the transition temperature of $300^{\circ}K$ the yield stress is nearly independent, but, as shown in Fig. 2.5 the yield stress variation with the number of zone passes at $296^{\circ}K$ there is nearly logarithmic decrease with further zone melting passes. In this temperature region, in most of the b.c.c. metals, the thermal fluctuations are large enough to free dislocations even at very small stress, however, in order that these dislocations may move, they still have to escape from their Snoek atmosphere. Schoeck and Seeger (1959) proposed a dynamic Snoek ordering in order to account for temperature independence and linear hardening with impurity behaviour. This effect should be additional to the inherent lattice friction stress (Keh and Nakada 1967).

Recently, Dorn and Rajnak (1964) proposed a criterion for the Peierls Nabarro mechanism using a line energy model of dislocation to estimate the saddle point activation energy, Un, for the nucleation of a pair of kinks as a function of stress, the height and shape of the Peierls Nabarro barrier. They found Un/2Uk, where 2Uk is the excess energy of a kink pair, was a unique function of τ^*/τ_p where τ^* is the effective stress and τ_p is the Peierls stress. The relationship found between

$Un/2Uk$ and τ^*/τ_p is expressed in terms of temperature, T, and the athermal temperature, Tc. Considering the strain rate of deformation for thermally activated process to be given by

$$\dot{\varepsilon} = \dot{\varepsilon}_0 e^{-2U_K/KT_c} = \dot{\varepsilon}_0 e^{-U_n/KT} \qquad (4.13)$$

where $\dot{\varepsilon}$ is a nearly constant then one obtains

$$Un/2Uk = T/Tc \qquad (4.14)$$

Dorn and Rajnak (1964), Mukherjee and Dorn (1964), Rosen, Mote and Dorn (1964), Wynblott, Rosen and Dorn (1965), Guyat and Dorn (1967) analysed the existing experimental data in this fashion and observed a good agreement to the expected curve. They emphasize that this agreement provides the best evidence in favour of the Peierls Nabarro mechanism. Fig. 4.10 illustrates the τ^*/τ_p against T/Tc of the present results one one and five zone passes crystals. As mentioned earlier, ther is some doubt as to the justification of extrapolating the yield stress of different purity crystals to the same value at 0^oK, however, at present τ_p is taken as 40.8 Kg/mm^2 by extrapolating the yield stress of one pass crystals towards 0^oK, and τ^* as the value at 373^oK, $Tc = 373^oK$. This plot reveals that the measured deviation from a linear relationship between yield stress and temperature is much greater than that predicted by the theory.

Although the present observation does not agree with the prediction from a single thermally activated overcoming of the Peierls-Nabarro barrier, the importance of this inherent lattice friction stress in the low temperature deformation behaviour of b.c.c. metals cannot be ignored. Also the present models of solution hardening do not give the observed magnitude of strenthening. From the evidence presented, it appears more likely that Gilman's reaction rate theory (1965) describes most suitably the low temperature deformation behaviour of b.c.c. metals.

Fig.4-10. Comparison of the Experimental Data with Dorn and Rajnak's Theoretical Curve.

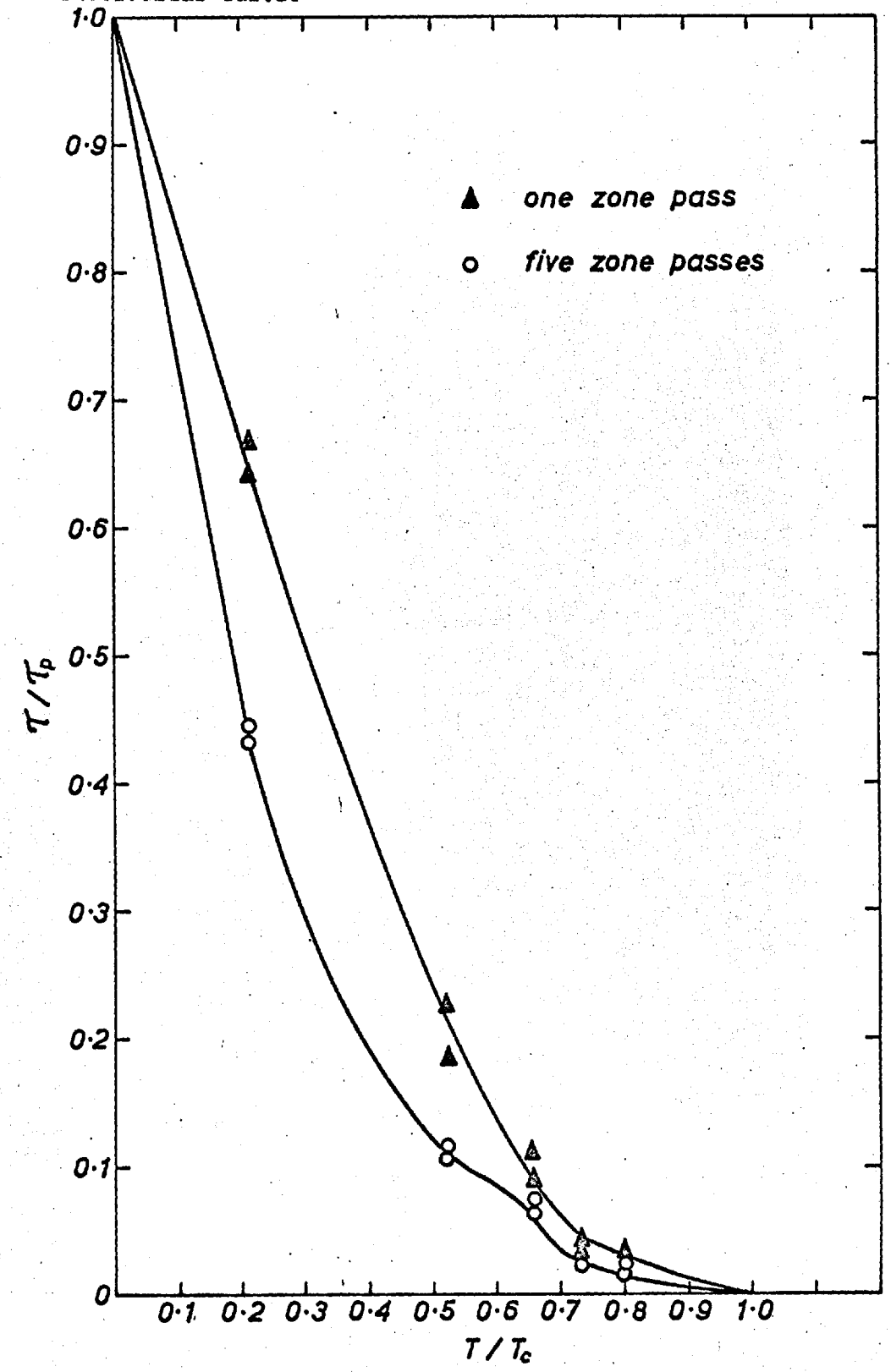

4.4 Strain ageing experiment

4.4.1 Introduction

Since the preceding observations indicate that pinning, which undoubtedly exists, does not seem to be very important the present experiments were undertaken as part of a study of the effect of interstitial impurities on the yielding and flow behaviour of niobium single crystals. Yield point return experiments were performed and the results compared with previous investigations. It was also intended to investigate the strain ageing behaviour of ⟨100⟩ and ⟨110⟩ oriented single crystals in which the latter orientation does not yield discontinuously at initial yielding. It was decided to investigate briefly the influence of ageing time, temperature and impurities and finally the orientation dependence of strain ageing for ⟨100⟩ and ⟨110⟩ orientation of comparable purity.

Three types of crystals were used for the ageing experiments:

Crystals A: one zone pass with ⟨110⟩ orientation, grown at vacuum pressure between $4.4 \rightarrow 3.9 \times 10^{-5}$ torr, at a zone speed of 2.5 mm/min.

Crystals B: one zone pass with ⟨110⟩ orientation, grown at vacuum pressure between $4.9 \rightarrow 3.0 \times 10^{-6}$ torr, at a zone speed of 2.5 mm/min.

Crystals C: one zone pass with ⟨100⟩ orientation, grown at vacuum pressure between $4.9 - 3.0 \times 10^{-6}$ torr at a zone speed of 2.5 mm/min.

4.4.2 Evidence of the influence of impurities

Two crystals, one an impure crystal (crystal A) and the other a standard purity (crystal B) of identical ⟨110⟩ orientation were pre-strained approximately 2% at room temperature, unloaded, then either immediately reloaded or aged for one hour

at 373°K. They were then strained and aged repeatedly.

The initial yielding of both specimens resulted in the characteristic upper and lower yield point of ⟨110⟩ oriented crystals. Immediate reloading produced stress-strain curves which exhibited no yield drop. Fig. 4.11 illustrates stress-strain curves for both crystals A and B. The purity has markedly affected the initial yielding. The impure crystal A showed a yield stress nearly 1.5 times and a yield drop two times larger than for crystal B at initial yielding. This is closely analogous to the effect of the number of zone passes on the stress-strain curve in Fig. 4.1 which is attributed to the effect of impurities. Crystal A also showed a larger susceptibility to the strain ageing at lower temperature and for a shorter ageing time than crystal B. The recovered yield point in crystal A was remarkably sharp without pre-yield microstrain and easily distinguishable from the initial yielding. Although the strain hardening rate remained unchanged after ageing, it can be seen that the level of flow stress was raised by the ageing treatment. However, the recovered yield point in pure crystal B was not as sharp as in crystal A and the level of the original extrapolated stress-strain curve was attained after a relatively short period and lower temperature ageing treatment. The most interesting features in crystal B was that there was a pre-yield microstrain preceding a more rounded yield drop. The observed general increase in flow stress seemed to depend very sensitively on the magnitude of solute which had migrated to the strain field of dislocation which was introduced by pre-straining. The age hardening was observed after 113 hours at room temperature, without any sign of a yield point. It was noted that the short time ageing does not change, or is almost insensitive to the amount of pre-straining. The same behaviour was reported by Wilson and Russel (1959) and independently by Nakada and Keh (1967) for iron-carbon and silicon-iron respectively.

Strain ageing in polycrystalline niobium was reported to occur at moderately elevated temperatures. Mincher and Sheely (1961) have suggested, on the basis of variation of strength with oxygen and nitrogen contents, that these elements cause the

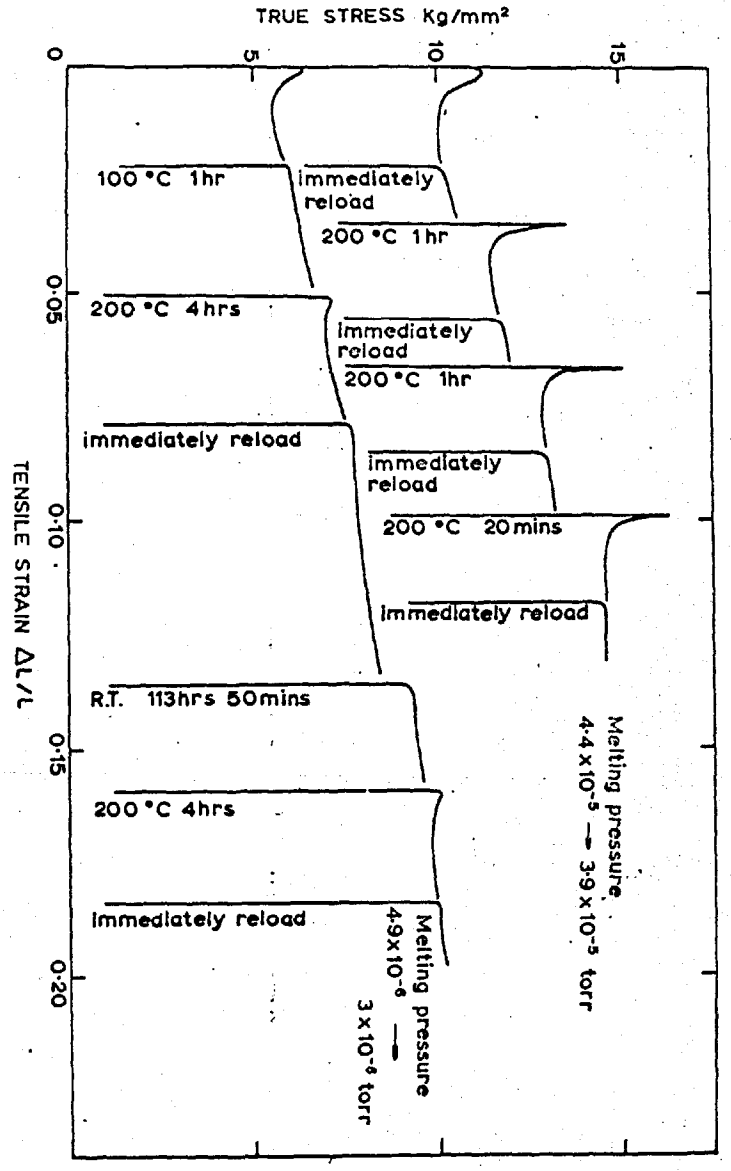

Fig.4-11. Strain Ageing Characteristics of Crystal A and B with <110> Orientation and Different Purities.

observed strain ageing between 573°K and 623°K. They also agree with Tankins and Maddin (1961). Dyson, Jones and Tegart (1958) note that this is in agreement with the prediction of Cottrell (1954) by which strain ageing occurs during the tensile test at temperature, where the diffusivity of interstitial is about 10^{-13} - 10^{-12} cm^2/sec in niobium. According to Cottrell this would be near 523°K to 573°K for oxygen and between 773°K and 873°K for nitrogen at a strain rate of 10^{-5} - 10^{-3} sec^{-1}. In the present investigation, the yield point return has been observed from 373°K after 10 minutes ageing treatment in crystal A and from 473°K after 4 hours ageing treatment in crystal B. In crystal B there were not sufficient impurities available at and near the neighbouring dislocation to cause a yield point return and it required a longer and higher temperature treatment to collect a sufficient amount of interstitials subsequently. This resulted in the smaller a ageing susceptibility of crystal B than that of impure crystal A, and the pre-yield microstrain with a rounded yield drop due to weak pinning. However, the temperature at which strain ageing took place in this investigation, did not agree with any previous investigations. The present results of 373°K and 473°K are substantially lower than reported values, despite the higher purity and perfection compared with materials used by previous workers.

4.4.3 Ageing time and temperature dependence of $\Delta\sigma$

The characteristics of strain ageing in crystal A for immediate reloading, and after 10, 20 min. ageing at 403°, 423° and 573°K are illustrated in Fig. 4.12. General features with varying temperature and time were very similar to the observation in section A.

The increase in yield stress with various ageing times and temperature, was taken as the difference between the new upper yield stress after strain ageing for time t, and the flow stress observed at the end of restraining. The results were summarized in Fig. 4.13 by $\Delta\sigma$ Vs $t^{2/3}$ plot. If we assume, for atmosphere formation, that $\Delta\sigma$ is proportional to

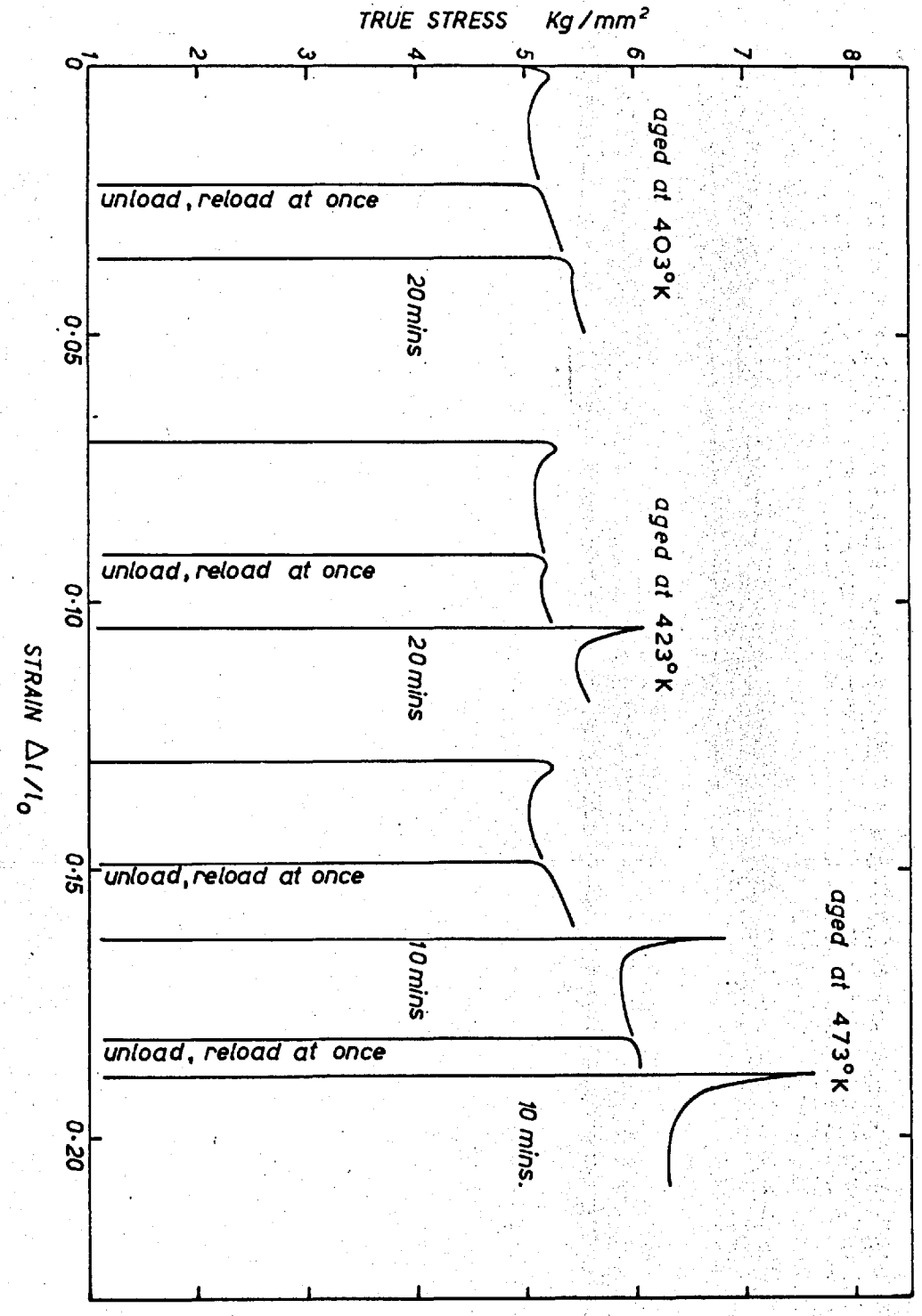

Fig.4-12. Strain Ageing Characteristics of Crystals with <110> Orientation at 403, 423 and 473°.

the amount of solute collected by the dislocations, then according to Cottrell and Bilby's equation, it should increase proportionately to $t^{2/3}$ during early stages of ageing. This is not always true, for example, Wilson and Russel (1960) and Hartley (private communication) found that the increase in yield stress was a linear function of t. They proposed that the apparent intercept at zero ageing time is positive if Snoek ordering is absent. In the present results of Fig. 4.13, the increase in yield stress can be fitted approximately by a straight line against t as well as to $t^{2/3}$ at 473°K. However, at 473°K the straight line cannot be fitted to either t or $t^{2/3}$. It is unrealistic to consider that this empirical fit is significant in the absence of more information. However, it was found that the increase in yield stress at 473°K was insensitive to the ageing time after 20 mins, which suggests that solute saturation of the stress field occurs in times less than this. The concept of locking by stress induced ordering has been used to explain the rapid return of the yield point by Wilson and Russel (1959). This model does not require long range diffusion but only atomic jumps between neighbouring lattice sites. Ageing will be naturally more rapid than is segregation to form an atmosphere. The magnitude of the effect due to such ordering would be expected to be proportional to the amount of dissolved interstitial solute at early stages, however. The effect will be small in the later stages however, when solute content of the matrix has been sufficiently reduced. This could explain the insensitivity of the yield stress to ageing for periods of longer than 20 minutes at 473°K.

It is unfortunate that insufficient and conflicting data are available for the diffusion of interstitial solutes in niobium; especially for the case of single crystals no information is available. There are several accounts of strain ageing experiments on unalloyed polycrystalline samples. Begley (1968) obtained an activation energy of 27.1 Kcal/mol for niobium and concluded that dislocation pinning was due to oxygen. Wilcox and Huggins (1961) obtained 10.5 and 16.9 Kcal/mol for niobium and tantalum respectively and decided that hydrogen was the cause of locking. Hartley and Wilson (1963) reported

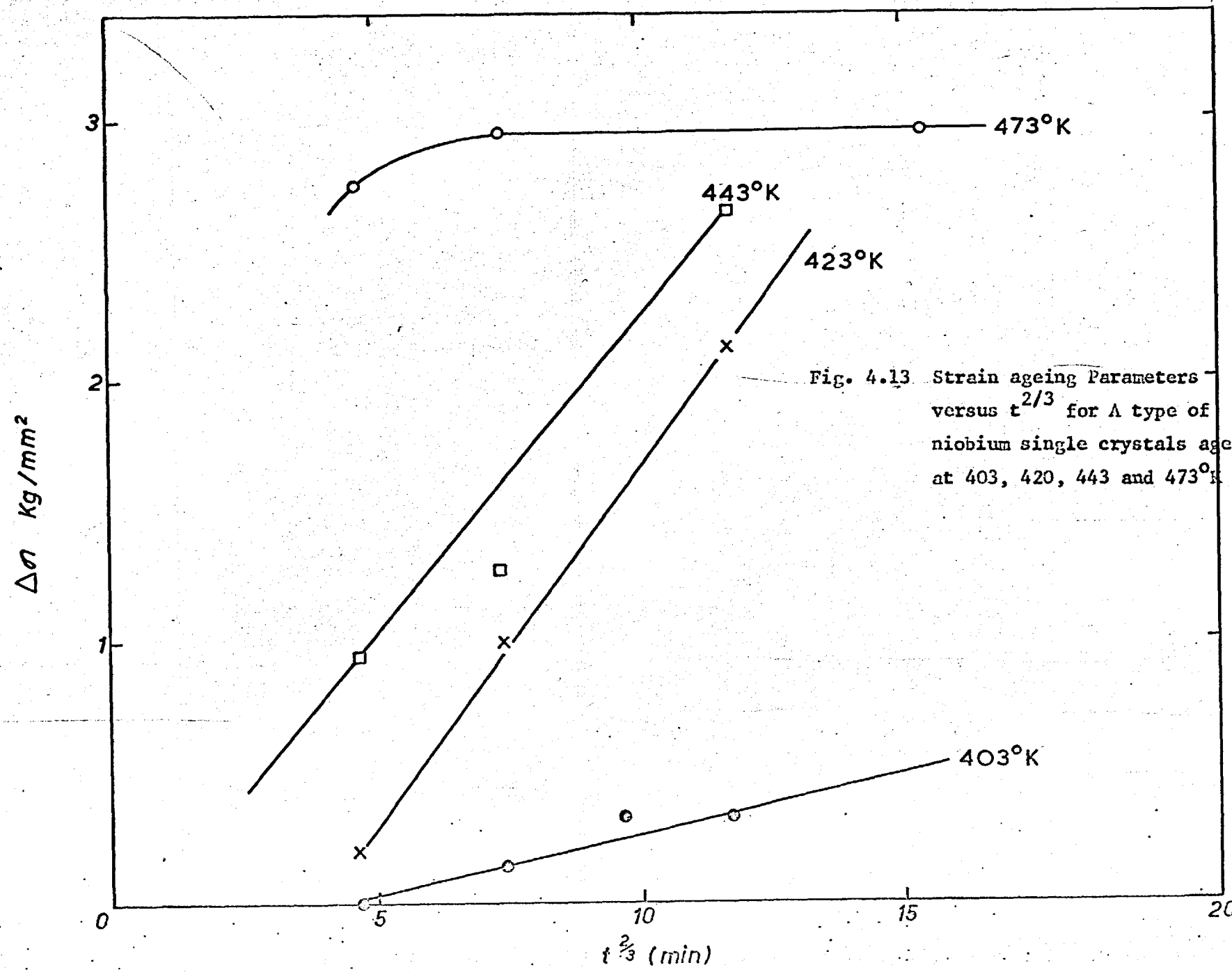

Fig. 4.13 Strain ageing Parameters versus $t^{2/3}$ for A type of niobium single crystals aged at 403, 420, 443 and 473°K

25.1 K cal/mol for molybdenum and suggest that oxygen and nitrogen are the diffusing elements. Stanley and Szkopiak (1962) proposed that oxygen was the cause of locking in niobium and the major activation energy of 26.9 K cal/mol. Data for the diffusion of interstitial atoms in niobium have been collected and referenced in Table 4.4 for convenience. A sample calculation of activation energy was found to give 19.8 K cal/mol for the return of yield point. Comparison of the activation energy obtained in this work with data in the Table (4.4). indicates that neither nitrogen nor oxygen are the diffusing elements responsible for ageing. The activation energy is too high for hydrogen, except on Ferro's theoretical calculation (see Table 4.4).

The disagreement with previous work is due in part to the fact that the materials which have been used by previous workers were polycrystalline niobium of commercial purity. Hence, the role of grain boundaries in the diffusion process, and the amount of interstitial impurities which existed in the material would probably give very different results to those obtained on the present crystals of zone refined ⟨110⟩ oriented single crystals. The values of Power and Doyle (1959) for the activation energy of diffusion of interstitials support this view; they obtained 32.2 K cal/mol from niobium containing 0.3 weight % of oxygen and 26.2 K cal/mol from purer niobium which contained 0.026 weight % oxygen. The higher activation energy for the crystal with the higher concentration of interstitials may be due to the effect of interaction between interstitials. Thus, the effect of interstitial concentration, the relative amount of interstitials, and the kind of interstitials in the diffusion process cannot be ignored and these factors may cause a substantial difference.

4.4.4 Effect of orientation on strain ageing behaviour

The discontinuous yielding is now generally accepted as a common feature of yielding in ⟨110⟩ oriented single crystals of b.c.c. metals whilst ⟨100⟩ oriented single crystals yield continuously with a high work hardening rate. Single crystals of ⟨100⟩ orientation were chosen to see whether the return of the yield point takes place after an ageing treatment.

TABLE 4.4

Summary of Diffusion Data for Interstitials in Niobium

Diffusing Elements and Activation Energy for Diffusion (K cal/mol)					
Oxygen	Nitrogen	Carbon	Hydrogen	Investigator	Method
1.70	20.0			Ferro (1957)	Theoretical
26.6	34.8	33.2		Powers and Doyle (1959)	Internal friction
27.6	38.6			Aug (1953)	Internal friction
27.1				Begley (1958)	Strain ageing
27.0				Tankins & Maddin (1961)	Strain ageing
26.9				Stanley and Szkipiak (1962)	Strain ageing
			9.37	Albrecht et al (1959)	Strain ageing
			10.5	Wilcox and Huggins (1961)	Strain ageing

This seems to provides some information about the anisotropic yielding behaviour of both orientations.

The strain ageing characteristics of both orientations are illustrated in Fig. 4.14. Both crystals were grown under identical conditions, such as growing zone speed and vacuum pressure. The purity therefore, can be assumed to be the same. In the initial yielding, ⟨110⟩ orientation yielded discontinuously and the ⟨100⟩ oriented single crystal yielded continuously. However, a sharp yield point appeared after ageing treatment for the ⟨100⟩ orientation, which was absent in the initial yielding. The ageing factor $\Delta\sigma$, of this orientation was approximately 2.3 times larger than the ⟨110⟩ orientation without any sign of pre-yield microstrain after the same ageing treatment.

There is no single satisfactory explanation, at the present time to account for the anomalous yielding behaviour of b.c.c. metals. One speculative explanation is that this ageing yield point in ⟨100⟩ orientation appeared after considerable pre-straining where the work hardening rate is relatively low, this lead to the Gilman's(1962) model of yielding where the effect of work hardening is the primary extinguisher of the yield point. Another plausible explanation is that this may be caused by the anisotropy of shear stress in the sense of shear direction in the vicinity of the dislocation core. Recent observation of slip systems in tension and compression in tungsten, niobium and molybdenum has revealed a considerable evidence for an asymmetry of shear stress in the {112} plane. Therefore, any explanation of this orientation dependence should be based on the geometrical properties of dislocations in the lattice. At present it is difficult to envisage the position of the interstitial, precipitate or point defects which are diffused and subsequently give rise to an anomalous strain ageing behaviour.

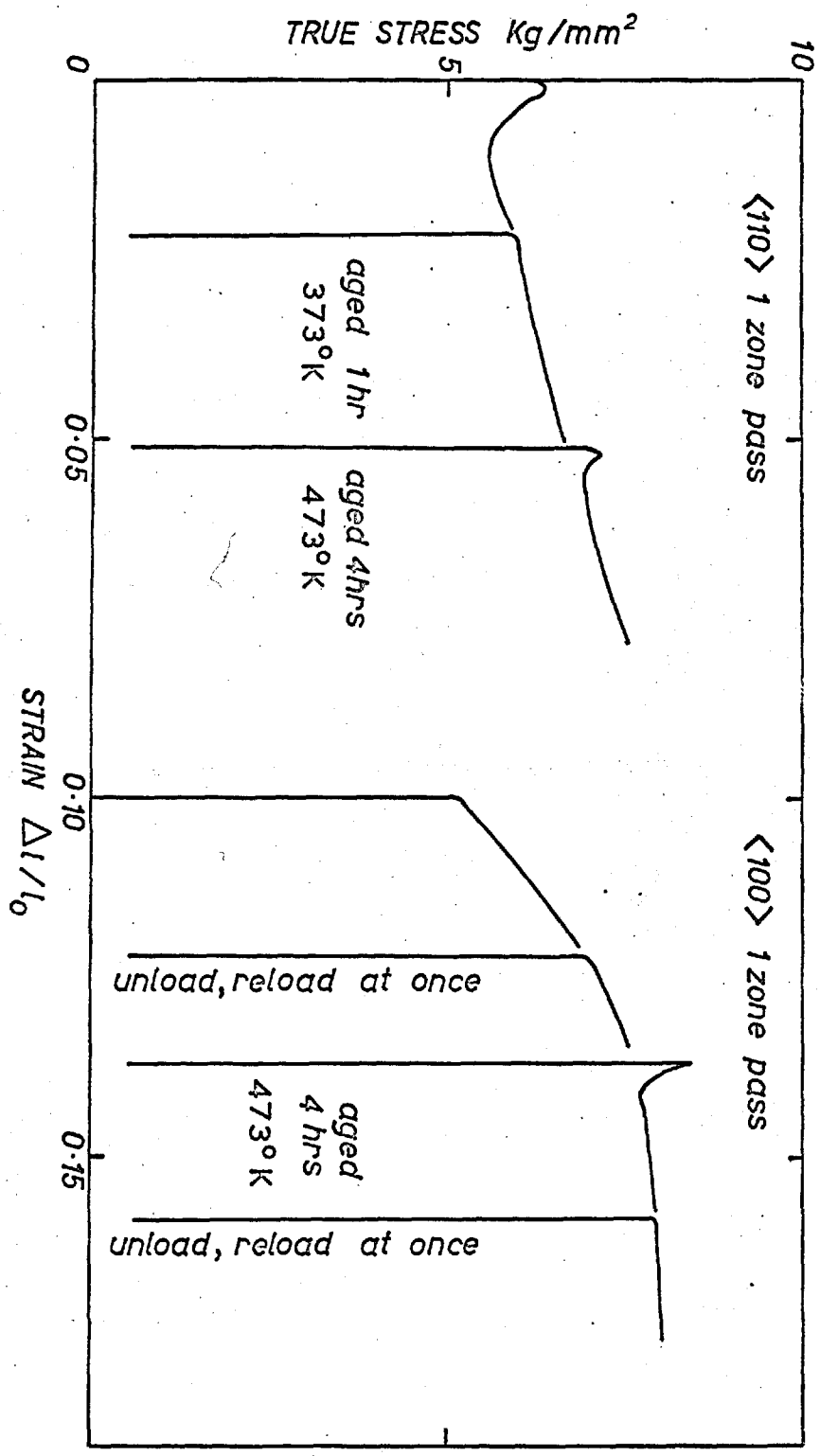

Fig.4-14. Strain Ageing of Niobium Single Crystals with <110> and <100> Axes.

4.4.5 Conclusion and Summary of the Strain ageing experiment

The mechanisms proposed so far to account for the observed strain ageing behaviour are:

Atmosphere formation -	Cottrell and Bilby 1949 Formby and Owen 1965
Stress-induced ordering -	Wilson, Russel and Eshelby 1959 Nakada and Keh 1967 Schoeck and Seeger 1959
Precipitation formation -	Hartley and Wilson 1963 Thomas and Leak 1952 Bullough and Newman 1962

Each of these processes of solute redistribution can occur during the strain ageing process, and the present observations suggest that the Cottrell-Bilby atmosphere formation is of prime importance in causing the return of the sharp yield point below 473°K, while the rapid increase in flow stress, insensitive to the ageing time at above 473°K is probably associated with stress-induced ordering. Though there are many theoretical and indirect indications of the precipitation formation, there has so far been no direct experimental evidence found. At the present time it is not possible to eliminate all impurities or to separate the effect of each element. Current analytical techniques do not permit reliable measurement of the level and species of interstitials in high purity niobium as used here, and therefore it is improper to point out the precise interstitial element which is responsible for the strain ageing process.

The present investigation is far from complete, however, it is summed up as follows:

(i) strain ageing took place at room temperature after long ageing periods,

(ii) the temperature at which strain ageing takes place was found to be significantly lower than previously reported,

(iii) pre-yield microstrain was observed after ageing treatment at 373°K for one hour for pure crystal of ⟨110⟩ orientation,

(iv) the strain ageing kinetics and consequently the activation energy of diffusion of interstitials are strongly influenced by the initial concentration and relative concentration of interstitials in the crystals,

(v) The development of yield point was observed for the crystal oriented along ⟨100⟩ axis.

CHAPTER 5

DEFORMATION BEHAVIOUR OF NIOBIUM SINGLE CRYSTALS

CHAPTER 5

5.1 Introduction

The nature of plastic deformation in b.c.c. metals is not fully understood although a considerable amount of work has been devoted to the problem. Most of the previous workers have studied the dependence of yield stress upon both strain rate and temperature without paying serious attention to the effect of purity and orientation. It has generally been considered in the past that the plastic deformation of single crystals of b.c.c. metals is isotropic because of the facility with which multiple slip takes place.

However, recent work on tungsten, molybdenum, niobium tantalum and iron has revealed that when the orientation of the crystal is properly chosen the yield stress and work hardening rate can exhibit a strong orientation dependence - particularly at low temperatures.

Furthermore, recent studies of the slip systems operating in tension and compression of the many b.c.c. metals have revealed considerable evidence for an asymmetry of the critical resolved shear stress.

So far there has been no systematic study of the yield stress and slip systems in both tension and compression at various temperatures and it was decided that the present investigation be directed at these effects with crystal axes in ⟨110⟩ ⟨100⟩ and ⟨$\bar{1}$11⟩ orientation. The experiments were performed with two zone pass single crystals and because of the uncertainty about the active slip system, unless otherwise stated, the true stress versus true strain rather than shear stress and strain are plotted.

5.2 Deformation behaviour of crystal with symmetrical orientation

5.2.1 Crystals with ⟨110⟩ orientation

Some typical true stress and strain curves of crystals with

Fig.5-1. Stress-Strain Curves of Niobium Single Crystals with <110> Axis in Tension.

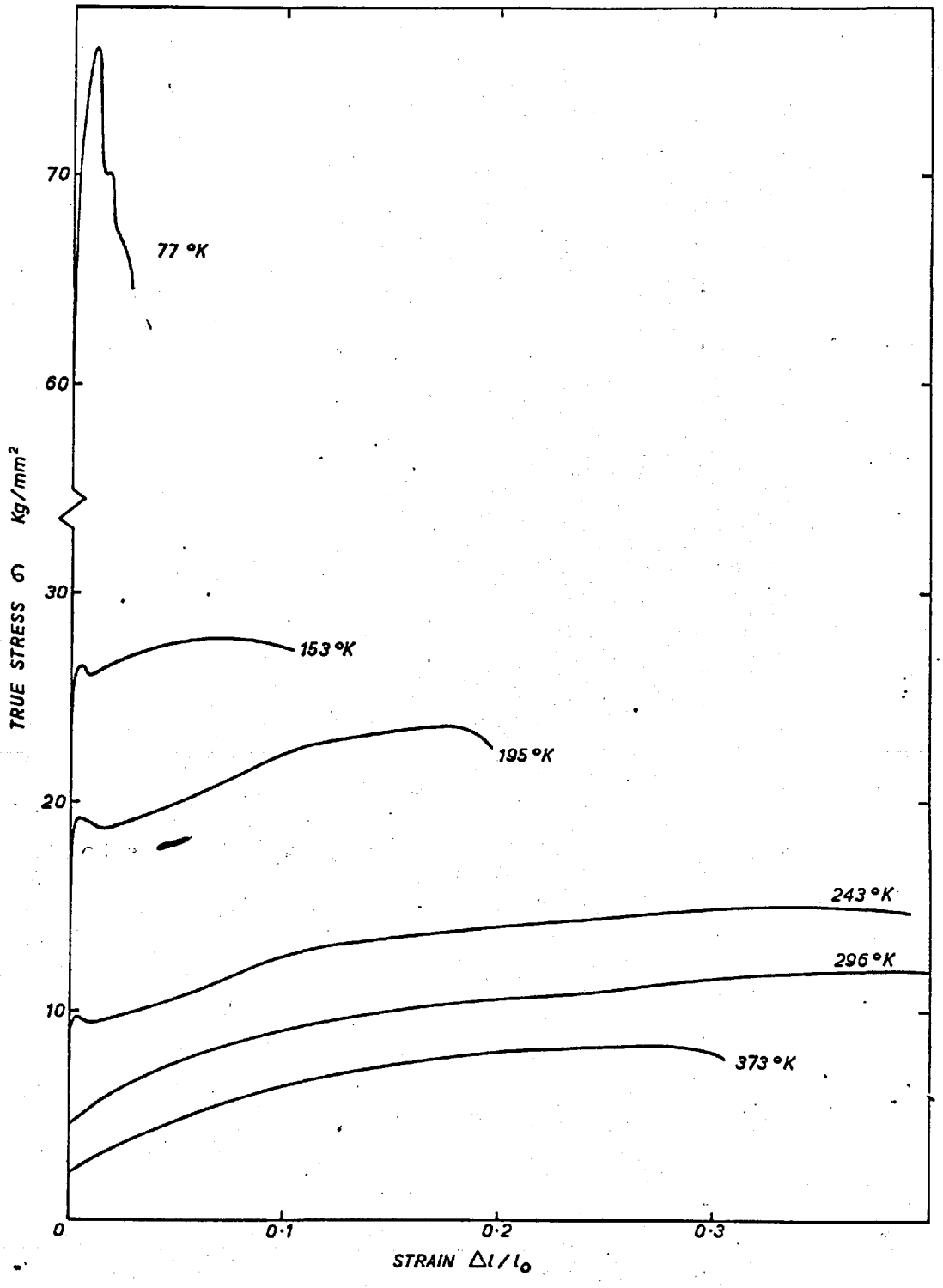

Fig.5-2. Stress-Strain Curves of Niobium Single Crystals with <110> Axis in Compression.

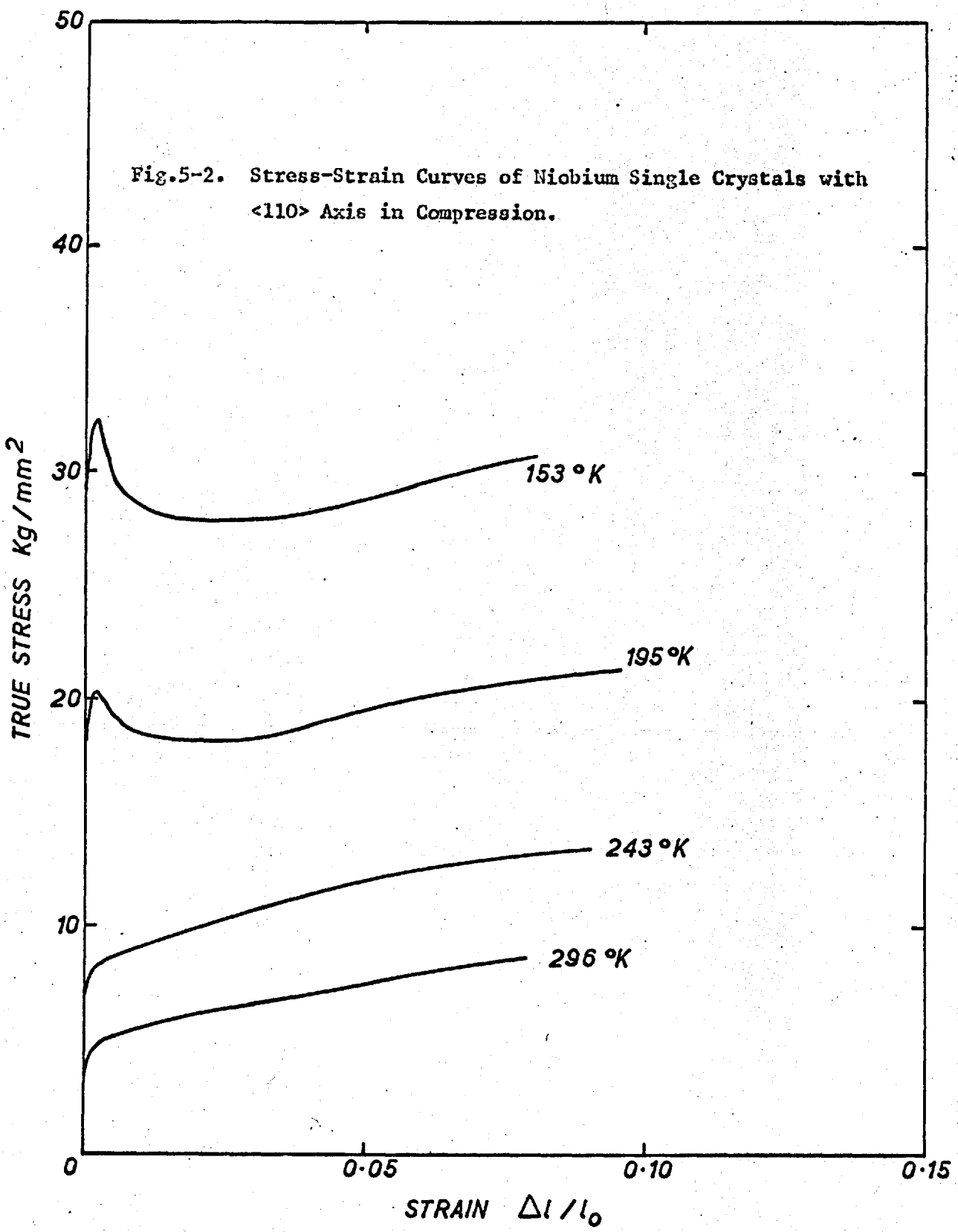

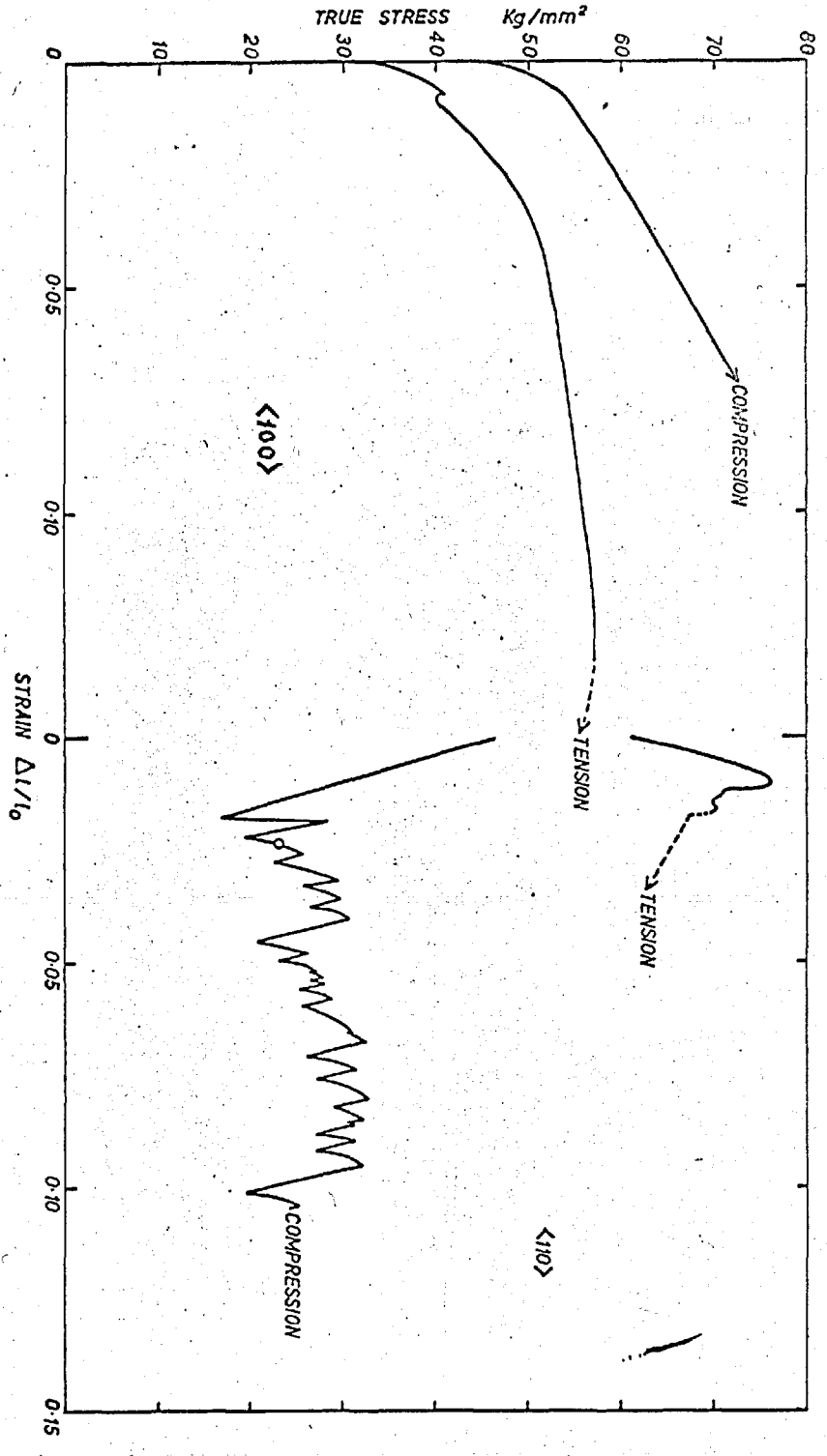

Fig.5-3. Stress-Strain Curves of Niobium Single Crystals with <110> and <100> Axes in Tension and Compression at 77°K.

TABLE 5.1

Proportional limit of single crystals with the deformation axis in the ⟨110⟩ direction

Temperature ^{o}K	Tension Kg/mm^2		Compression Kg/mm^2	
		σ_k {112}		σ_k {112}
373	2.715	1.28		
	2.65	1.25		
296	5.272	2.485	3.976	1.877
	4.658	2.196	3.8	1.894
273	5.368	2.53		
243	9.68	4.562	7.45	3.51
	8.85	4.174	7.5	3.54
195	16.63	7.843	17.28	8.15
			17.7	8.34
	16.29	7.68	18.13	8.55
153	23.55	11.2	28.62	13.49
			30.28	14.29
			25.14	11.87
77	60.72	28.65		
			TW 41.5	TW 19.5
	60.2	28.4		
24.4			TW 30.5	TW 14.3

TABLE 5.2

Slip and twin planes observed in single crystals stressed in the <110> and <100> directions

(T = tension, C = compression, TW = twinning)

		Ta		Nb		Mo		W	
		⟨110⟩	⟨100⟩	⟨110⟩	⟨100⟩	⟨110⟩	⟨100⟩	⟨110⟩	⟨100⟩
High stressed	T					413°K	TW 77°K		
{112}			TW 77°K				413°K		450 - 77°K
Schmid factor									
0.472	C	77°K		TW 77°K		293° & 77°K		450 - 77°K	
{110}	T	77°K	293°K	77°K	77°K		293° - 193°K		450 - 77°K
Schmid factor	C								
0.408			77°K		77°K		293°K		
Low stressed	T								
{112}		TW 77°K						450 - 77°K	
Schmid factor	C								
0.236									

* Data from Argon and Maloop (1966)

** Data from Sherwood, Guiu, Kim and Pratt (1967)

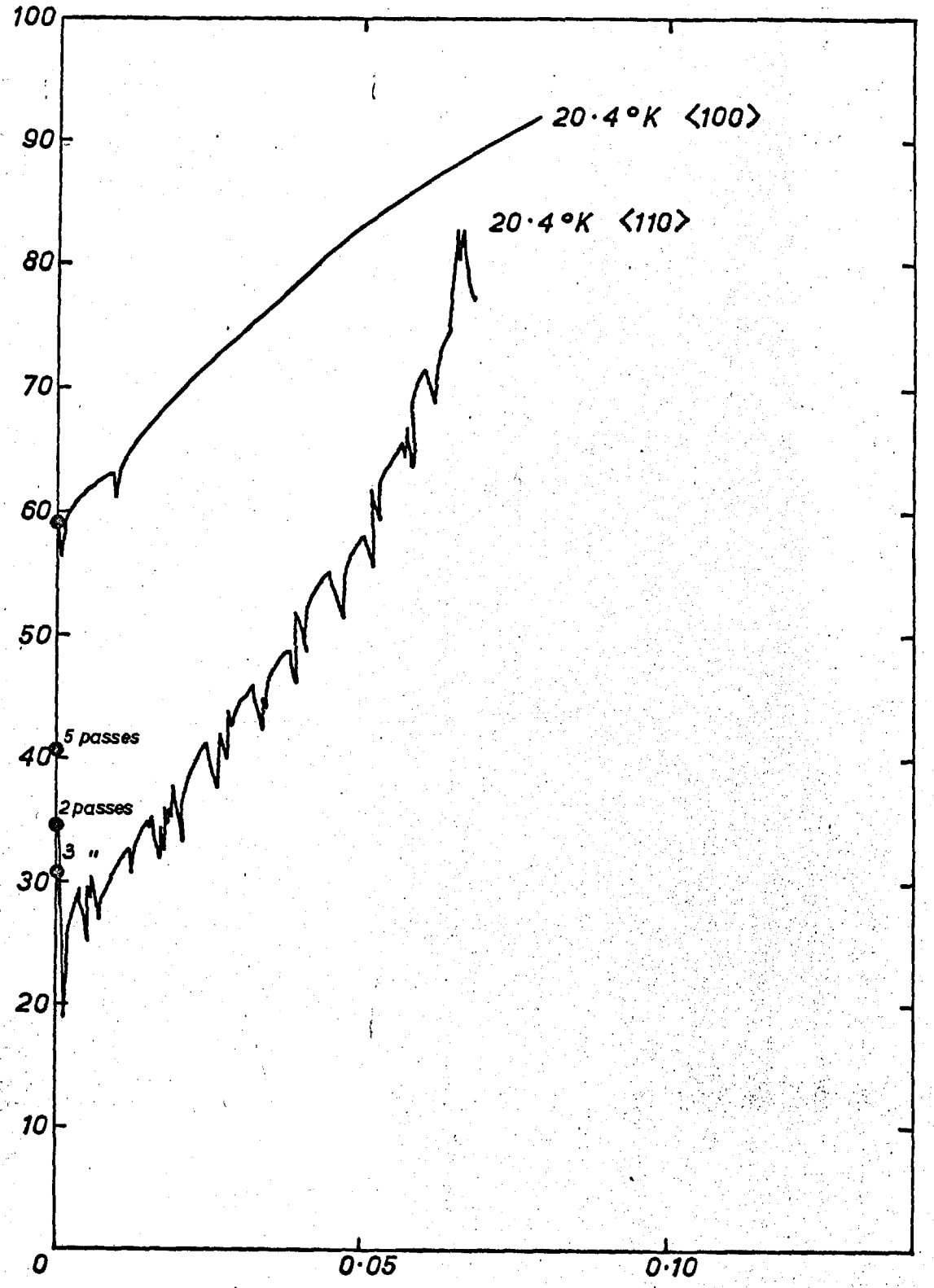

Fig.5-4. Stress-Strain Curves of Niobium Single Crystals with <110> and <100> Axes in Compression at 20.4°K.

⟨110⟩ orientation at various testing temperatures are shown in Fig. 5.1 Table 5.1 summarizes the value of the proportional limit. The characteristic features of this orientation were a pre-yield microstrain followed by a rounded yield drop in the crystals deformed at and below room temperature, and the subsequent work-hardening rate was rather low and almost temperature insensitive. However, the yield drop and pre-yield microstrain are increased at decreasing testing temperature. The yield point disappeared at 373°K and necking was always localized. Fracture occurred after 100% reduction in area causing a perfect chisel-type fracture and symmetry considerations indicated that this crystal must be oriented for double slip. The crystal, at 77°K, deformed entirely by slip and necked immediately upon yielding leading to a chisel edge fracture. The slip systems observed are summarized in Table 5.2.

In Fig. 5.2 the true stress and strain curves for compression are illustrated. The specimen yielded discontinuously with pre-yield microstrain below 195°K in the same manner as in tension; however, at 77°K it underwent prolific twinning with audible clicking before slip took place at a stress of 41.5 Kg/mm^2. This twinning produced a load drop of more than 50% and yielding at much lower stresses followed by repeated twinning and slip without any sign of work-hardening at much lower stresses than the first twinning stress as shown in Fig. 5.3. The specimen deformed at 20.4°K is illustrated in Fig. 5.4 and repeated twinning and slip took place in the same manner at 77°K, however, the specimen continued to work-harden with increasing plastic deformation. There was no big load drop after the first twinning as in the case of 77°K and this behaviour is in strong contrast to the behaviour at 77°K.

5.2.2 Crystals with ⟨100⟩ deformation axis

In Fig. 5.5 the true stress versus true strain curves of crystals with ⟨100⟩ axis in tension are shown at various temperatures. The crystals tested in this orientation yielded smoothly at lower stress and showed a larger initial work-hardening. The rate of work-hardening increased with decreasing temperature. The value of the proportional limits of the crystals

TABLE 5.3

Proportional limit of Single crystals with the deformation axis in the ⟨100⟩ direction

Temperature °K	Tension Kg/mm² on {112}		Compression Kg/mm² on {112}	
373	2.607	1.229		
	2.55	1.20		
296	3.84	1.80	4.13	1.95
	4.28	2.02	3.52	1.66
243	7.85	3.7	9.608	4.53
	7.8	3.68	9.60	4.26
195	14.35	6.77	13.62	6.25
	13.22	6.24	15.3	7.2
153	21.69	10.23	22.66	10.69
			21.04	9.93
	19.25	9.08	18.79	8.87
77	33.2[illegible]	15.26	45.05	21.24
	35.99	16.97	45.14	21.28
24.4			59.0	27.58

Fig.5-5. Stress-Strain Curves of Niobium Single Crystals with <100>Axis in Tension.

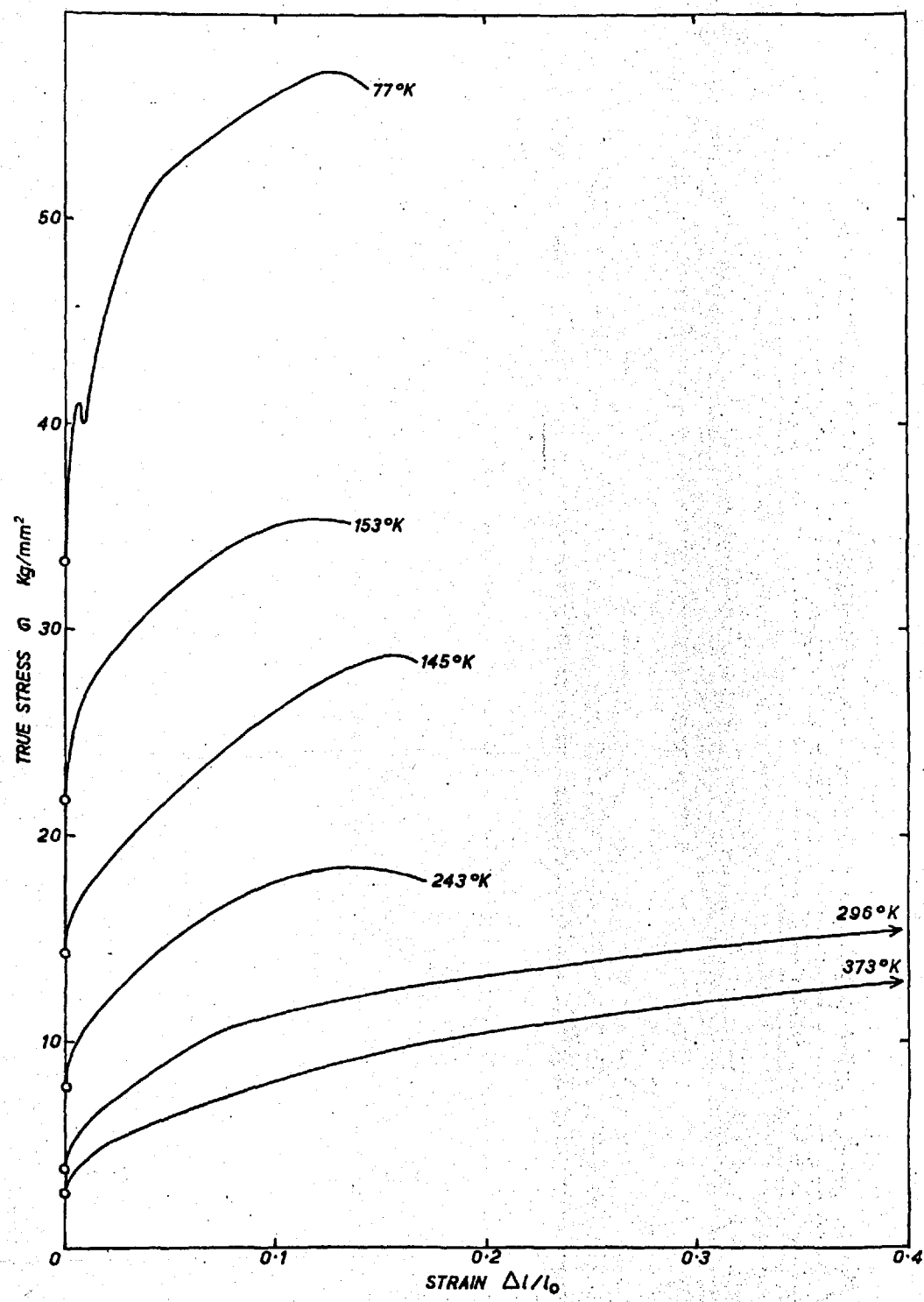

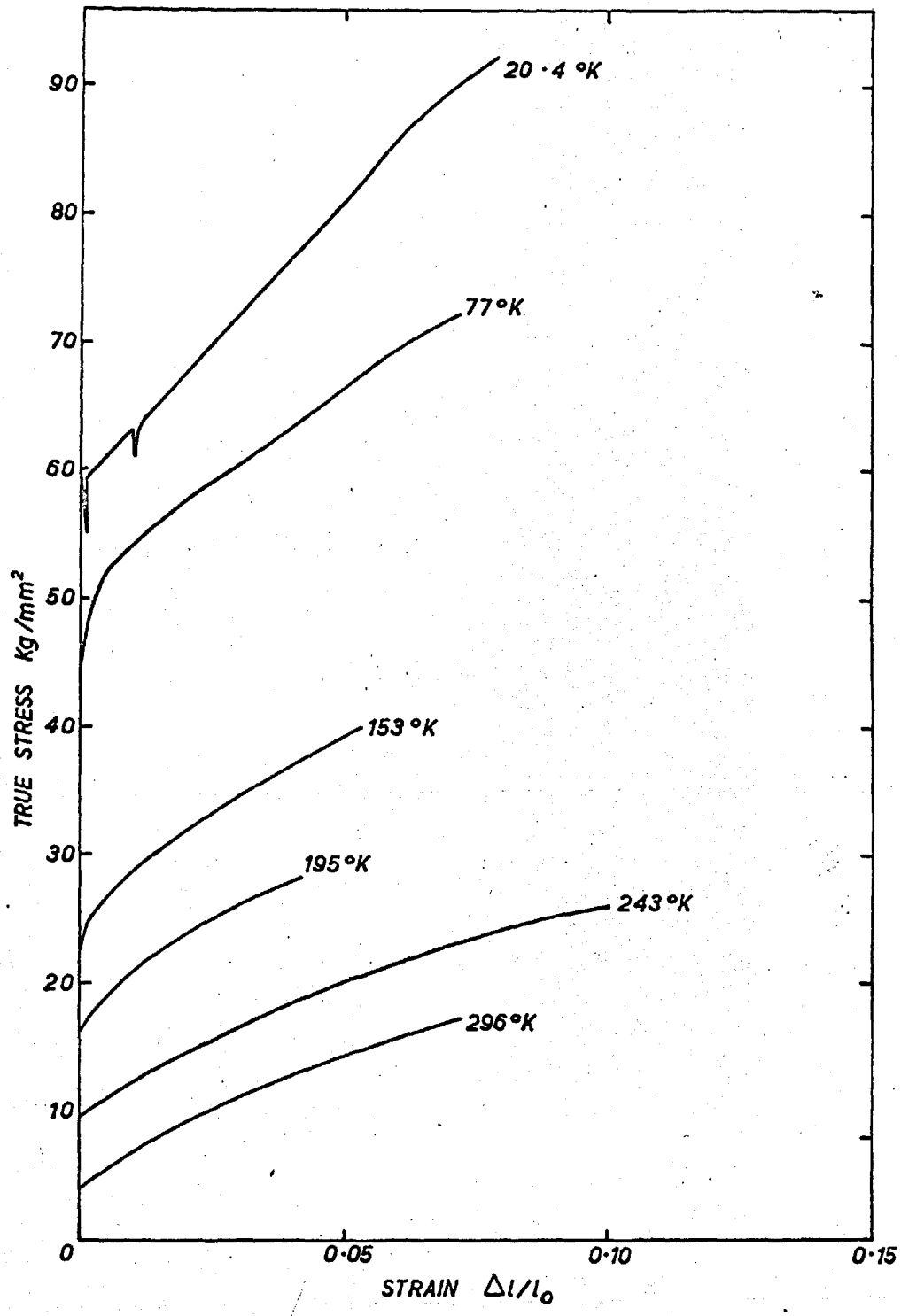

Fig.5-6. Stress-Strain Curves of Niobium Single Crystals with <100> Axis in Compression.

tested are listed in Table 5.3. It is note-worthy that the crystal deformed at 77°K extended about 12.5% before reaching the U.T.S. and showed a small yield drop at the beginning of the plastic flow without any sign of twinning.

The true stress and true strain curves of crystals deformed in compression are shown in Fig. 5.6. The proportional limit, which in this case was taken from the linear part of the stress strain curve in the same way as in the tension tests, is always greater than in tension below 300°K. The specimen was deformed into a perfect barrel shape in this case, and this is in good agreement with the symmetrical character of the slip element with respect to the compression axis. There are no signs of yield drops or of twinning, except at 20.4°K and even at this temperature, as shown in Fig. 5.6, only sporadic load drops were observed after considerable amounts of plastic strain.

5.2.3 Deformation axis with ⟨111⟩ orientation

It is clear from the stress strain curves of Fig. 5.7 that this orientation is characterised in tension by an unusually severe shear deformation. The initial discontinuous yielding was followed by rapid work-hardening, and then by a large rounded load drop leading to local necking. This has been directly observed in a room-temperature test. The cross-section of the specimen changed from a circular to a markedly elliptical shape which implies that strain associated with local necking is very severe, and therefore, the load drop in the stress-strain curves does not necessarily represent the true softening effect. Occasionally a second elliptical necking in the specimen yet to be deformed was observed at room-temperature testing. As shown in Fig. 5.8 there was shear necking in the specimens tested at all temperatures which was especially pronounced in the specimens tested at 77° and 195°K. The specimens necked with single shear necking, undergoing extremely severe deformation with no evidence of twinning. At 77°K, these lamellae lay close to the {011} plane and the shear direction approached ⟨100⟩. There were also a few clearly visible secondary slip lines.

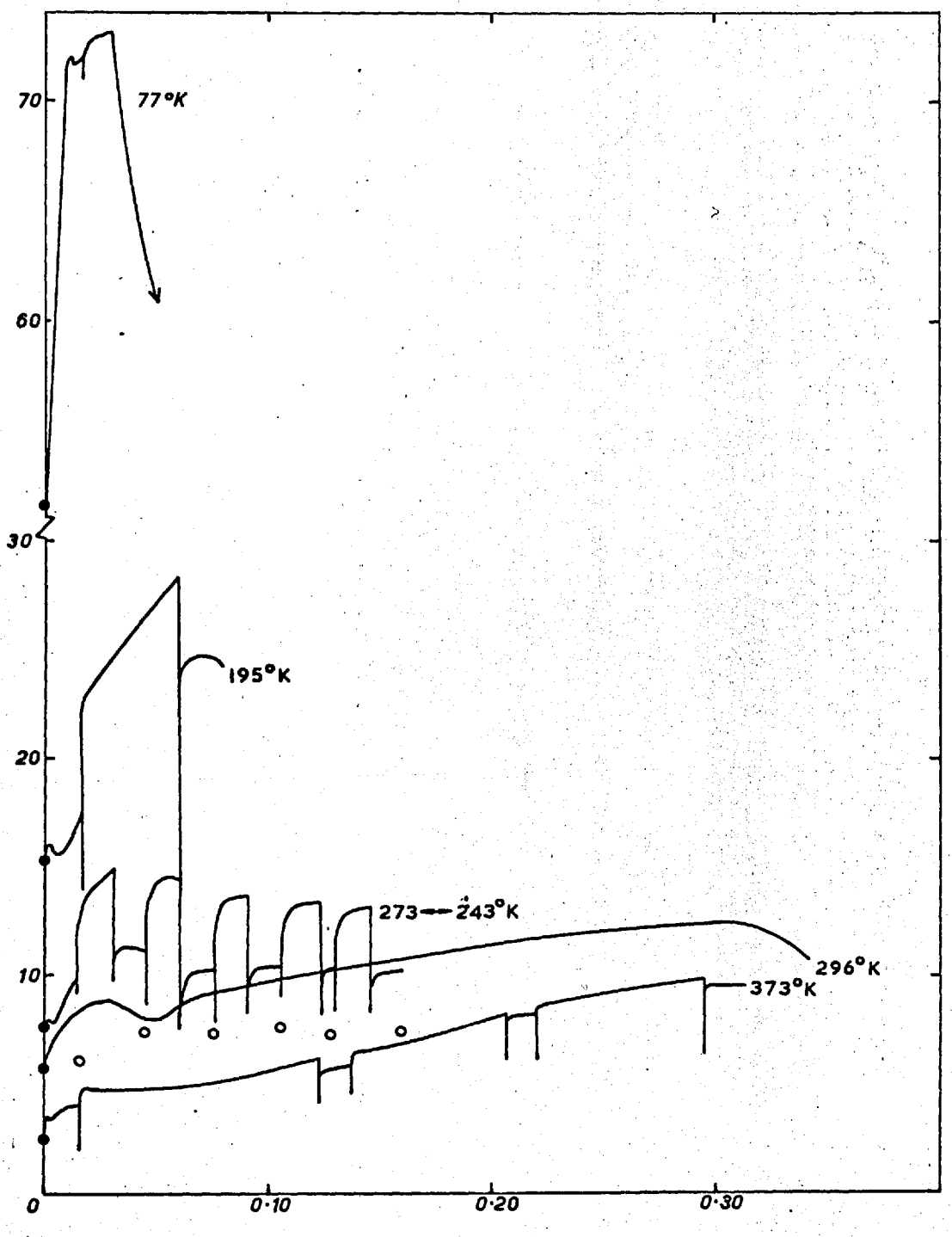

Fig.5-7. Stress-Strain Curves of Niobium Single Crystals with <111> Axis in Tension

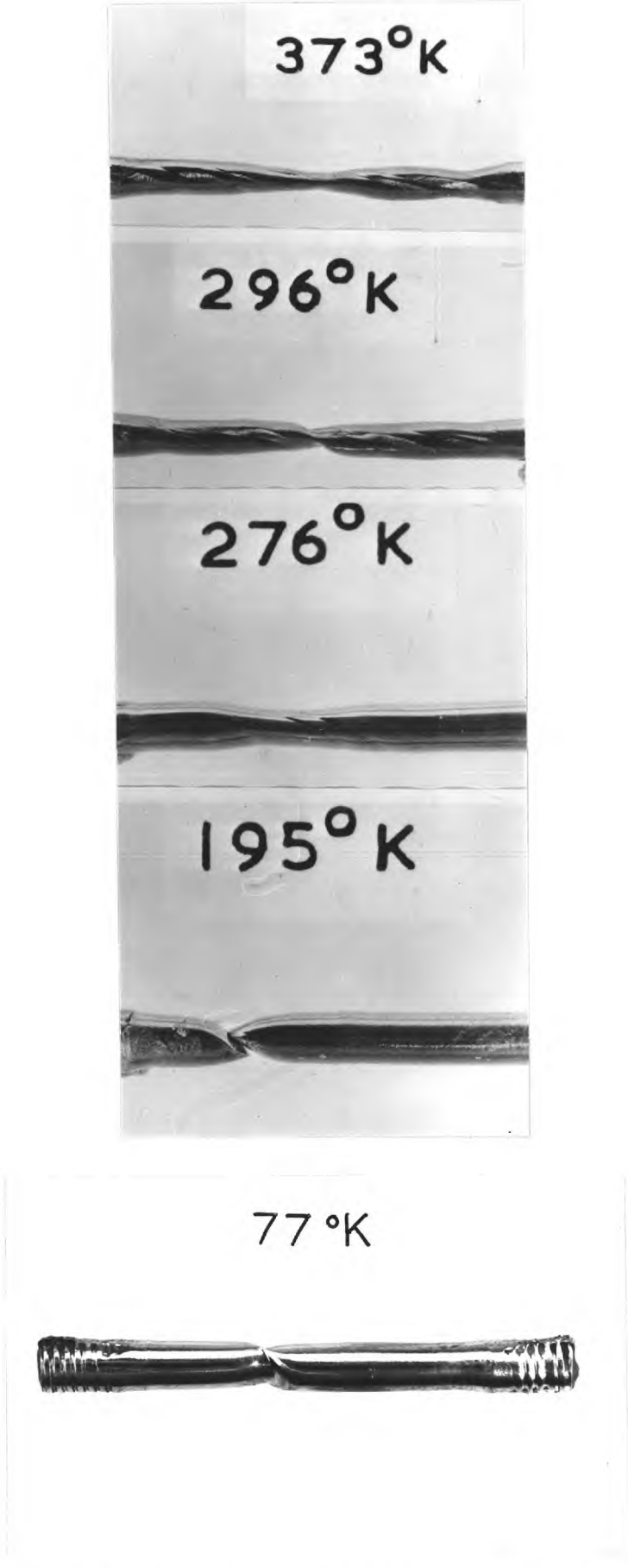

Fig. 5.8 Deformed specimens of niobium single crystals with <111> axis in tension

5.3 Discussion

5.3.1 Orientation and Temperature dependence of the proportional limit of ⟨110⟩ and ⟨100⟩ orientation in tension and compression

It would be expected that for a critical resolved shear stress law to hold the resolved shear stresses to initiate the same slip systems in ⟨110⟩ and ⟨100⟩ directions must be similar. This would be expected because the Schmid factor for {110}, ⟨111⟩, {112}, ⟨111⟩ and {123}, ⟨111⟩ slip systems in ⟨110⟩ orientation are virtually identical to the respective Schmid factors for ⟨100⟩ orientation.

Recent observations on molybdenum (Guiu and Pratt 1966, Stein 1967), tungsten (Rose et al 1962, Garlick and Probst 1964) tantalum (Sherwood, private communication) and iron (Stein and Low 1966) in tension tests have shown that a high proportional limit is exhibited by crystals with ⟨110⟩ orientation A yield drop and low work-hardening rate were the characteristics of this orientation, whereas the ⟨100⟩ orientation yielded continuously with high work-hardening rate. Beardmore and Hull (1965) have examined the crystals with orientation along the edge of the stereographic triangle and found a gradual increase in yield stress from ⟨100⟩ toward ⟨110⟩ orientation. It appears that the effect of orientation is essentially of crystallographic or geometric nature, and is common to all b.c.c. metals. This observation suggests that the resolved shear stress necessary to initiate slip in the same slip system in both ⟨110⟩ and ⟨100⟩ orientations is strongly dependent on the deformation axis of the crystals. This conclusion is contrary to the critical resolved shear stress criterion.

The temperature dependence of the proportional limit for single crystals of niobium in tension and compression are shown in Fig. 5.9 and Fig. 5.10 respectively. The value of the proportional limit, or deviation from the linear region in the stress strain curves, are chosen for comparison, since crystals with ⟨110⟩ orientation yield discontinuously, while the ⟨100⟩ oriented crystals exhibit parabolic work-hardening from the onset

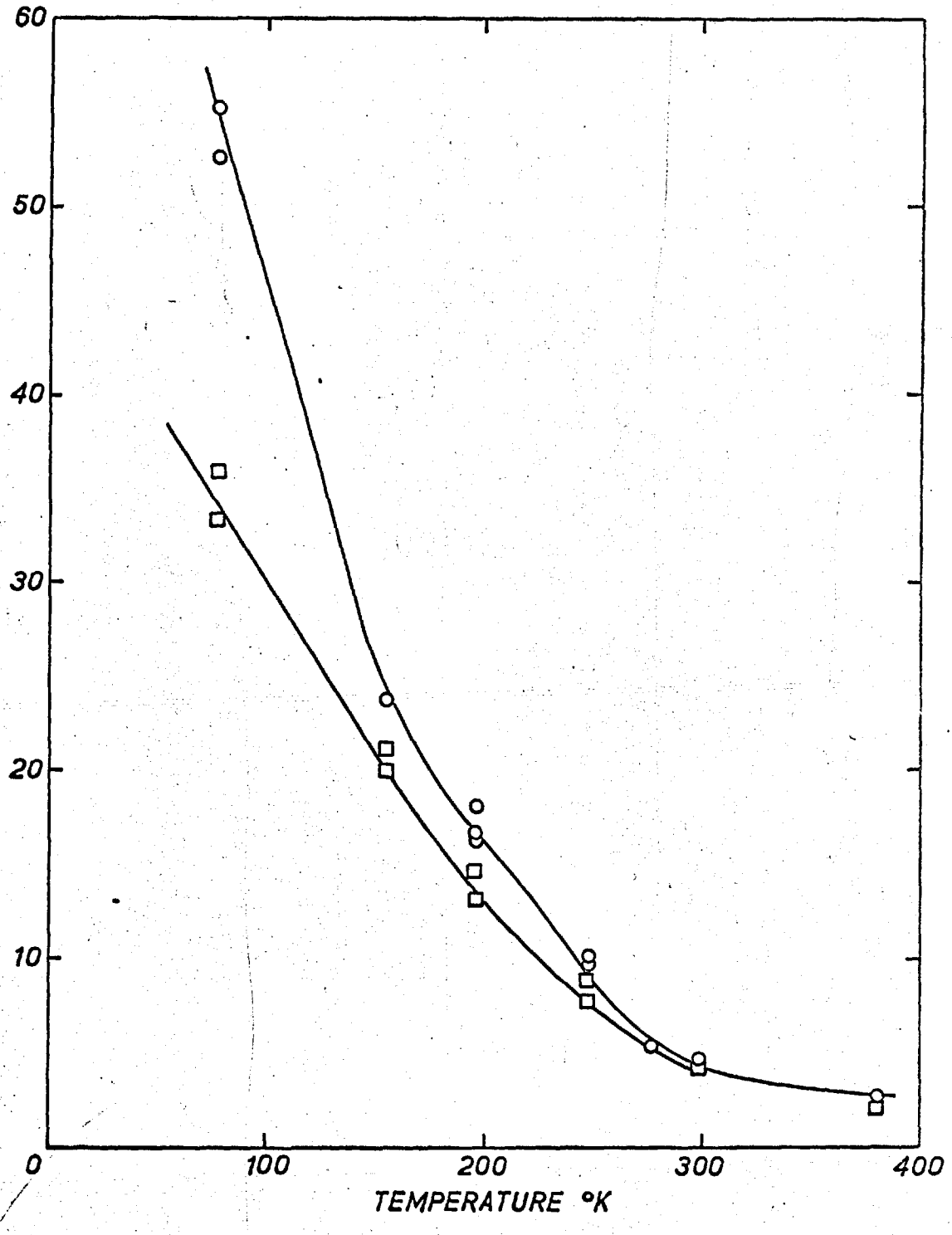

Fig. 5.9 Temperature dependence of the proportional limit for niobium single crystals of <110> and <100> orientations in tension. O = <110> axis. □ = <100> axis.

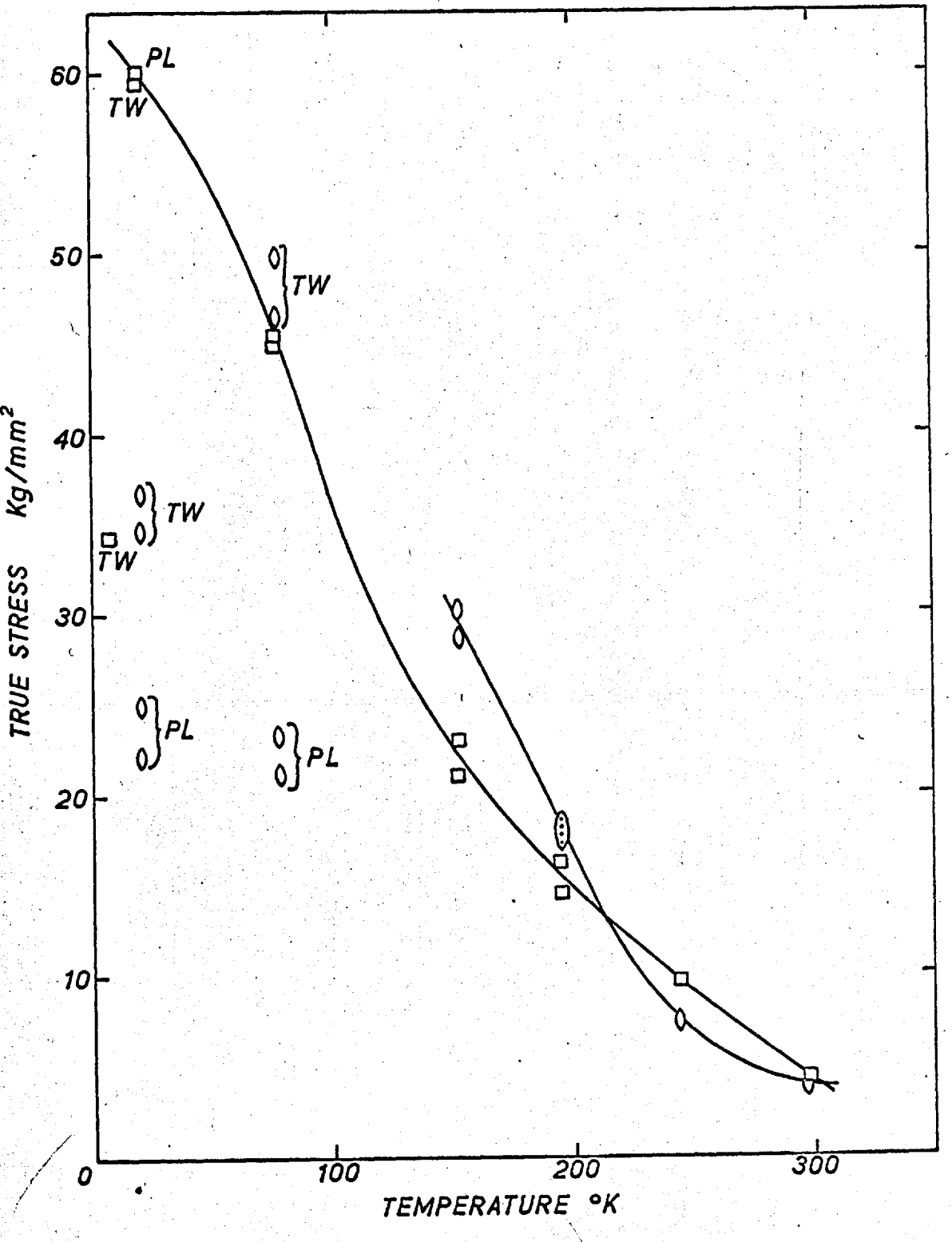

Fig. 5.10 Temperature dependence of the proportional limit for niobium single crystals of <110> and <100> orientations in compression. O = <110> axis. □ = <100>axis.

of macroscopic flow.

The proportional limit of a ⟨110⟩ orientation in tension is always higher and more strongly temperature dependent than that of a ⟨100⟩ orientation. This observation in tension, generally agrees with previous work on molybdenum (Guiu and Pratt 1966; Stein 1967), tungsten (Rose et al 1962; Garlick and Probat 1966; Beardmore and Hull 1965) and tantalum (Sherwood private communication).

However, the behaviour in compression is more complex; the proportional limit of ⟨110⟩ orientation at temperatures above 243°K exhibited a lower value than the ⟨100⟩ orientation, but at 196° and 148°K exhibited higher values and even exceeded the value of tension in ⟨110⟩ orientation. The proportional limit for the ⟨110⟩ orientation in compression was always higher than that in tension. Above 153°K the ⟨110⟩ oriented crystal yielded discontinuously with relatively low work-hardening rates, whilst ⟨100⟩ oriented crystals yielded smoothly with high work hardening rates similar to the behaviour in tension for both orientations. However, at 77°K twinning was observed in crystals with ⟨110⟩ orientation before slip and this produced a load drop of more than 50%, and subsequently yielding occurred at a much lower stress and repeated twinning and slip took place.

In contrast the ⟨100⟩ oriented crystals yielded continuously without any sign of either a load drop or twinning. This behaviour was more pronounced at 20.4°K where, in ⟨110⟩ oriented crystals, twinning and slip took place repeatedly with increasing strain, whereas only sporadic load drops were observed in the case of the ⟨100⟩ oriented crystals.

The observed marked orientation dependence of the yielding behaviour and yield stress at low temperature in tension and compression is difficult to explain with previously proposed theories, because their interactions are essentially isotropic in nature, It is therefore, tempting to consider either double cross slip, movement of jogs on screw dislocations, or asymmetry arguments as the mechanism capable of giving rise to

anisotropic behaviour.

Rose et al (1962), Guiu and Pratt (1966) and Beardmore and Hull (1965) have explained this anisotropic behaviour in tension as arising from the geometry of jog formation, assuming that most jogs arise from the interaction of the dislocations of two or more active slip systems. When two dislocations come into contact at more than one point they may form a repulsive junction (Saada 1961). A stress is then required to bring them close to each other. On the other hand some dislocations can also interact according to the reaction:

$$\frac{a}{2}\ [111] + \frac{a}{2}\ [1\bar{1}1] \rightarrow a\ [100] \qquad (5.1)$$

forming an attractive junction (Saada 1961, 1963), this type of junction may be an important source of internal stress, and it produces the hexagonal network of dislocations predicted by Amelinckx and Dekeyser (1959) and observed in many b.c.c. metals, (Carrington et al 1960; Benson et al 1962; Keh and Weissman 1963). When the crystal is deformed along ⟨110⟩ orientation the jogs produced by the interaction of mobile dislocations will have $[\bar{1}11]$ and $[1\bar{1}1]$ active Burgers vectors, then the plane of jogs formed in screw dislocations is $\{011\}$ on which the resolved shear stress is zero because this plane is normal to the stress axis. It will therefore, be difficult to move them conservatively. Since the dislocation multiplication mechanism involves the movement of the screw dislocations over large distances (Low and Turkalo 1962) the macroscopic yielding is believed to occur as soon as the jogs become mobile. Rose et al (1962) suggested that this would happen when, as a result of slight mis-orientation, the stress on the jogs reached a value high enough to move them conservatively. On the other hand, Guiu and Pratt (1966) suggested non-conservative movement of jogs based on the fact that the screw dislocations may become mobile when jogs move non-conservatively, producing point defects. They explained the yield point phenomenon exhibited by the ⟨100⟩ orientation as resulting from the combined effect of a rapid increase in the number of mobile dislocations, the high value of the strain rate sensitivity after the proportional limit, and the low work-hardening rate.

In the ⟨100⟩ orientation the jogs are on planes on which the resolved shear stress is of the same order as that acting on the dislocations themselves. As a result, the screw dislocations will be able to move under relatively low stresses, both because there will be a large number of jogs and dislocation segments available for thermal activation, and because the enhanced conservative movements of jogs may give rise to a larger equilibrium jog spacing. The behaviour above room temperature is explained also in terms of non-conservative movement of jogs with the help of thermal activation on a large number of sites.

Although many workers (Schoeck 1961; Mordike 1962; Gregory 1963; Gregory et al 1963; Lawley and Gaigher 1964) have suggested that the jog movement plays an important role in the deformation of b.c.c. metals, the evidence for the actual mechanism which determines the mobility of the jogs has always been difficult to obtain. The value of the activation energy H is too small to be in agreement with the idea that yielding is controlled by the movement of jogs. The presently obtained value of H of 0.6 eV_A (see Table 5.4) is also much smaller than the energy for vacancy diffusion in niobium. Gregory (1963) and Gregory et al (1963) have reported H of the order of 3 to 4 eV in their polycrystalline niobium close to that for vacancy formation, but this seems to be an exceptional case. In tantalum, Mordike (1962) suggested that the low value of H is determined by the conservative motion of extended interstitial jogs in screw dislocations, but this is not likely because of the high stacking fault energy in b.c.c. metals. There is another difficulty in that it is difficult to accept that a sufficiently high jog density could be built up at the beginning of the plastic deformation. Finally it is difficult to envisage how this mechanism can give rise to the observed difference in tension and compression, unless the jogs are extended, and this possibility is considered unlikely (Schoeck 1961) in view of the high stacking fault energy.

TABLE 5.4

Activation Volume (V) and Energy (H) at 296°K

Stress Axis	V at yielding	V 7.6% total strain	V 20% total strain	H at yielding
⟨110⟩	48.3 b^3	51.48 b^3	52.06 b^3	0.604 eV
⟨100⟩	82.05 b^3	83.21 b^3	83.21 b^3	0.613 eV

The orientation dependence is also expected from the asymmetry in the critical resolved shear stress to move screw dislocations. This asymmetry effect was discovered by Taylor (1928) on single crystals of β brass where the resistance to slip in ⟨111⟩ direction on a given plane is not equivalent to slip in the opposite sense, and that, for a particular orientation of the deformation axis, the slip planes chosen in tension and compression are not equivalent.

If slip occurs naturally on the {112} planes or involves elements of slip on these planes as proposed by Sestak and Zarubova (1965) an asymmetry of the critical resolved shear stress {112} would be predicted if the dislocations are dissociated on these planes. This follows from the non-equivalence of the positive and negative ⟨111⟩ twinning direction on {112} planes in the b.c.c. lattice. Edge dislocations can only dissociate asymmetrically on {112} planes according to the reaction (Frank and Nicholas 1953).

$$\frac{a}{2}\langle 111\rangle \rightarrow \frac{a}{3}\langle 111\rangle + \frac{a}{6}\langle 111\rangle \qquad (5.2)$$

The dissociation occurs in such a way that, if a shear stress acts in the sense of twinning, the $\frac{a}{6}$ ⟨111⟩ twinning partial will glide first. Conversely, if the sense of an applied stress is unfavourable for twinning, the complementary partial $\frac{a}{3}$ ⟨111⟩ will glide first. It is expected that the stress required to move the dislocation in these two cases will be different, since a larger energy change is involved in moving the complementary partial first.

It has also been proposed by Hirsch (1960) and independently by Sleeswyk (1963) that screw dislocations can dissociate into three $\frac{a}{6}\langle 111\rangle$ partials on the $\{112\}$ planes which intersect along the axis of the original screw dislocation. An analysis of the geometry of the partials under an applied stress also predicts that there should be an asymmetry of the stress to move screw dislocations on these planes. As pointed out by Hirsch (1960), the stress required to constrict a dissociated screw dislocation in the b.c.c. lattice may be thermally activated, and may possibly account for the magnitude of the low temperature flow stress. If this is so, it should give rise to an anisotropic Peierls type of stress. Recently, Duesberry and Foxall (1965) and Argon and Maloof (1966) have invoked this argument to explain the asymmetry of the observed slip planes in niobium and tungsten and the difference in yield strength in tension and compression for certain orientation.

Considering the deformation axis in the $\langle 001\rangle$ and $\langle 110\rangle$ directions, the $\{112\}\langle 11\bar{1}\rangle$ slip system is the most highly stressed $\{112\}\langle 111\rangle$ system in both cases, but for compression in $\langle 001\rangle$ and $\langle 110\rangle$ the senses of slip are opposite, so that the sense of slip for tension in $\langle 001\rangle$ is exactly equivalent to that in compression in $\langle 110\rangle$ and vice versa, the only difference is that the components of stress normal to the slip plane are opposite. Any asymmetrical effect will be manifested by a difference in flow stress.

The dissociation of screw dislocations on the $\{112\}$ planes should result in a higher yield stress in the $\langle 110\rangle$ direction for tension than for compression, and the reverse effect in the $\langle 100\rangle$ direction. Even if the stacking fault energy is too high to allow a stacking fault to form, it is expected that there will be an asymmetry of the dislocation core, and a similar anisotropy of the yield stress should result. For the sense of the resolved shear stress on the highly stresses $\{112\}$ planes, unfavourable for twinning, it is predicted that slip will occur either on the lowly stressed planes, or on the highly stressed $\{112\}$ planes, if thermal activation can constrict the partials back on to the slip plane.

Several favourable dissociations of $\frac{a}{2}\langle 111\rangle$ dislocations on the $\{110\}$ planes have also been proposed (Hirsch 1960; Cohen, Hinton, Lay and Sass 1962; Crussard 1962; Kroupa and Vitek 1964). However, a consideration of the sense of slip and the geometry of the partials lying on the $\{110\}$ planes does not lead to an asymmetry of the critical resolved shear stress to move screw dislocations on these planes.

If the core dissociation on the $\{112\}$ planes is the only factor determining the magnitude of the stress to move screw dislocations, the proportional limit for $\langle 001\rangle$ in compression should equal the proportional limit for $\langle 110\rangle$ in tension and vice versa. From the above discussion the difference in the proportional limits in tension and compression can only be accounted for in terms of an asymmetry of the critical resolved shear stress on the $\{112\}$ planes, however, this was not the case in the present investigation. It appears that the orientation dependence of the yield stress in tension and compression cannot be accounted for simply in terms of an anisotropic Peierls-Nabarro stress due to dislocation core asymmetry, some other mechanism must be involved.

5.3.2 Slip and twinning systems

At low temperature only $\{110\}$ slip planes were observed. When the sense of the resolved shear stress on the highly stressed $\{112\}$ slip planes was unfavourable for twinning slip occurred on the $\{110\}$ planes with a Schmid factor of 0.408. In Table 5.2 the data for molybdenum and tantalum (Sherwood et al 1967), and tungsten (Argon and Maloof 1966) are included for comparison.

It can be seen that in niobium and tantalum, slip occurs on $\{110\}$ planes, whereas in molybdenum and tungsten slip occurs on $\{112\}$ planes with a Schmid factor of 0.236. There is another anomaly in the slip and twinning behaviour which cannot be readily accounted for by the splitting of dislocations on the $\{112\}$ planes; at 77°K in niobium, slip occurs on the $\{110\}$. Similar behaviour has been reported at 77°K by Reid et al (1966) in electron beam-melted niobium single crystals.

The causes of the difference in the behaviour of the group VA and group VIA metals with regard to the slip plane may be related to the differences in the stacking fault energy. It has generally been believed that the stacking fault energy on the $\{112\}$ planes is considerably higher for the group VIA metals. Hartley (1966) has calculated, from a consideration of the changes in atomic configuration of faulting, the stacking fault energies and width of the dissociated edge dislocation on the $\{112\}$ planes:

TABLE 5.5

Calculated stacking fault energies and width on the $\{112\}$ planes (d = width of dissociation, a = lattice parameter)

	γ erg/cm^2	d/a		γ ergcm^2	d/a
Nb	150	3.6	Mo	430	3.4
Ta	210	4.5	W	500	3.7

It is likely that the stacking fault energy determines the extent of the core asymmetry, and hence affects the stress required to move screw dislocations on the $\{112\}$ planes. When the sense of the applied stress is unfavourable for twinning, whether dislocations will slip on $\{110\}$ planes or the low stressed $\{112\}$ planes will be determined by τ_{112}/τ_{110}, and ultimately this may be determined by $\{112\}$ slip plane, and hence by the stress required to constrict the partials into the favourable $\{112\}$ slip plane, and hence by the magnitude of the stacking fault energy.

It has been frequently observed in iron and silicon iron (Opinsky and Smoluchowski 1951; Vogel and Brick 1953; Steijn and Brick 1954; Erickson 1962) that the ratio $\tau_{112}/\tau_{110} > 1$ and increases with decreasing temperature and increasing alloy content Thus, for a crystal oriented with the Schmid factor highest for $\{112\}$ slip, there may be a transition to $\{110\}$ slip on lowering the testing temperature. With the deformation axis in the $\langle 110\rangle$ and $\langle 100\rangle$ direction, slip will occur on the $\{110\}$ planes if the following inequality holds:

$$\tau_{112}/0.472 > \tau_{110}/0.408 \qquad (5.3)$$

where τ_{112} and τ_{110} are the critical resolved shear stresses

and 0.472 and 0.408 are the respective Schmid factors on the {112} and {110} planes. This inequality was valid in niobium at 77°K for the sense of stress unfavourable for twinning.

– From the above discussion, the slip planes in niobium cannot be accounted for simply in terms of an asymmetric core dissociation of screw dislocations on the {112} planes.

5.3.3 The occurrence of twinning

There are fewer studies of the twinning mechanism compared with deformation by slipping. The understanding of the twinning mechanism is far from satisfactory; the crystallography, morphology and the effect of temperature, strain-rate, composition pre-straining and specimen dimension and shape are still in dispute. Table 5.6 shows the allowed and forbidden twinning systems in crystals with ⟨011⟩ and ⟨001⟩ orientation in tension and compression.

As shown in Fig. 5.3 and Fig. 5.4 the present observation does not agree with previous predictions and observations. In the crystal with ⟨011⟩ orientation, two allowed systems are more highly stressed in compression tests at 20.4 and 77°K. In the ⟨001⟩ orientation, as seen in Table 5.5, there are no allowed twinning systems in compression, accordingly, no twinning took place at 77°K, but a sporadic load drop was observed at 20.4°K. However, tension in ⟨001⟩ orientation is an ideal orientation for twinning on the Schmid-Boas system of 8 (1$\bar{1}$2) ⟨$\bar{1}$11⟩ with a Schmid factor of 0.500. Nevertheless, no twinning was observed, and on the contrary, the specimen elongated about 12.5% up to U.T.S. after a small rounded load drop at the initial yielding without a further load drop or twinning. This observation is inconsistent with the previous predictions (Sleeswyk 1963; Mitchell 1968). Similar observations on niobium were reported by Reid et al (1966), however, it is not understood why compression along ⟨011⟩ should be more conducive to twinning than tension along ⟨011⟩.

Many workers have reported that the transition fron slip to twinning in b.c.c. metals takes place at higher temperature as

TABLE 5.6

The Schmid factors of the most highly stressed {110} and {112} shear systems

Crystal axis	Most highly stress twinning system		Schmid Boas twinning system	Schmid factor
<011> tension	$(\bar{2}11)\ [11\bar{1}]$	f	3	0.473
	$(211)\ [\bar{1}11]$	f	4	0.442
	$(\bar{1}\bar{1}2)\ [11\bar{1}]$	a	7	0.341
	$(112)\ [\bar{1}11]$	a	8	0.339
Compression	$(\bar{2}11)\ [11\bar{1}]$	a	3	0.468
	$(211)\ [\bar{1}11]$	a	4	0.448
	$(121)\ [1\bar{1}1]$	a	6	0.097
<001> tension	$(\bar{1}12)\ [1\bar{1}1]$	a	1	0.394
	$(112)\ [\bar{1}\bar{1}1]$	a	2	0.463
	$(\bar{1}\bar{1}2)\ [11\bar{1}]$	a	7	0.463
	$(1\bar{1}2)\ [\bar{1}11]$	a	8	0.500
Compression	$(\bar{1}12)\ [1\bar{1}1]$	f	1	0.433
	$(112)\ [\bar{1}\bar{1}1]$	f	2	0.460
	$(\bar{1}\bar{1}2)\ [11\bar{1}]$	f	7	0.474
	$(1\bar{1}2)\ [\bar{1}11]$	f	8	0.494

a = allowed system

f = forbidden system

interstitial impurities are removed (Anderson and Boronis 1959; Simonson 1960; Wellings and Maddin 1962; Koo 1963). McHargue and McCoy (1963) reported the concentration of oxygen, nitrogen and argon in binary niobium alloys above which twinning was not obtained under compression test at 77°K. Their data suggests that twinning is inhibited by the onset of the precipitation of the oxide, nitride or carbide. However, Bowen et al (1967) reported that no twinning was observed in tension at 77°K for an unspecified orientation of ultra pure niobium single crystals. Their crystals were purer than those used in the present work because of a further purification heat treatment near the melting point under ultra high vacuum pressure. This finding is contradictory to the above prediction.

Table 5.6 shows the first twinning stress of ⟨011⟩ oriented single crystals with a different number of zone passes in compression:

TABLE 5.6

Number of zone passes	Testing temperature	
	at 77°K	at 20.4°K
2	41.5 Kg/mm^2	34.6 Kg/mm^2
3	not tested	30.7 Kg/mm^2
5	not tested	40.5 Kg/mm^2

Table 5.6 indicates that firstly, the primary twinning stress at 20.4°K does not vary systematically with increas ng numbers of zone passes, i.e. increasing purity. The present observation does not agree with the previous observation that an increase in the overall purity facilitates deformation by twinning in pure and alloyed b.c.c. metals. However, this opposite effect has also been reported by Low and Fenstel (1953) and the present result of non-systematic change of twinning stress with increasing purity agrees with the observation in ultra pure iron, by Altshuler and Christian (1966).

Secondly, it was observed that the first twinning stress at

20.4°K was found to be much lower than that at 77°K and that the twinning behaviour was remarkably different at the two temperatures. This anomalous twinning behaviour at these two temperatures has not been previously reported. The specimen at 77°K underwent prolific twinning with audible clicking before slip took place, this twinning produced a load drop of more than 50% and was then followed by repeated twinning and slip without any work-hardening at a much lower stress level than the first twinning stress. In the specimen at 20.4°K, however, repeated twinning and slip took place in the same manner as at 77°K after a relatively small load drop at the first twinning, but the specimen continued to work-harden with increasing plastic deformation. The compression specimens had the following dimensions: for the 77°K test, gauge length 6 mm, gauge diameter 2.5 mm, whilst the specimen for 20.4°K had 2.5 mm gauge length and 1.27 mm gauge diameter. The 77°K test was performed on an Instron machine with a 10 ton load cell, whereas the 20.4°K test was performed by a screw driven Polanyi type machine. Therefore, it was impossible to decide whether this marked difference in the first twinning stress and subsequent twinning behaviour was due to the variations in the hardness of the testing machines, or to differences in the specimen dimension or genuinely had arisen from differences due to the testing temperature.

5.3.4 Special features of the crystals with ⟨111⟩ orientation

The conventional geometrical softening which has been observed in hexagonal zinc and cadmium (Chalmers 1959; Schmid and Boas 1935) is associated with large initial values of Θ and λ. If the angle between the operative slip plane and the tensile axis is defined as λ, and the angle between the slip direction and the tensile axis is defined as Θ, the factor $\sin\Theta\cos\lambda$ will increase during rotation if both Θ and λ are initially greater than 45°. The resulting deformation is not uniform but takes place by a type of yield phenomenon in which the first part of the crystal to yield undergoes considerable extension, and the stretched part then gradually spreads along the crystal under substantially constant stress if the stress is maintained. This process cannot occur without the slip plane at the end of

the slipped region being considerably bent. The bend can be accounted for by a pile-up of dislocations which subsequently leave the crystal as the slip planes again become straightened. In this case one slip system predominates throughout deformation.

Brindley et al (1962) found geometrical Luders propagation in copper base alloys of the so-called 'soft orientation' in a region extending inward from the ⟨110⟩ corner orientation. They observed that during the Luders extension a geometrical front passed along the crystal, the cross-section changed from circular to elliptical, and the measured flow stress varied by about 10% giving rise to an undulating curve between 77° and 473°K. However, this phenomenon would be very difficult in the b.c.c. metals, especially for an orientation where multiple slip occurs at an early stage of deformation.

At lower temperatures, 77°, 195° and 276°K, as seen in Fig. 5.8 most deformation was confined to a single lamella in which the shear strain was extremely high, however, as the testing temperature increased, the degree of severe shear d deformation was less remarkable and apparent kink bands were formed along the gauge length. A large rounded load drop in the load elongation curves was associated with the formation of a lamella due to the severe shear necking, and occasionally, a large rise in flow stress produced a second elliptical transition region in the crystal yet to be deformed, leading to the second reduction in the flow stress. These were directly observed in a room temperature test.

Previously Votava (1964) has reported catastrophic flow behaviour in niobium single crystals of similar orientation at room temperature. He observed a small load drop, each of which was associated with the formation of a planar constriction in the crystal and he attributed the effect to geometrical softening by intensification of the applied stress due to lattice rotation. However, the crystallographic observation or illustration are not presented in his work, therefore, it is not certain at present whether Votava was reporting the same phenomenon as that observed here. His tensile specimen, however, was prepared by varying the

power supplied during zone-melting, and this technique could lead to variation in specimen diameter and straightness along the gauge length, which could give bending of the specimen and could affect the yielding and flow behaviour. Jaoul and Gonzalez (1961) have considered geometrical softening and shown that the maximum rate at which the shear stress on a slip system increases with respect to strain, occurs in crystals with longitudinal axes initially near ⟨111⟩ axis. Since the strain rate in b.c.c. metals is a very sensitive function of the applied stress, he predicted that this process may contribute significantly to the occurrence of the plastic instability after a short incubation period.

The present observation shows that the catastrophic flow behaviour becomes more marked with decreasing test temperature. This implies that local adiabatic heating is related in some way with this anomalous behaviour. Basinski (1957) and Basinski and Sleeswyk (1957) proposed a "thermal instability" in order to explain serrated flow behaviour of polycrystalline iron and aluminium at 4.2°K. They ascribed the thermal instability to adiabatic heating of specimens as a consequence of plastic deformation. Owing to the small specific heat and low thermal conductivity at low temperature, the temperature of the slipped region increases significantly and the flow stress is lowered. This effect produces the load drop. However, this possibility has been denied by Reid et al (1966) by determining the temperature rise of $\Delta T = 0.3°C$ for their niobium single crystals at 77°K using Basinski's formula (1957) and concluded this effect is negligible by comparison with geometrical softening.

At 77°K Reid et al (1966) observed very localized shear deformation very similar to the present result in Fig. 5.8 and reported the shear direction to be near ⟨100⟩ and the plane of shear {011}. Similarly, in the present work, the same shear direction and plane were found to {011} plane. They suggested that the dislocations with ⟨100⟩ Burgers vector are mobile on {110} plane and that such dislocations are originally generated in this crystal by the association of dislocations with ⟨111⟩ Burgers vectors and this is a result of the low value of the anisotropy factor $A = \frac{2C_{44}}{C_{11} - C_{12}} = 0.53$ at 77°K.

Their suggestion was based on the estimation of dislocation width and ease of motion which have been made for various low index dislocations in the manner described by Reid (1966) involving elastic constants. However, according to recent work on the temperature dependence of the elastic constants of niobium single crystal by Armstrong et al (1967) the anisotropy factor A decreased to a broad minimum value of 0.49 around 203°K, then increased to a value at 923°K which was 10% higher than that at room temperature. Thus, as the temperature increased, the anisotropy factor A indicated a trend toward greater isotropy. If the low value of the anisotropy factor is the only reason for this catastrophic behaviour at this temperature, then there should be a maximum effect observed at this temperature (around 203°K) where the anisotropy factor A is minimal. But this was not the case in the present investigation.

The direct observation of mobile ⟨100⟩ dislocations has been reported by Dingley and Hale (1966) in electron microscopy studies of iron and iron alloys. The value of $\underline{g}$ used to distinguish between ⟨111⟩, ⟨110⟩ and ⟨100⟩ dislocations were $\underline{g} = (123)$, $\underline{g} = (222)$ and $\underline{g} = (013)$ respectively, and about 20% of total dislocations were found to be of the ⟨100⟩ type. The proportion was unaffected by the temperature of deformation, alloy content, the amount of strain or strain rate. In contrast, Lorreto and Reid (private communication) observed less than one percent of the total dislocations to be of the ⟨100⟩ type. Thus, the explanation in terms of mobile dislocation of ⟨100⟩ type appears to be premature at this time.

It appears from the preceding discussion that the plastic instability observed in this orientation between 77° and 373°K in tension may arise from neither of the above-mentioned theories alone. The change of cross-section of the specimen from circular to elliptical shape and local shear deformation was so extreme, that the load drop in the load elongation chart does not necessarily represent true geometrical softening. It is thus difficult to adopt the conventional sense of geometrical softening. If a large number of dislocations move simultaneously, then a load drop will be produced in the load elongation curve by the rapid multiplication and motion of dislocations. This effect could be less

important at intermediate temperatures because of the ease of cross slip. Although the load drop was observed not only at 77°K but also between 195° and 373°K in the present case, the catastrophy on the specimen was more pronounced with decreasing testing temperature. This suggests that the contribution of adiabatic heating may be also responsible in certain degrees.

5.3.5 Orientation dependence of yielding and work-hardening

From the observation of the orientation dependence of yielding and work hardening in Fig. 5.1 and Fig. 5.5, it can be said in general terms, that the initial work-hardening is dependent on the number of active slip systems, consequently this work-hardening rate determines the type of yielding.

In the case of the ⟨001⟩ deformation axis, ther are approximately twice as many active slip systems as for the deformation axis in ⟨011⟩ direction. Considering the barriers formed by dislocations resulting from a reaction of the type

$$\frac{a}{2}\langle 111\rangle + \frac{a}{2}\langle 1\bar{1}1\rangle \longrightarrow a\langle 100\rangle \qquad (5.4)$$

When the deformation axis is in the ⟨011⟩ direction, and if only the plane with the maximum resolved shear stress is considered to be active, the a⟨001⟩ may lie in three different directions on each slip plane (Guiu 1965).

When the deformation axis is in the ⟨001⟩ direction there are four active slip directions and, as a result, six different reactions as described by Rose et al (1962). At the same time these dislocations may lie in five or six different directions depending on whether the slip is of {110} or {112} type. As a result a higher dislocation density and smaller and denser network of obstacles would be expected on each slip plane. By analogy of the role of Cottrell-Lommer sessile dislocations, in the hardening of f.c.c. metals, this would result in a more profuse dislocation tangling (Benson et al 1962; Ohr and Beshers 1964), higher dislocation density and smaller cell structure (Keh 1965) and a strong long range internal stress (Li 1963).

The dislocation etch pit studies also revealed significant anisotropy on the same etching plane for various crystal orientations. Argon and Maloof (1966) observed that the rate of dislocation multiplication in the crystal with ⟨011⟩ deformation axis is about twenty times less than the rate of multiplication in all other orientations of zone-melted tungsten crystal. Guiu (1965) observed some indication of cell structure in the crystal with ⟨011⟩ deformation axis in molybdenum single crystals. He suggested that multiple splitting of the Laue spot after deformation may be an indication of cell structure which will produce a similar effect to forming within the lattice roughly defined sub-boundaries (McLean 1962; Li 1963).

Weissman (1962), in examining the strain distribution before and after the upper yield point, found some evidence that the upper yield point is associated with initiation of the secondary slip system. In the deformation of single crystal tantalum and tungsten, if the deformation axis is such that many systems can operate simultaneously, no yield point will appear. If the orientation is such that one or two systems are active first and the rest are activated by the internal stress, at later stages of deformation, a yield point appears due to the relaxation of the internal stress. Johnston (1962), in his calculated stress-strain curves, demonstrated that a severe work-hardening rate completely eliminates the yield drop, although there is still a definite yield point.

The mechanism of work-hardening in b.c.c. metals has been so little investigated in the past that it would be premature to aim at a reasonable understanding of the orientation dependence of the work-hardening without more precise knowledge. However, it appears important to realise from the evidence presented, that it is feasible to correlate a large work-hardening with a larger number of slip systems which result in the yield point phenomenon. For instance, the crystal with ⟨001⟩ tensile axis exhibits a sharp yield point after strain ageing treatment where the work hardening is relatively low.

CHAPTER 6

CONCLUSIONS AND SUMMARIES

and

SUGGESTIONS FOR FUTURE WORK

CHAPTER 6

6.1 Conclusions

The work in the first part of the present study has been devoted to the evaluation of the various pertinent parameters in the electron beam zone melting of niobium crystals. The effects of these parameters on certain measurable properties were:

i. A good agreement was found between yield stress, hardness, strain ageing behaviour, electrical resistiv y ratio and chemical analysis in the evaluation of the purification caused by varying the zone-melting parameters.

ii. The improvement in overall purity achieved with increasing number of zone passes was found to be greater between one and two zone passes, then diminishing between subsequent zone passes.

iii. A fast zone speed resulted in a crystal of low purity and caused a considerable gradient in impurity distribution along a single crystal rod. This arose from an increase in the value of the effective distribution coefficient.

iv. No significant difference in the impurity distribution profile was observed between zone-levelled and zone-refined crystals when the same zone speed was used.

v. The vacuum pressure during the zone-melting process was found to be the most influential parameter in controlling the purity of the crystal.

vi. The progress of purification, and the improvement in the vacuum pressure of the furnace with time were in good agreement. This implied that the removal of the products of volatilisation and degassing by the vacuum system, was a major part of the purification. Vacuum distillation of lower melting point elements would also be promoted by decreasing the furnace pressure.

vii. Chemical analysis showed that improvement in overall purity due to further zone passes was most likely due to the reduction of carbon or nitrogen contents. This might be associated with the observed higher yield stress and the discontinuous yielding behaviour in the crystals with the least number of zone passes.

The results on the effect of the overall impurities on the yielding and strain ageing behaviour has shown:

i. The temperature dependence of the yield stress was decreased markedly with increasing overall purity for both ⟨110⟩ and ⟨100⟩ orientations. It was found that the temperature dependence of the yield stress was followed linearly by $\log \sigma - T$ relationship, and the difference in the yield stress between pure and less pure crystals can be expressed as $\Delta\sigma = A e^{-BT}$.

ii. Gilman's "reaction rate theory" which is based on the multiplication and velocity characteristics of dislocations provided the best explanation of the yielding and temperature dependence of the yield stress in the present work. This suggests that the impurity contribution to the yield stress is proportional to the square root of the concentration of interstitial impurities - a result that was found by Stein and Low (1966) for iron.

iii. The strain rate sensitivity of pure and less pure crystals cannot be adequately explained on the basis of a single thermally activated process.

iv. The strain ageing kinetics may be divided into two stages: the one stage below 473°K where the Cottrell-Bilby $t^{2/3}$ law is obeyed, and the second stage above 473°K where the ageing factor is insensitive to the ageing time when stress-induced ordering takes place.

v. The strain ageing kinetics and consequently the activation energy of diffusion of interstitials are strongly influenced by the initial and relative concentration of interstitials present in the crystal.

vi. After strain ageing yield points were observed for the crystals with ⟨100⟩ tensile axis. This may be caused by the low work-hardening where the strain ageingg took place, or by the anisotropy of shear stress in the sense of shear direction in the vicinity of the dislocation core.

Mechanical tests on niobium single crystals with a symmetrical orientation has shown:

i. At high temperatures the yield stress was found to be independent of the orientation of the crystal and of the sense of the applied stress.

ii. At low temperatures, the yield stress was strongly dependent on the orientation and the sense of applied stress. In tension ⟨110⟩ orientation showed a higher yield stress compared with the ⟨100⟩ orientation, however, the yield stress in compression for ⟨110⟩ was higher than for ⟨100⟩ above 200° and below 100°K.

iii. The observed difference in the yield stress in tension and compression may be accounted for in terms of an asymmetry of the critical resolved shear stress on the {112} plane. If the core dissociation on the {112} plane is the only factor determining the magnitude of the stress to move screw dislocations, then the yield stress for ⟨100⟩ in compression should be equal to the yield stress for ⟨110⟩ in tension, however, this was not so in the case of the present observation.

iv. No current theory of orientation dependence is thought to be adequate, however, there seems to be rough correlation between the number of slip systems and the low value of the yield stress with a high work-hardening rate which subsequently affects the yielding behaviour.

v. The crystal orientation most favourable for twinning under compression is the ⟨110⟩ orientation; although

equivalent in terms of shear stress, the crystals with ⟨100⟩ axis in tension did not twin.

vi. There was no systematic variation in the first twinning stress with the interstitial impurity content of the crystals.

vii. Catastrophic, very loca-lized flow behaviour was observed for crystals with ⟨111⟩ tensile axis: the plane of shear was found to be near {110} and the shear direction near ⟨100⟩. However, it is still premature to be interpreted in terms of mobile dislocations with ⟨100⟩ Burgers vectors. The load drop in the load elongation curve which was caused by the change of cross-section of the specimen from a circular to an elliptical shape and local shear necking does not necessarily correspond to geometrical softening. However, the catastrophic shear necking of the specimens was more pronounced with decreasing testing temperature which suggests that this behaviour may be caused by a combination of adiabatic h heating at localized necked regions and geometrical softening.

SUGGESTIONS FOR FUTURE WORK

It has been shown that inherent lattice hardening is not the dominant source of low temperature strength in b.c.c. metals, and the interstitial impurities do contribute a major part of the strength. It would be interesting to investigate the interaction of dislocations with interstitial impurities by strain ageing experiments, microstrain measurement in the region of 10^{-6} - 10^{-8} strain and internal friction measurements. These experiments could be carried out for various crystal orientations as a function of temperature, strain rate and impurity content.. This could enable a comparison to be made of the amount of interstitial dislocation interaction determined by three different methods, In the present work Gilman's reaction rate theory (1965) gave fair agreement to the temperature dependence of the yield stress, however, further experiments would be necessary to differentiate between the two models involving lattice hardening and solution hardening. Mechanical testing both in tension and compression at very low temperatures, say between 4.2 and 20°K, for various orientations doped with known amounts of interstitials, should help in this.

At the moment, it appears that there is no acceptable explanation of the observed orientation dependence of the deformation behaviour of b.c.c. metals, or its dependence on the sense of the applied stress. There is an asymmetry in the critical resolved shear stress for slip on $\{112\}$ planes at low temperature, but it is difficult at this stage to predict the right magnitude of the asymmetry since the value depends on the value of the stacking fault energy and on the elastic anisotropy factor of the particular plane and no reliable values are known for these factors. It would be of great value to investigate the effect of temperature upon the orientation dependence of the slip plane both in tension and compression since there is no general agreement on the operative slip planes. The observation of a $\{110\}$ $\langle 100 \rangle$ slip system with marked shear necking at 77°K for $\langle 111 \rangle$ orientation in tension, both in the present work and in that of Reid et al (1966), posed another difficulty in this subject. Examination of the specimen deformed

under this condition with electron microscopy would be of great interest. However, in this study one must use the low order diffracting vectors because of anomalous dislocation invisibility with high order diffracting vectors in Burgers vector determination (France and Loretto 1968; Dingley 1968). The jog theory however, predicts the correct variation with orientation to explain the work-hardening, but the difficulty with this theory is that it is difficult to believe a sufficiently high jog density could be attained. Further experiments would be necessary before the effect of the orientation and the difference between tension and compression could be properly explained. Measurements of the resistivity ratio, in conjunction with a transmission electron microscopy study might indicate the number of jogs which are moving non-conservatively, which on the jog theory, would be different for ⟨110⟩ and ⟨100⟩ orientations.

phys. stat. sol. 14, K151 (1966)

Department of Metallurgy, Imperial College, London

Yielding and Strain Ageing of Niobium Crystals

By

H.C. KIM and P.L. PRATT

One of the characteristics of the b.c.c. metals is a rapid increase in yield stress with decreasing test temperature followed by a transition from ductile to brittle behaviour. Generally the yield stress decreases and ductility increases with increase in purity. To account for these effects various theories have been proposed (1, 2, 3). Due to the lack of detailed experimental work on various high purity single crystals a reliable quantitative comparison between theories and experimental data is still lacking.

Previous investigations of some b.c.c. metals purified either by electron bombardment zone melting (4, 5), or by the decarburizing technique (6, 7), showed a large decrease in the temperature dependence of the yield stress by increasing the overall purity. In this note, some effects of impurity on the mechanical properties of single crystals of niobium are presented.

Single crystals of niobium, 3 mm in diameter 25 cm in length, were grown by an electron beam zone melting technique at a zone speed of 2.5 mm/min, in an initial vacuum of 6×10^{-6} Torr which gradually improved to 3.5×10^{-6} Torr at the end of one zone pass. The purity of the single crystals reached the limit of detection by chemical analysis after one pass, and no significant differences could be seen between one and four zone passes. However tensile tests, hardness tests, and the electric resistivity ratio $\left(R_{273^\circ K}/R_{77^\circ K}\right)$, showed a pronounced difference between one and two zone passes and a less pronounced difference beyond two zone passes. The results are plotted as a function of the number of zone passes in Fig. 1. The decrease in yield stress, and hardness, and the increase in resistivity ratio indicates an increase in overall purity with further zoning. Similar results were reported by Lawley et al. on zone melted molybdenum single crystals (4).

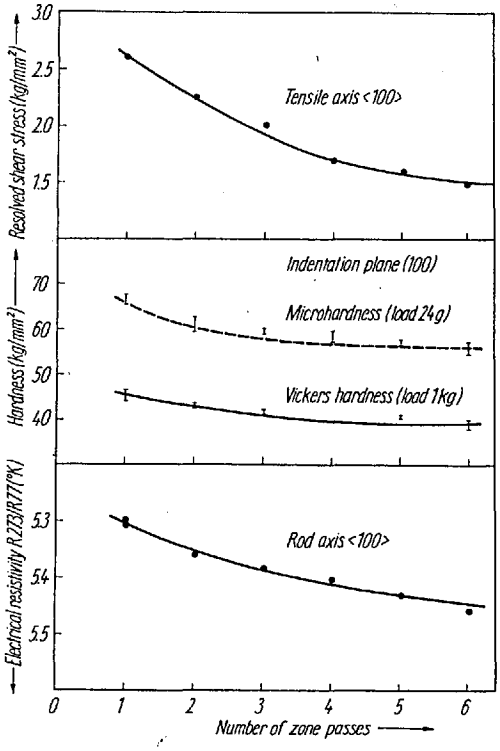

Fig. 1. Variation of resolved shear stress, hardness, and electrical resistivity ratio with number of zone passes

Tensile specimens with a gauge diameter of 2.8 mm and a gauge length of 16 mm were sparkmachined with a shoulder radius of 6 mm and subsequently electropolished. Tensile tests were performed in Instron Universal testing machine at a cross head speed of 0.05 cm/min at temperatures of 373, 296, 273, 245, 195, and 77 °K.

The stress-strain curves were very anisotropic and an orientation dependence similar to that observed in molybdenum (9), tungsten (8), and tantalum (10) was noted below 245 °K. The <110> orientation yielded smoothly at 373 °K but below room temperature yielded discontinuously with a preyield microstrain followed by an upper and lower yield point. The amount of yield drop depended on the purity level. The <100> orientation yielded smoothly at all temperatures with a lower proportional limit and higher work hardening rate than the 110 orientation. The yield stress was determined at the limit of proportionality to enable a comparison between the two orientations to be made.

In Fig. 2 the temperature dependence of the proportional limit of <110> crystals is shown for the different number of zone passes. From this it can be seen that by increasing overall purity the temperature dependence of the yield stress is decreased significantly. A similar trend was also observed for the <100> orientation. A similar behaviour has been reported by Lawley et al. on molybdenum (4), by Koo on tungsten

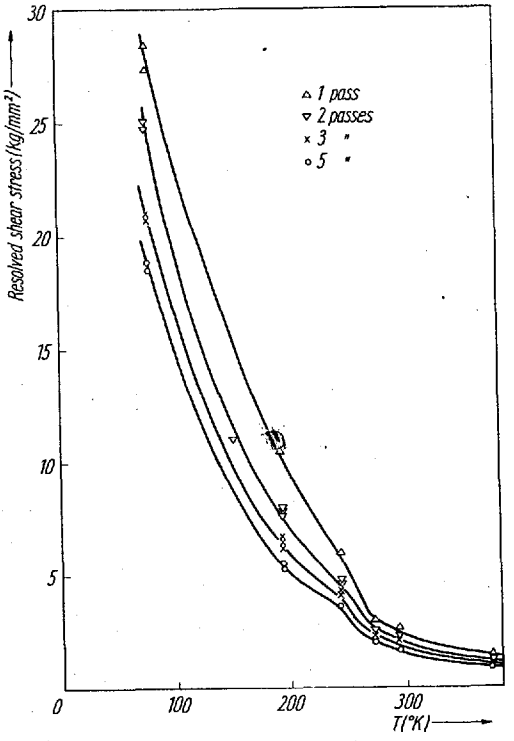

Fig. 2. The effect of temperature on the proportional limit of crystals with tensile axis in the <110> direction with cross head speed of 0.05 cm/min.

(5), and by Stein et al. on iron containing < 10 ppm C (6, 7).

All the specimens deformed entirely by slip at all the temperatures investigated. Twinning was never observed. The crystals with <110> orientation necked down immediately after the upper yield point but <100> crystals with two zone passes extended 12.5% before the UTS at 77 ^{o}K.

The effects of impurity were also prominent on the strain ageing. A series of experiments were carried out on one zone pass crystals of <110> and <100> orientations. For the <110> orientation, specimens of two different purity levels were tested at room temperature, one batch of a standard purity and the other grown under a vacuum of 4×10^{-5} Torr.

As seen in Fig. 3: the less pure crystals showed a higher proportional limit, and higher upper and lower yield stresses at the initial yielding. They showed a larger yield drop after a shorter ageing time, and at a lower temperature, than the purer crystals. The activation energy for the return of the yield drop was found to be 19.8 kcal/mol. This is less than the values obtained by Power and Doyle (11) for the diffusion in niobium of oxygen, nitrogen or hydrogen, (27 kcal/mol for oxygen being the smallest value they obtained). The major difference between the initial yielding and the yielding after

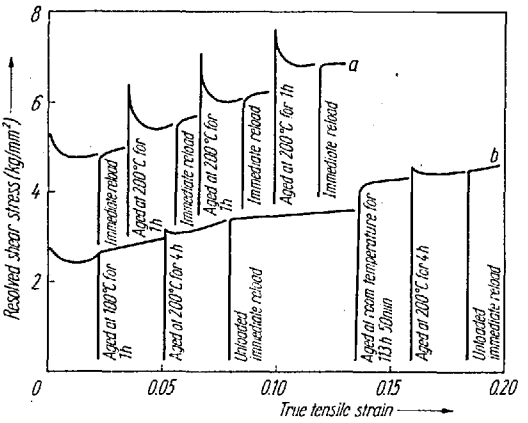

Fig. 3. The effects of impurity on the strain ageing characteristics of one zone pass crystals with tensile axis in the ⟨110⟩.
a) pressure during melting; $4 \rightarrow 3\times10^{-5}$ Torr,
b) pressure during melting; $6 \rightarrow 3\times10^{-6}$ Torr

strain ageing was that in the former preyield microstrain was followed by a round yield drop, whilst in the latter the yield drop was sharp with no preyield microstrain. The crystals with ⟨100⟩ orientation which did not yield discontinuously at initial yielding showed sharp yield drops after strain ageing as also observed in tungsten single crystals (12).

Further results with a detailed discussion will be presented in a later paper.

The authors would like to thank Prof. J.G. Ball for providing laboratory facilities in the Department of Metallurgy, and the members of the b.c.c. group in this department for helpful discussions. We are grateful to C.E.G.B. for financial support, and to the D.S.I.R. (now S.R.C.) for providing the Instron machine.

References

(1) A.H. COTTRELL and B. BILBY, Proc. Phys. Soc. 49, A 62 (1949).
(2) H. CONRAD, Symposium on Structure and Mech. Props. of Metals, N.P.L. 1963.
(3) R.L. FLEISCHER, Acta metall. 10, 835 (1962).
(4) A. LAWLEY, J. VAN DEN SYPE, and R. MADDIN, J. Inst. Metals 91, 23 (1962).
(5) R.C. KOO, Acta metall. 11, 1083 (1963).
(6) D. STEIN, J.R. LOW, and A.U. SEYBOLT, Acta metall. 11,

1253 (1963).
(7) D. STEIN, Acta metall. 14, 99 (1966).
(8) R.M. ROSE, D.P. FERISS, and J. WULFF, Trans. AIME 224, 981 (1962).
(9) F. GUIU and PH.D. THESIS, London University 1965.
(10) P.J. SHERWOOD, Private Communication.
(11) R.W. POWER and M.V. DOYLE, J. appl. Phys. 30, 514-524 (1959).
(12) H.W. SCHADLER and J.R. LOW Jr., General Electric Res. Rep. No. 62-GC-206, 1962.

(Received February 14, 1966)

Mat. Res. Bull. Vol. 2, pp. 323-335, 1967. Pergamon Press, Inc. Printed in the United States.

THE PROPERTIES OF NIOBIUM CRYSTALS PRODUCED BY ZONE-MELTING

H. C. Kim and P. L. Pratt
Department of Metallurgy
Imperial College
London S. W. 7., England

(Received January 9, 1967; Communicated by P. L. Pratt)

ABSTRACT

The effects of the number of passes, the zone speed and direction, and the vacuum pressure during zone melting of niobium were evaluated by measurements of electric resistivity ratio, hardness, and yield stress, and by strain ageing experiments and chemical analysis. High zone speeds resulted in a significant increase in the effective distribution coefficient in the zone levelling process. The most important contribution to purification was found to be the vacuum pressure in the furnace during melting. The carbon and nitrogen contents were reduced with increasing number of zone passes, and this may be associated with the lower yield stress and less marked discontinuous yielding behaviour.

Introduction

The electron beam zone melting technique has been used by many workers for preparing pure single crystals of the b. c. c. transition metals for mechanical tests. The purity of the crystals has commonly been assessed by measurements of resistivity ratio (1), hardness (2, 3), tensile strength (4) and by chemical analysis (5). However, in this investigation strain-ageing experiments were also used for the purpose of this evaluation.

Experimental Apparatus and Techniques

Description of Electron Beam Apparatus

The cylindrical furnace chamber, made from mild steel protected by nickel plating, is cooled by running water. This chamber is evacuated from

below by an oil diffusion pump, 6 inches in diameter and with a capacity of 300 litre/sec. A liquid nitrogen cold trap between the diffusion pump and the chamber reduces the back-streaming of oil vapour. On one side of the furnace wall there is a quartz window protected by a moveable radiation shield and a silica glass plate. The pressure is measured by an ionisation gauge with its head connected to the side of the chamber.

A stainless steel 'cold finger', filled with liquid nitrogen, attached to the lid of the chamber, acts as a getter, thereby improving the vacuum.

The cathode is mounted on a lead screw driven by a variable speed motor with a reduction gear. The cathode travels at speeds between zero and 30 mm./min. The specimen and all other parts of the furnace are earthed, while the cathode, run at a high negative voltage, is insulated by two 'pyrophylite' blocks.

The cathode assembly used in the initial stages is similar to the one developed by Cole et al. (6). In this the filament is hidden from the molten zone to avoid contamination of the crystals by metallic elements emitted from the filament, and to avoid coating of the filament with the metal ejected or evaporated from the molten zone. Because of the high impedance of this design, the emission current was very low, making power control difficult and resulting in poorly shaped crystals. In addition no sputtering from the molten zone was encountered when niobium crystals were grown, and so a direct focussing cathode of low impedance was constructed, in collaboration with P. J. Sherwood. The top and bottom focussing plates are made of molybdenum, while a tungsten filament, 0.5 mm. in diameter, is supported horizontally by a leg resting on the bottom focussing plate. This ensures that the plates are at the same potential so that the electrons are focussed electrostatically. The high voltage power supply is controlled by a circuit similar to that of Birbeck and Calverly (7).

Operating Characteristics and Procedure

With water cooling of the furnace chamber, the vacuum pressure in the furnace was about 6×10^{-6} torr. When the cold finger was filled with liquid nitrogen the pressure improved to 2.5×10^{-6} torr. On maintaining the rod at

the melting point the pressure rose to 9×10^{-6} torr., but after several minutes decreased to about 4×10^{-6} torr.

A stable molten zone 3 mm. long, in a 3 mm. diameter rod, could be formed using a voltage of 2.5-2.6 KV and emission current of 77-80 mA during the first zone pass. This gave a melting power of 200 watts. The second pass required slightly less power, about 184 watts. A 6 mm. diameter rod of the same material required 558 watts at 6.2 KV and 90 mA. Figure 1 shows the cathode assembly and the configuration of the molten zone of a 3 mm. diameter rod for the downward pass.

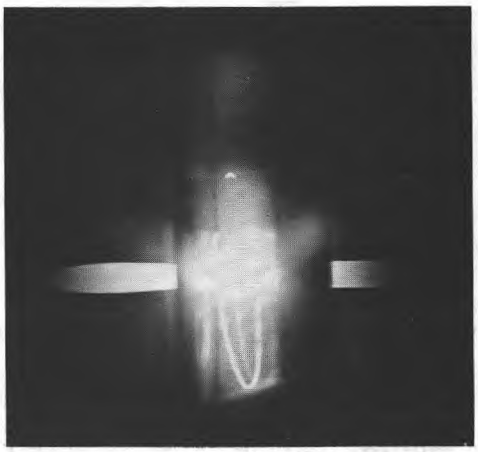

FIG. 1.
Cathode Assembly

The starting material in the form of electron beam melted rod was supplied by Fansteel-Hoboken, Belgium. A chemical analysis of the starting material, made by E. I. Du Pont de Nemours & Company, U.S.A., is shown in Table 1.

The polycrystalline rod, 3 mm. in diameter and 28 cm. long, was mounted in the furnace and subjected to zone melting. After completing the first zone pass, the power was decreased taking the crystal below its melting temperature. Uniformity in the distribution of impurity along the crystal can be achieved by a zone levelling (8) technique, with a number of zone passes alternately in opposite directions. For zone levelling the crystal was remelted at a distance of 7 zone lengths from the last freezing zone and the second pass resumed. This procedure was adopted to avoid disturbances in orientation, and also to avoid contamination from heating of the chuck and from the solute accumulated at the end of the rod after the first zone pass.

The variation of vacuum pressure with time using the zone refining process, the zone levelling process, and fast zone levelling, are shown in Fig. 2. In all three cases there is an appreciable fall in pressure after the first pass. Thereafter the decrease is less with subsequent zone passes.

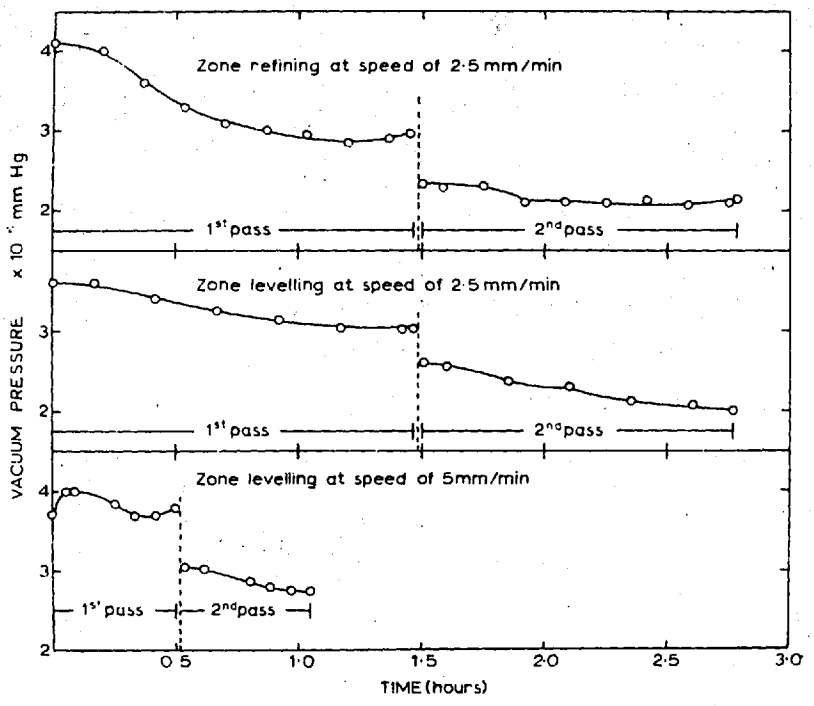

FIG. 2.

Variation of Vacuum Pressure During Zone Melting

To evaluate the influence of the variables controlling electron beam zone melting, single crystals were grown as follows:

Type A crystals	By zone levelling at a zone speed of 2.5 mm./min. with various numbers of zone passes.
Type B crystals	By zone levelling at a zone speed of 5 mm./min. with two zone passes.
Type C crystals	By zone refining at a speed of 2.5 mm./min. using two zone passes.
Type D crystals	By zone refining at a speed of 2.5 mm./min. at different vacuum pressures with one zone pass.

Seeding of Oriented Crystals

A randomly oriented crystal was fixed to a 6 mm. diameter stainless steel cap which was then sliced through a plane normal to the desired orientation. The cut surface was attached by a screw to the horizontal plane of the holder so that the seeding direction coincided with the vertical axis of the rod.

Subsequent crystals of the same orientation were grown by using a length of previously grown crystal as a seed. The misorientation of the axis of crystals grown by this method was less than 3° from the desired orientation.

There was no definite preferred orientation of crystals, grown without seeding, after one zone pass. However, the crystals tended to grow with their axes closer to <110> than to any other orientation. Similar results were reported on iron single crystals grown by strain annealing, using zone refined iron (9).

TABLE 1.

Chemical Analysis of Starting Material, and of Single Crystals After One and Four Zone Passes

		Weight in p. p. m. O_2	H_2	C	N_2
Starting Material		29	1	7-8	63
One pass	(1)	12	*	7-9	28
	(3)	21	*	*	35
4 passes	(1)	37	*	4	20
	(3)	29	*	*	31

Precision of Method: O ± 3 p. p. m.
H ± <1 p. p. m.
* not determined. C ± 5 p. p. m.
N ± 2 p. p. m.

Preparation of Single Crystals

In order to avoid the complexity which may arise from crystallographic geometry all the tests were carried out on specimens oriented in the <110> orientation. This orientation was chosen because preliminary experiments showed that the yielding behaviour was influenced by impurities to a greater extent than in any other orientation.

Tensile specimens were produced using a Servomet SMD Spark machine. As-grown single crystals of 3 mm. diameter were cut into 3 cm. lengths by the spark slicer. They were then spark lathed, starting from range 3 and finishing at range 7, which is the finest range. In this way the tensile specimens were given a 16 mm. gauge length with a shoulder radius of 3 mm. The final diameter of the specimens was 2. 7-2. 8 mm. depending on the uniformity of the diameter of the as-grown crystal. The deformed layer, 100 microns thick due to the spark lathing, was subsequently removed by electropolishing for 1 hour at a voltage of 15-17 volts and 0. 3-0. 4 Amp.

Evaluation of Specimens

The resistivity ratio has long been used as a measure of impurity content present in solid solution. This has been described in detail by Kunzler and Wernick (1). In the present investigation, resistances were determined at

low temperatures in a liquid nitrogen bath (77°K) and at high temperatures in a mixture of ice and water (273°K), for varying numbers of zone passes.

Hardness measurements were made on a cross section at one end of the tensile specimen, after preparation by spark planing and subsequent chemical polishing for 45 sec. in 7 parts of HNO_3 and 3 parts of HF. Since it is well known that the microhardness value under low load is higher than the value obtained from macrohardness it was decided to carry out both types of hardness measurements.

Indentations were made with a Reichert microhardness tester using a load of 24 gms. and a Vickers hardness tester using a load of 1 Kg.

Tensile tests were performed at a strain rate of 4.9×10^{-4} sec.$^{-1}$. The stress at the first deviation from linearity on the stress-strain curve was taken as the yield stress of each crystal, i.e. the proportional limit.

For the strain ageing experiments two single zone pass crystals of identical orientation were grown at the same zone speed. However, one was grown at pressures between $4.4\text{-}3.9 \times 10^{-5}$ torr. and the other, at pressures between $4.9\text{-}3.0 \times 10^{-6}$ torr. They were then prestrained at room temperature at a strain rate of 4.9×10^{-4} sec.$^{-1}$, unloaded, and then given ageing treatments at 296°, 373° and 473°K for various times.

Experimental Results and Discussion

Effect of Number of Zone Passes, Type A Crystals

In the zone melting technique the degree of purification depends on the purity of the starting material, because the amount of solute removed by each pass is only a fraction of the amount present beforehand. Hence, under identical conditions of zone length, vacuum pressure during melting, zoning speed and direction, and starting material, the purification achieved should depend solely on the number of zone passes. This fact has been confirmed by previous workers on electron beam melted niobium (4) and tungsten (10) by means of yield stress, and on molybdenum by means of hardness (11).

The present results of resistivity ratio $R_{273}/R_{77°K}$, microhardness and Vickers hardness, and yield stress, are presented in Fig. 3 as a function

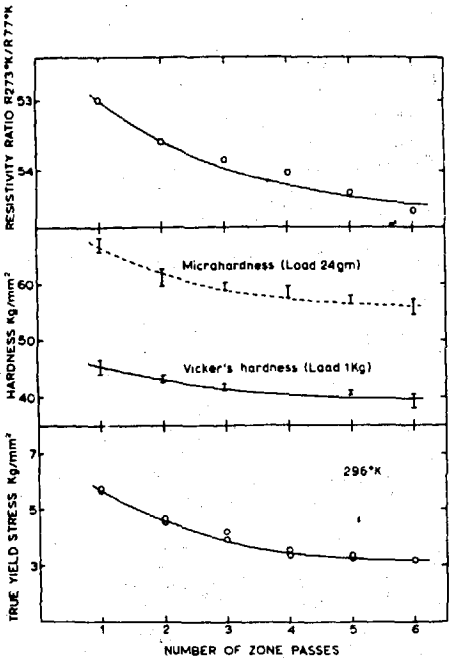

FIG. 3.

Variation of Resistivity Ratio, and Hardness and Yield Stress at Room Temperature with Number of Zone Passes.

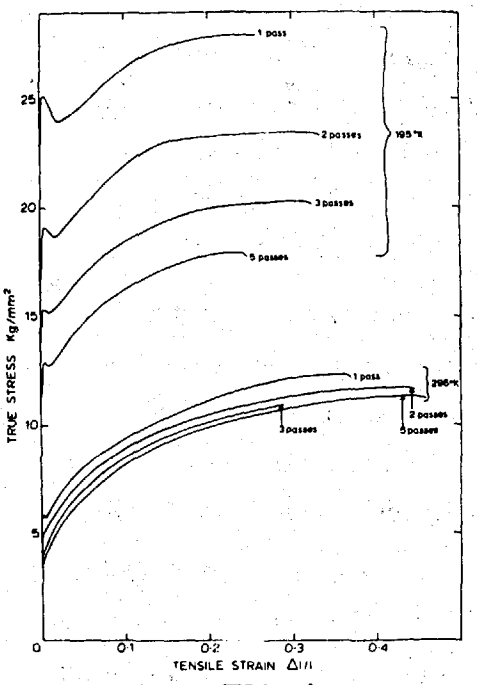

FIG. 4.

Stress-Strain Curves of Crystals With Various Numbers of Zone Passes at 193° and 296°K.

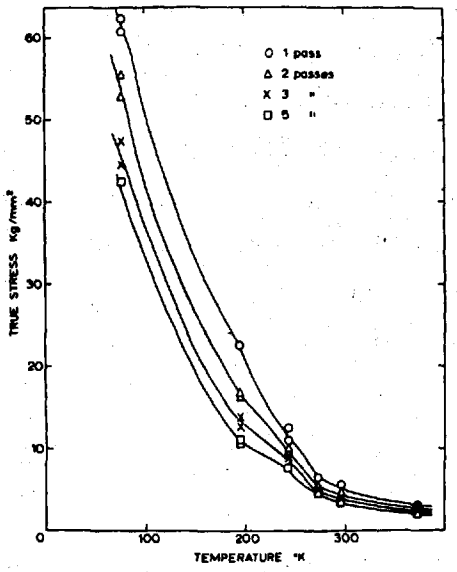

FIG. 5.

Temperature Dependence of the Yield Stress of Crystals with Various Numbers of Zone Passes.

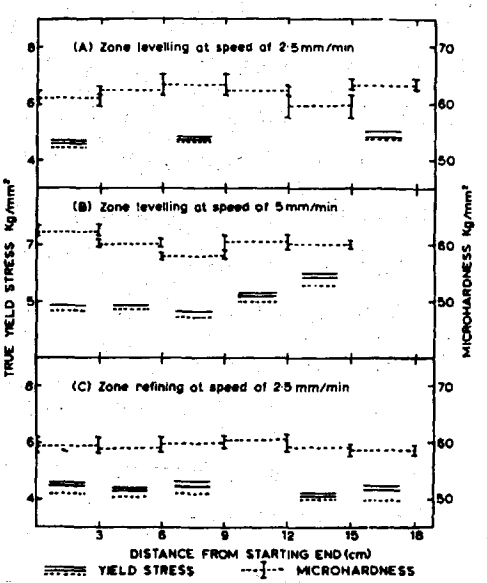

FIG. 6.

Variation of Hardness and Yield Stress at Room Temperature with Distance from the Starting End.

of the number of zone passes. The values of resistivity ratio of 5. 30-5. 46 for 1 zone pass are slightly higher than the values reported by Votava of 5. 05, 5. 15, 5. 10 for 8, 16 and 27 zone pass niobium. This discrepancy may result either from different compositions of starting material or of zone speed, or from both factors. Votava (2) used niobium supplied by Murex Co. and a zone speed of 14 mm. / min., about 5. 6 times faster than that used in this work.

Variations of both microhardness and Vickers hardness were also apparent but these decreased as the number of zone passes increased. For one to six zone passes the microhardness varied from 67 to 56 Kg/ mm.^{2} whereas the Vickers hardness varied from 45 to 40 Kg/ mm.^{2}. Votava's (2) Vickers hardness varied from 44-48 Kg/ mm.^{2}.

The decrease in yield stress with increasing number of zone passes was more rapid than the variation observed using the other methods. The yield drop, Fig. 4, and the temperature dependence of the yield stress, Fig. 5, changed markedly with increasing number of zone passes.

Effect of Zone Levelling Speed with Two Zone Passes, Types A and B Crystals

As shown in Fig. 6A and B, the variation of hardness along the rod for both fast and slow zone levelling speeds was hardly detectable, whilst the yield stress was generally higher and increased significantly with distance from the starting end in the case of the fast zone speed. In this work the speed differed by a factor of two, and this caused a significant change in the impurity distribution profile along the rod, and in the overall purity. These changes may have arisen from differences in the time available for purification during the zone melting. However, Drangler and Murray (3) found that the slower zoning speed improved the crystals near the starting end only, and the rest of the crystal did not vary in electron beam melted tungsten and molybdenum.

Effect of Zone Refining and Zone Levelling, Types A and C Crystals

A considerable impurity gradient is unavoidable in the zone refining process, but in contrast, a more uniform concentration profile could be expected in the zone levelling process. The results of hardness measurements and of yield stresses along zone refined and zone levelled rods after two zone

passes at the same speed are compared in Fig. 6A and C. No significant differences in hardness along and between the two differently prepared crystals were observed. However, the yield stress was slightly lower and decreased towards the finishing end in the case of the zone refined crystal. Whether this slight difference is caused by the characteristics of the zone refining process or by experimental scatter in the measurements is not clear. By contrast Koo (9) has found that in zone refined tungsten single crystals, the yield stress increased rather steeply up to 7.6 cm. from the starting end and then remained constant up to the finishing end. Theory suggests that, for the case of niobium, k must be >1 for the impurity controlling the yield stress.

Effect of Vacuum Pressure During Zone Melting, Type D Crystals

Previously it has been accepted that the purification mechanism involved in electron beam zone melting entails the vacuum distillation of lower melting point elements and the volatilization of oxides and nitrides as well as zone refining (2, 3, 12, 13, 14). In the present investigation the vacuum pressure was found to be much more influential than the number of zone passes or the zone speed in controlling the purity of the crystals. In Fig. 7 the crystal grown at poor vacuum pressure shows a much higher proportional limit, larger yield drop, and larger susceptibility to strain ageing than the crystal grown in a better vacuum. This suggests that the removal of gaseous impurities is the most important process in the zone melting of niobium crystals.

The proposed purification mechanisms of vacuum distillation and volatilization may be a contributing factor. The vapour pressures of many elements are sufficiently high to bring about distillation at and near the zone melting temperature. They are transferred through the vapour phase to a cooler part of the furnace such as the liquid nitrogen cold finger or the water cooled furnace wall. However, in the case of dissolved gaseous elements such as nitrogen and oxygen, the solubility is proportional to their partial pressures. By improving the vacuum pressure in the furnace the solubility is correspondingly reduced and this leads to the higher crystal purity. Furthermore, the observed similarity between the improvement of vacuum pressure with time and with the number of zone passes, and the improvement of purity achieved

with increasing number of zone passes also provides substantial evidence to support this view of the purification mechanism.

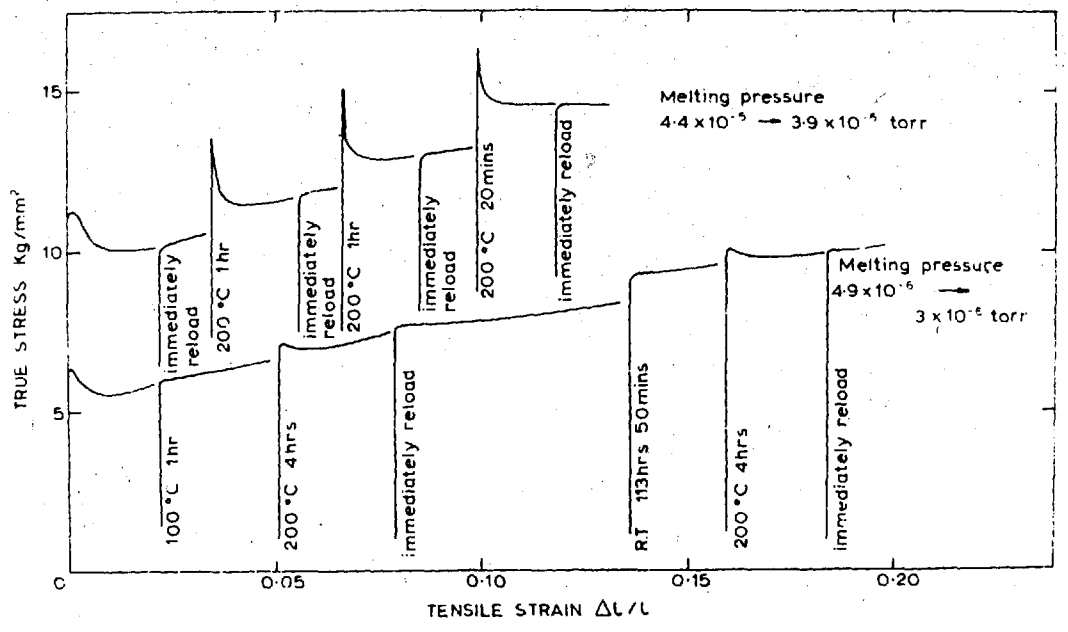

FIG. 7.

Strain-Ageing Characteristics of Crystals of Different Purity

Chemical Analysis

It is unfortunate that during the current work the chemical analysis of metallic elements was not carried out. The extensive chemical analysis of Reed (5) shows that the tantalum and tungsten contents have not been altered after 12 zone passes. This suggests that the considerable concern about contamination by tungsten from the filament of the cathode assembly is not so serious as has been suggested by previous workers. The vapour pressure of pure tungsten and tantalum are comparatively low at the zone melting temperature, and these values are further reduced due to their small concentrations in the niobium crystals. On the other hand, analysis of the interstitials showed that the carbon content increased with increasing number of zone passes, whilst the nitrogen content markedly decreased. The oxygen results were rather scattered.

The results of analysis for interstitial impurities are shown in Table 1 for the present work.

In contrast to Reed, the analysis indicates that the carbon content was reduced to half after four zone passes and the nitrogen content reduced similarly after the first zone pass. The oxygen content decreased after the first zone pass and then increased to a level in excess of that found in the starting metal.

A comparison between the report of Reed and the present analysis implies that carbon contamination due to back-streaming from the vacuum system took place in his case, whilst, due to the better cold trap, this did not occur here.

In the case of dissolved gaseous elements such as nitrogen and oxygen the solubility is found to be decreased by increasing the temperature and by decreasing the vacuum pressure. However, an increase in oxygen in the present case with further zone passes is not unreasonable. Consider the thermodynamics of oxide formation calculated from the free energy of formation of NbO; the equilibrium partial pressure of the Nb/NbO system at approximately 2,400°C is 10^{-10} torr. (15), and the oxygen partial pressure in the vacuum furnace is probably less than that, so no NbO is formed in the molten zone. However, as the temperature drops immediately behind the molten zone, the partial pressure of the oxygen will be sufficient to form NbO because the equilibrium partial pressure of oxygen in the Nb/NbO system decreases rapidly with temperature. This suggests that NbO is formed after the zone has passed over the crystal. The oxygen content could be further reduced only by further improvement in the vacuum pressure and by increasing the temperature gradient near the molten zone.

The larger yield drops and higher yield stresses occurred in the crystals with the least number of zone passes, as shown in Fig. 4; the chemical analysis suggests that this effect is very likely due to the carbon or nitrogen interstitial impurities.

Conclusions

A good agreement was found between resistivity ratio, hardness and yield stress in the evaluation of purity caused by varying the zone melting parameters.

The improvement in overall purity achieved with increasing number of zone passes was found to be greater between one and two zone passes, and then diminished between subsequent zone passes.

A fast zone speed results in poor purity of crystal and causes a considerable gradient in impurity distribution along a single crystal rod. This arises from an increase in the value of the effective distribution coefficient.

No significant differences in the impurity distribution profile are observed between zone levelled and refined crystals when the same zone speed is used.

The vacuum pressure during the zone melting process was found to be the most influential parameter in controlling the purity of crystals.

The progress of purification and the improvement in the vacuum pressure with time agrees very well. This implies that the removal of the products of volatilization and degassing by the vacuum system is a major part of purification. Vacuum distillation of lower melting point elements would also be promoted by decreasing the furnace pressure.

Chemical analyses show that the improvement in overall purity due to further zone passes is most likely due to the reduction of carbon or nitrogen contents. This may be associated with higher yield stresses and the discontinuous yielding behaviour observed in the crystals with the least number of zone passes.

Acknowledgements

The authors would like to express their thanks to Professor J. G. Ball for providing research facilities in the Department of Metallurgy, to C. E. G. B. and U. K. A. E. A. for financial support, to many colleagues for useful discussions including Miss S. Zador for help with the Nb/NbO equilibrium, to Mr. B. Dalgleish for preparing diagrams, and Miss P. Martins for photographic help.

References

1. J. E. Kunzler and J. H. Wernick, Trans. A. I. M. E. 212, 856 (1958).
2. E. Votava, Phys. Stat. Sol. 5, 421 (1964).

3. I. Drangel and G. Murray; Materials Research Corp. Res. Rept., New York (1964).

4. T. E. Mitchell, R. A. Foxall and R. B. Hirsch, Phil. Mag. 8, 1895 (1963).

5. R. E. Reed, ORNL-3949 and 4020, UC-25 Metals, Ceramics and Materials, Oak Ridge National Laboratory, U. S. A. (July 1966).

6. M. Cole, I. A. Bucklow and C. W. B. Grigson, Brit. J. Appl. Phys. 12, 296 (1961).

7. F. E. Birbeck and A. J. Calverley, J. Sci. Inst. 36, 460 (1959).

8. W. G. Pfann, Zone Melting, p. 154, Wiley & Sons, New York (1958).

9. J. T. Michalak, Acta Met. 13, 213 (1965).

10. R. C. Koo, Acta Met. 11, 1083 (1963).

11. A. Lawley, van den Sype and R. Maddin, J. Inst. Met. 91, 23 (1962).

12. J. Wulff, Hochvacuumtechnik m. Auwartter Wissenschaftlich Verlag-Ges MBH, p. 272, Stuttgart.

13. O. Winkler, Met. Rev. 5, 1 (1960).

14. H. R. Smith, Vacuum Metallurgy, p. 221, Reinhold Pub. Co., New York, U.S.A.

15. B. C. H. Steele, Ph. D. Thesis, University of London (1965).

PLASTIC ANISOTROPY OF TANTALUM, NIOBIUM, AND MOLYBDENUM[1]

P. J. SHERWOOD, F. GUIU, H. C. KIM, AND P. L. PRATT
Department of Metallurgy, Imperial College, University of London, London, England

The stress–strain behavior of single crystals of tantalum, niobium, and molybdenum has been studied in both tension and compression in the temperature range 4.2–400 °K. The crystals were stressed in both the ⟨100⟩ and the ⟨110⟩ directions.

At high temperatures, the yield stress of all three metals is independent of the direction and sense of the applied stress. At low temperatures, the yield stress depends markedly on the orientation of the crystals and the sense of the applied stress. This anisotropic behavior cannot be satisfactorily explained in terms of any of the mechanisms proposed so far, such as the mobility of jogs in screw dislocations, or the dissociation of $a/2$ ⟨111⟩ screw dislocations on {112} planes.

1. INTRODUCTION

Although the elastic properties of the b.c.c. metals, with the exception of tungsten, are known to be anisotropic, the plastic properties of single crystals of b.c.c. metals have in the past often been considered to be isotropic, because of the facility with which multiple slip may occur.

Early work by Taylor (1928) on single crystals of β brass was the first to show that the resistance to slip in a ⟨111⟩ direction on a given plane is not equivalent to slip in the opposite sense, and that, for a particular orientation of the deformation axis, the slip planes chosen in tension and compression are not equivalent. Subsequent work on iron and iron–silicon alloys (Vogel and Brick 1953; Steijn and Brick 1954; Taoka, Takeuchi, and Furubayashi 1964; Šesták and Zárubová 1965) has shown a similar asymmetry in the operative slip planes in tension and compression.

If slip naturally occurs on the {112} planes or involves elements of slip on these planes (as proposed by Šesták and Zárubová 1965), an asymmetry of the critical resolved shear stress, $\tau_{(112)}$, would be predicted if the dislocations are dissociated on these planes. This follows from the nonequivalence of the positive and negative ⟨111⟩ twinning direction on {112} planes in the b.c.c. lattice. Edge dislocations can only dissociate asymmetrically on {112} planes according to the reaction (Frank and Nicholas 1953),

$$a/2\ \langle 111\rangle \rightarrow a/3\ \langle 111\rangle + a/6\ \langle 111\rangle.$$

The dissociation occurs in such a way that, if a shear stress acts in the sense of twinning, the $a/6$ ⟨111⟩ twinning partial will glide first. Conversely, if the sense of an applied stress is unfavorable for twinning, the complementary partial $a/3$ ⟨111⟩ will glide first. It is expected that the stresses required to move the dislocation in these two cases will be different, since a larger energy change is involved in moving the complementary partial first.

[1]Presented at an international conference on the Deformation of Crystalline Solids, held in Ottawa, August 22–26, 1966.

It has also been proposed by Hirsch (1960) and independently by Sleeswyk (1963) that screw dislocations can dissociate into three $a/6$ ⟨111⟩ partials on the {112} planes which intersect along the axis of the original screw dislocation. An analysis of the geometry of the partials under an applied stress also predicts that there should be an asymmetry of the stress to move screw dislocations on these planes. As pointed out by Hirsch (1960), the stress required to constrict a dissociated screw dislocation in the b.c.c. lattice may be thermally activated, and may possibly account for the magnitude of the low-temperature flow stress. If this is so, it should give rise to an anisotropic Peierls type of stress. Recently, Duesbery and Foxall (1965) and Argon and Maloof (1966) have invoked this argument to explain the asymmetry of the observed slip planes in niobium and tungsten and the differing yield strengths in tension and compression for certain orientations.

To investigate whether there is, in fact, an anisotropy of the yield stress in tension and compression which can be explained by an asymmetry of the critical resolved shear stress on the {112} planes, it is most advantageous to study crystal orientations with the applied stress in the ⟨100⟩ and ⟨110⟩ directions. From Schmid-factor considerations, these orientations are the most conducive to {112} slip, and also, for a given applied stress, the resolved shear stresses on the most highly stressed {112} plane are equal. A consideration of the crystallography of slip on this plane also shows that for both orientations the senses of slip in the ⟨111⟩ direction are opposite in tension and compression. So far no systematic investigations of the yield stresses and slip planes in both tension and compression have been reported for these two orientations. This paper is concerned with the results of such an investigation in tantalum, niobium, and molybdenum.

Previous investigations in tension on tungsten single crystals (Rose, Ferris, and Wulff 1962), on molybdenum single crystals (Guiu and Pratt 1966), and on niobium single crystals (Kim and Pratt 1966) have shown that, when the stress is applied in the ⟨100⟩ and ⟨110⟩ directions, the yield stress and work-hardening rate can exhibit a strong orientation dependence, particularly at low temperatures. These effects and certain other aspects of the yielding behavior have been explained in terms of either the conservative movement of jogs (Rose *et al.* 1962) or the nonconservative movement of jogs (Guiu and Pratt 1966) in screw dislocations. Another feature of the plastic anisotropy of b.c.c. metals which will not be dealt with in this paper is the appearance of a region of easy glide and three stages of work hardening in the stress–strain curve under suitable conditions of orientation, temperature, and strain rate. This has been observed in niobium (Mitchell, Foxall, and Hirsch 1963; Votava 1964), tantalum (Mitchell and Spitzig 1965), iron (Keh 1965), and molybdenum (Guiu and Pratt 1966).

2. EXPERIMENTAL TECHNIQUES

2.1. Preparation of Single-Crystal Specimens

Single crystals of molybdenum, tantalum, and niobium were grown by the electron-beam zone-melting technique in a dynamic vacuum of 10^{-6}–10^{-7} Torr in the case of molybdenum, and 3–5 × 10^{-6} Torr in the case of tantalum and

niobium. The molybdenum was supplied by Murex Ltd. in the form of a sintered rod 6 mm in diameter, and the tantalum and niobium were supplied by Société Générale Métallurgique de Hoboken in the form of rods 3 mm in diameter, swaged from double electron-beam melted ingots.

To ensure an even distribution of impurities within the single crystals, the rods were given two zone passes in opposite directions at a zone speed of 2.5 mm/minute. Chemical analyses of the single crystals for carbon and gaseous impurities are given in Table I.

TABLE I

Chemical analysis of single crystals of tantalum, niobium, and molybdenum

Element	Ta	Nb (Content (wt. p.p.m.))	Mo
C	36±5	4–8±5	2–3
O	11±3	13–25±3	<1
N	7±3	26–32±2	≪10
H	11±1	Not detected (<1)	<0.01

The tantalum was analyzed by the National Physical Laboratory, Teddington, the niobium by Du Pont De Nemours and Co., U.S.A., and the molybdenum by the British Non-Ferrous Metals Research Association, London.

Tensile specimens of molybdenum with a rectangular cross section were prepared by surface grinding, using cuts only 0.001 2 mm deep. The cold-worked layer was removed by electropolishing in concentrated H_2SO_4. The approximate dimensions of the tensile specimens were as follows:

cross section	2.1 × 2.3 mm²
gauge length	12.7 mm
radius of shoulder	1.5 mm
total length	20 mm

Tensile specimens of tantalum and niobium were prepared by spark lathing in a Servomet spark machine, and subsequently were electropolished in a solution of one part 47% HF and 9 parts concentrated H_2SO_4 to remove the surface damage. The final specimen dimensions were: gauge diameter 2.3–2.7 mm, gauge length 17 mm with a shoulder radius of 3 mm.

Compression specimens of molybdenum were cut from the gauge length of the rectangular tensile specimens. The ends were polished flat to give a final gauge length of approximately 7 mm. Compression specimens of tantalum and niobium were prepared by slicing previously spark-lathed and electropolished lengths of single crystal with a carborundum slitting wheel. The compression faces were ground on 600 grade silicon carbide papers, using a specially designed jig to ensure that the faces were accurately parallel. The compression specimens had the following approximate dimensions: gauge diameter 2.5 mm, gauge length 6 mm, except for tests between 4.2 and 20 °K, when the gauge diameter was 1.27–1.68 mm and the gauge length 2.5 mm.

2.2. Methods of Testing

Tension and compression tests were conducted over the temperature range 77–400 °K in an Instron machine, model TT-CM. In the case of molybdenum,

a standard cross-head speed of 0.005 cm/minute was used in both tension and compression, which corresponded to total strain rates of specimen and machine of 7×10^{-5} and 10^{-4} sec^{-1} respectively. In the case of tantalum and niobium, standard cross-head speeds of 0.05 cm/minute in tension, and 0.02 cm/minute in compression were used, corresponding to strain rates of 4.9×10^{-4} and 4.5×10^{-4} sec^{-1} respectively. Compression tests between 4.2 and 20 °K were performed at a strain rate of 9×10^{-4} sec^{-1}.

3. EXPERIMENTAL RESULTS

The temperature dependence of the proportional limit for single crystals of tantalum, niobium, and molybdenum stressed in both tension and compression in the ⟨110⟩ and ⟨100⟩ directions are shown in Figs. 1, 2, and 3 respectively. The values of the proportional limit, or deviation from the linear region in the stress–strain curves, have been chosen for comparison, since crystals with

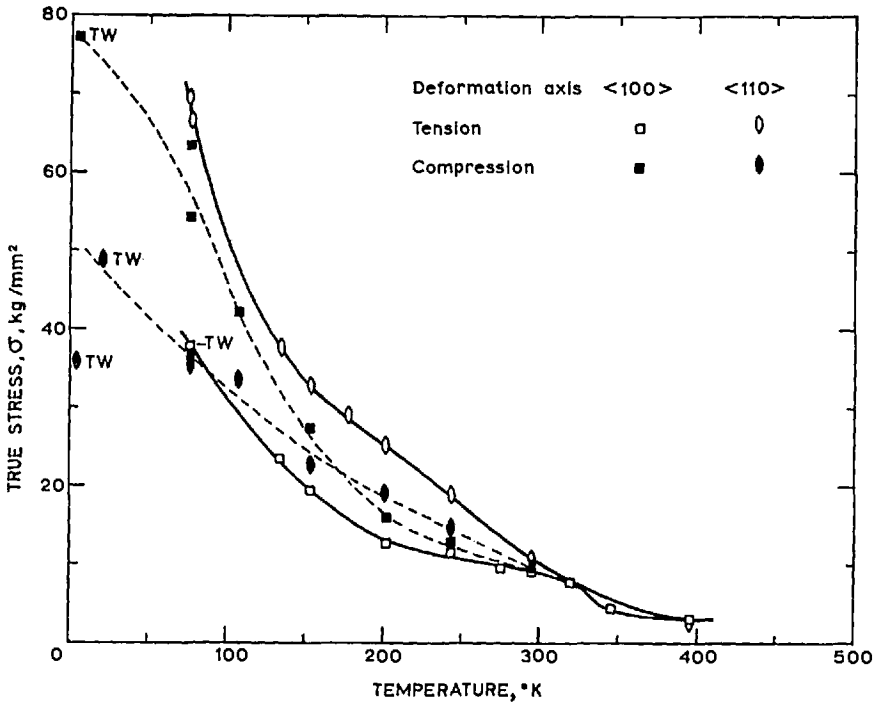

FIG. 1. Temperature dependence of the proportional limit for tantalum single crystals.

⟨110⟩ orientation show discontinuous yielding, while the ⟨100⟩ oriented crystals exhibit parabolic hardening from the onset of macroscopic flow. It is clear from Figs. 1–3 that all three metals exhibit an anisotropic behavior that is more pronounced at low temperatures.

Stress–strain curves of crystals deformed at 77 °K are shown in Figs. 4, 5, and 6. The single crystals of tantalum and niobium yield in tension at a higher stress than in compression when the applied stress is in the ⟨110⟩ direction.

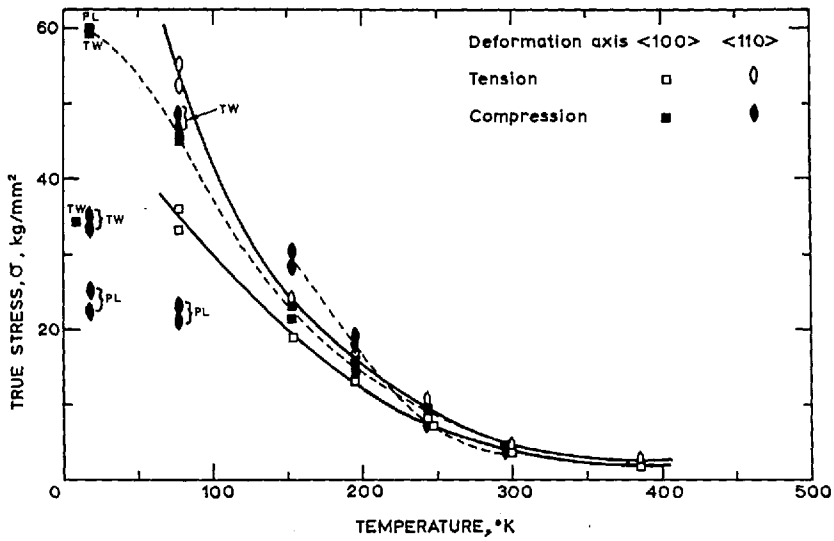

FIG. 2. Temperature dependence of the proportional limit for niobium single crystals.

The reverse effect is observed for crystals stressed in the ⟨100⟩ direction. However, the proportional limit of crystals of molybdenum is always higher when the stress is applied in the ⟨110⟩ direction. In the case of tantalum, twinning without slip occurred in tension in the ⟨100⟩ direction, whereas in compression in the ⟨110⟩ direction repeated discontinuous slip occurred after a strain of 0.03. In niobium, however, twinning occurred before slip at a stress of 46.8 kg/mm² for compression in the ⟨110⟩ direction and this produced a drop in load of more than 50%. Subsequently, the crystals yielded at a much lower stress and repeated twinning and slip were observed. In molybdenum, twinning and simultaneous fracture occurred in tension for both ⟨110⟩ and ⟨110⟩ orientations after a relatively large amount of plastic strain. Twinning in compression was never observed in molybdenum at any temperature, while in tantalum and niobium it always occurred at temperatures between 4.2 and 20 °K.

At temperatures above 77 °K, plastic deformation occurred only by slip in all three metals. Crystals deformed in the ⟨100⟩ direction showed no yield point and a high work-hardening rate, whereas crystals deformed in the ⟨110⟩ direction showed discontinuous yielding and a relatively low work-hardening rate.

Slip-line observations were made in tantalum, niobium, and molybdenum at the temperatures shown in Table II, where the slip planes and the corresponding Schmid factors are tabulated. The temperature dependence of the resolved shear stresses at the proportional limit, calculated from the data of Table II, is shown in Figs. 7, 8, and 9. At temperatures where slip line observations were not made, stresses were resolved on those planes that were more consistent with the data of Table II.

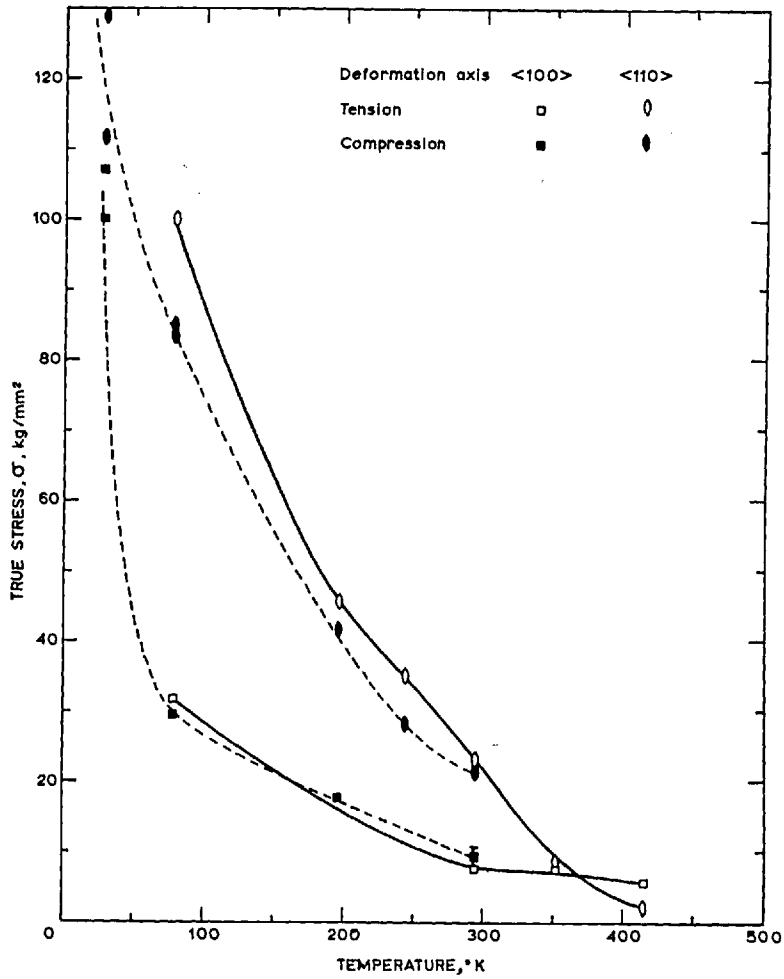

FIG. 3. Temperature dependence of the proportional limit for molybdenum single crystals.

4. DISCUSSION

4.1. Orientation Dependence of the Proportional Limit in Tension and Compression

The most striking features of the results presented in this paper are (*a*) the large differences in proportional limits for all three metals for crystals extended in the ⟨100⟩ and ⟨110⟩ directions, particularly at low temperatures, and (*b*) the differences between the proportional limits in tension and compression. Before discussing possible mechanisms giving rise to these phenomena, the differences and the similarities in the behavior of the three metals will be summarized. In tension, they all show a relatively high proportional limit in the ⟨110⟩ direction, compared with that in the ⟨100⟩ direction, but at sufficiently high temperatures the effect of orientation disappears. In contrast, the behavior in compression is somewhat more complex. Tantalum, at temperatures above 153 °K, shows a higher proportional limit for the ⟨110⟩ direction, but

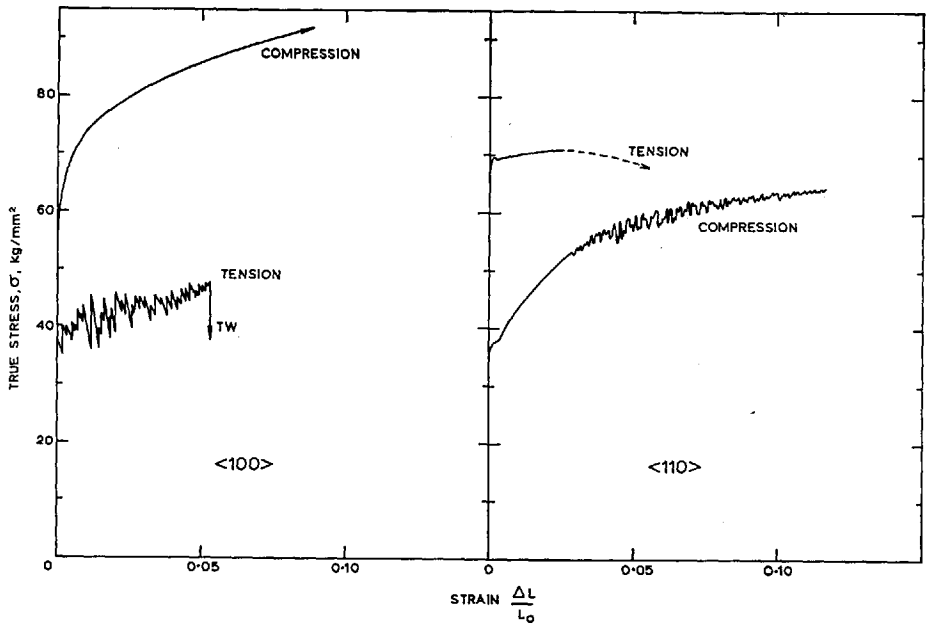

FIG. 4. Stress–strain curves of tantalum single crystals at 77 °K.

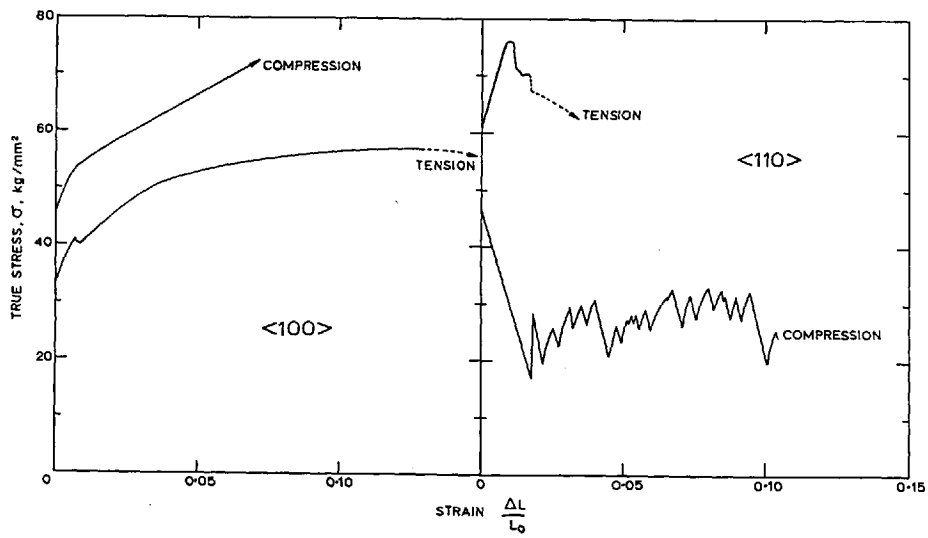

FIG. 5. Stress–strain curves of niobium single crystals at 77 °K.

on lowering the temperature the proportional limit for ⟨100⟩ becomes increasingly higher than that for ⟨110⟩. Niobium, above 200 °K and below 100 °K also shows a lower proportional limit for ⟨110⟩ than for ⟨100⟩, but between these temperatures the behavior is similar to that in tension. Molybdenum shows a consistently higher proportional limit for ⟨110⟩ at all temperatures.

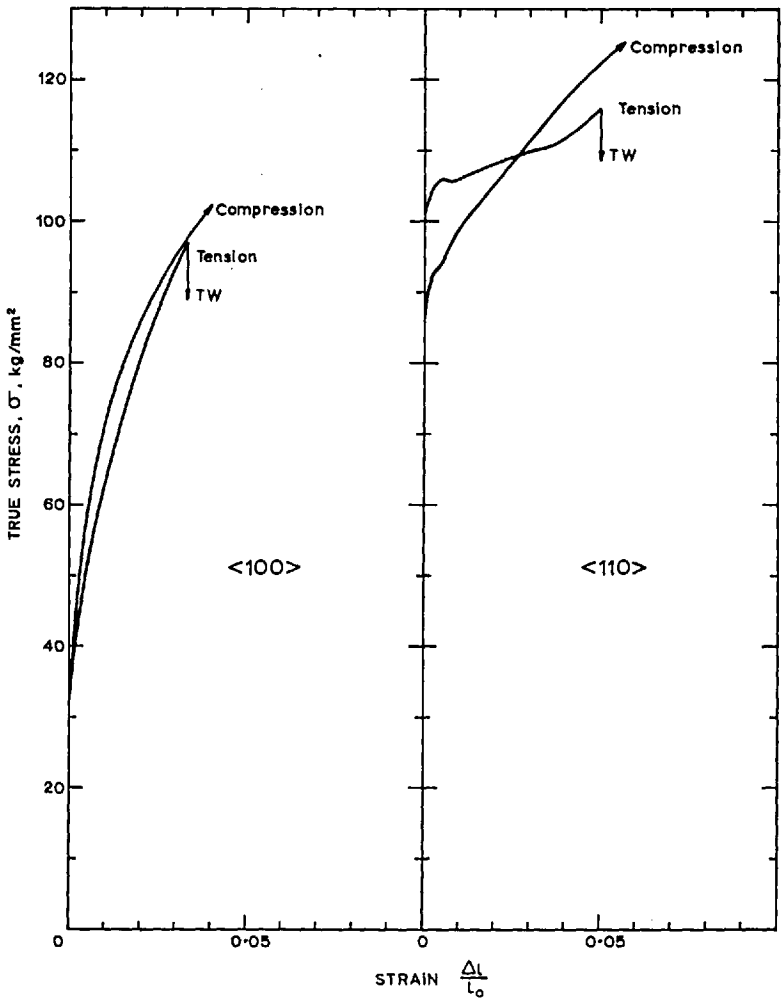

FIG. 6. Stress–strain curves of molybdenum single crystals at 77 °K.

However, in comparing the data in tension and compression for each orientation, it becomes obvious that the effects are reversed for the two orientations. In all three metals, the proportional limit for ⟨110⟩ in compression is lower than that in tension, except for the anomalous behavior of niobium between 100 and 200 °K. However, the proportional limit for ⟨100⟩ in compression is higher than that in tension, except in molybdenum where the values are approximately equal.

Although the data in tension may be satisfactorily explained in terms of the mobility of jogs in screw dislocations (Rose *et al.* 1962; Guiu and Pratt 1966), it is difficult to envisage how this mechanism could give rise to the observed differences in tension and compression, unless the jogs are extended. However, this possibility is considered unlikely (Schoeck 1961) in view of the high stacking-fault energies in b.c.c. metals. Since the macroscopic proportional limit is

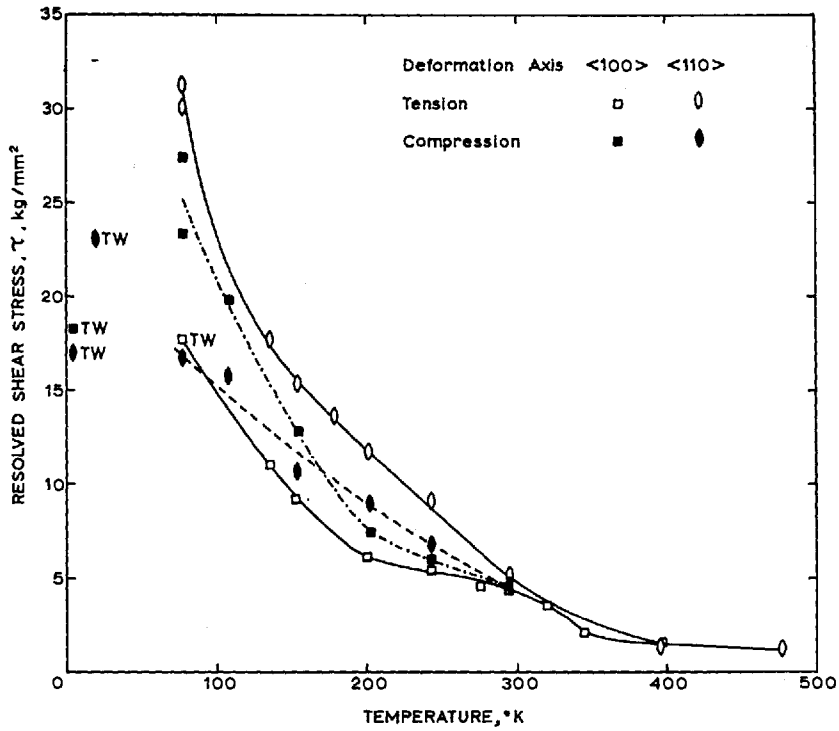

FIG. 7. Temperature dependence of the resolved shear stress at the proportional limit for tantalum single crystals.

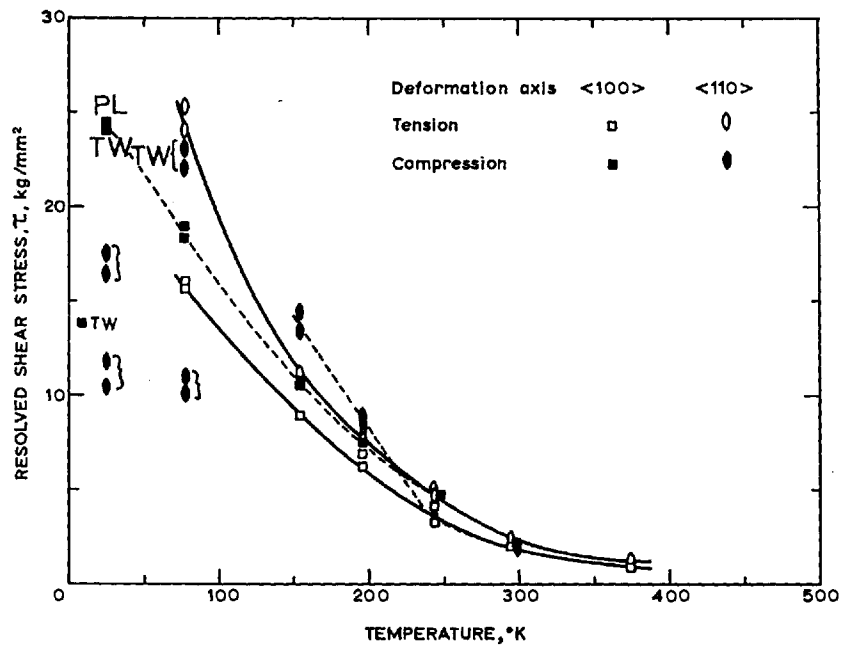

FIG. 8. Temperature dependence of the resolved shear stress at the proportional limit for niobium single crystals.

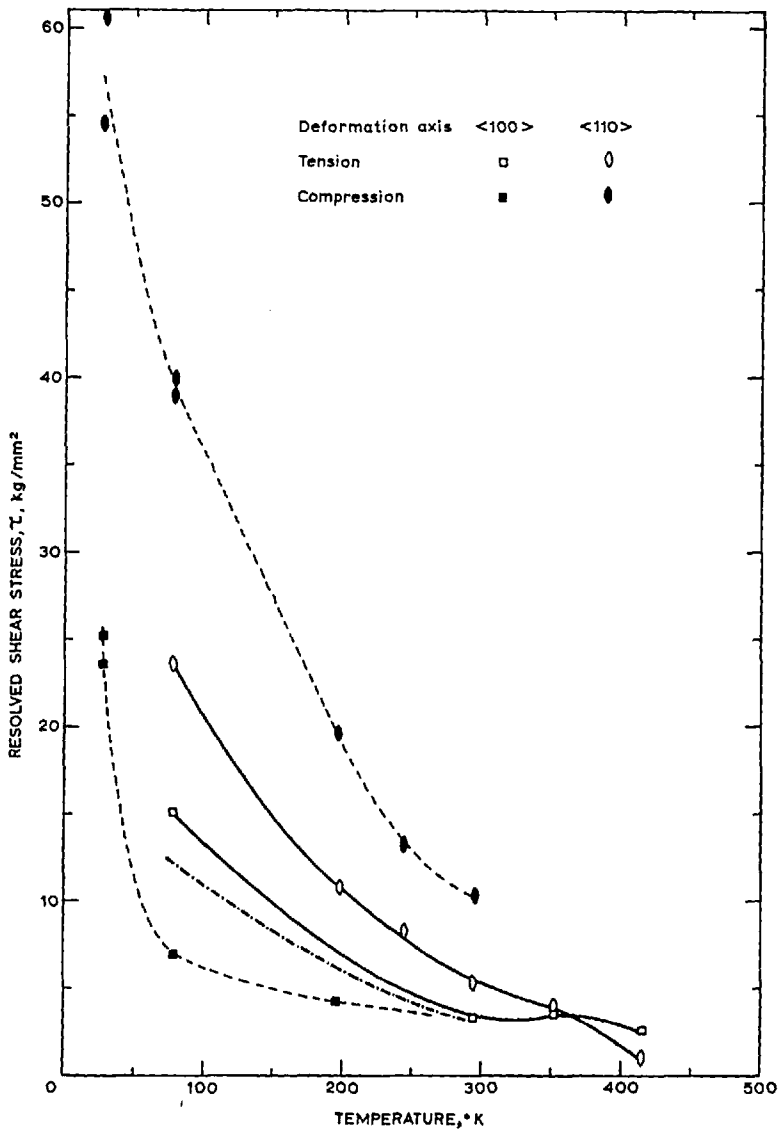

FIG. 9. Temperature dependence of the resolved shear stress at the proportional limit for molybdenum single crystals.

generally believed to correspond to the movement of screw dislocations over large distances, any explanation for these effects should be based on an asymmetry of the stress to move screw dislocations.

Considering the deformation axis in the [001] and [110] directions, the (112) [11$\bar{1}$] slip system is the most highly stressed {112} ⟨111⟩ system in both cases, but for compression in [001] and [110] the senses of slip are opposite, so that the sense of slip for tension in [001] is exactly equivalent to that in compression

TABLE II

Slip and twin planes observed in single crystals stressed in the ⟨110⟩ and ⟨100⟩ directions
(T = tension, C = compression, TW = twinning)

		Ta		Nb		Mo		W*	
		⟨110⟩	⟨100⟩	⟨110⟩	⟨100⟩	⟨110⟩	⟨100⟩	⟨110⟩	⟨100⟩
High stressed {112} Schmid factor 0.472	T		TW 77 °K				TW 77 °K 413 °K		450–77 °K
	C	77 °K		TW 77 °K		293 and 77 °K		450–77 °K	
{110} Schmid factor 0.408	T	77 °K	293 °K	77 °K	77 °K		293–193 °K		450–77 °K
	C		77 °K		77 °K		293 °K		
Low stressed {112} Schmid factor 0.236	T	TW 77 °K				293–77 °K TW 77 °K		450–77 °K	
	C								

*Data from Argon and Maloof (1966)

in [110], and vice versa. The only difference is that the components of the stress normal to the slip plane are opposite.

The dissociation of screw dislocations on the {112} planes described previously should result in a higher yield stress in the ⟨110⟩ direction for tension than for compression, and the reverse effect in the ⟨100⟩ direction. Even if the stacking-fault energy is too high to allow a stacking fault to form, it is expected that there will be an asymmetry of the dislocation core, and a similar anisotropy of the yield stress should result. For the sense of the resolved shear stress on the highly stressed {112} planes, unfavorable for twinning, it is predicted that slip will occur either on the lowly stressed {112} planes, or on the highly stressed {112} planes, if thermal activation can constrict the partials back onto the slip plane.

Several favorable dissociations of $a/2$ ⟨111⟩ dislocations on the {110} planes have also been proposed (Hirsch 1960; Cohen, Hinton, Lay, and Sass 1962; Crussard 1962; Kroupa and Vitek 1964). However, a consideration of the sense of slip and the geometry of the partials lying on the {110} planes does not lead to a similar asymmetry of the critical resolved shear stress to move screw dislocations on these planes.

From the preceding paragraphs it can be seen that many of the observed differences in the proportional limits in tension and compression can only be accounted for in terms of an asymmetry of the critical resolved shear stress on the {112} planes. However, if the core dissociation on the {112} planes is the only factor determining the magnitude of the stress to move screw dislocations, then the proportional limit for ⟨100⟩ in compression should equal the proportional limit for ⟨110⟩ in tension and vice versa (assuming the same slip system is operative). This is manifestly not the case in the present investigation, especially for molybdenum. It appears, therefore, that the orientation dependence of the yield stress in these three metals cannot be accounted for simply in terms of an "anisotropic Peierls stress" due to dislocation core asymmetry, but some other mechanism such as the mobility of jogs must also be invoked.

4.2. Slip Systems in Tension and Compression

At low temperatures only {110} and {112} slip planes were observed, and it can be seen from Table II, where the data of Argon and Maloof on tungsten have been included for comparison, that the Group VIA metals, molybdenum and tungsten, behave differently from those of Group VA, tantalum and niobium. When the sense of the resolved shear stress on the highly stressed {112} slip planes is unfavorable for twinning, in tantalum and niobium slip occurs on the {110} planes with a Schmid factor of 0.408, whereas in molybdenum and tungsten slip occurs on the {112} planes with a Schmid factor of 0.236. In the latter two, however, no slip lines could be detected for compression in the ⟨100⟩ direction at 77 °K. There are also some other anomalies in the slip and twinning behavior, which cannot readily be accounted for by the splitting of dislocations on the {112} planes. For instance, at 77 °K tantalum twins in tension in ⟨100⟩, but slips on {112} in compression in ⟨110⟩, whereas niobium slips on {110} in tension in ⟨100⟩, but twins in compression in ⟨110⟩. However, below 20 °K both orientations can be made to twin in compression.

Very similar observations in niobium have been made at 77 °K by Reid, Gilbert, and Hahn (1966).

The causes of the difference in behavior of the Group VA and VIA metals with regard to the slip plane chosen may be related to the differences in stacking-fault energy. It has been generally believed, and Hartley (1966) has recently shown from a consideration of the changes in atomic arrangements on faulting, that the stacking-fault energy on the {112} planes is considerably higher for Group VIA metals. The calculated stacking-fault energies and widths of dissociated edge dislocations on the {112} planes are summarized in Table III, where d is the width of dissociation, and a is the lattice parameter.

TABLE III

Calculated stacking-fault energies and widths on the {112} planes

	Group VA			Group VIA	
	γ erg/cm^2	d/a		γ erg/cm^2	d/a
Nb	150	3.6	Mo	430	3.4
Ta	210	4.5	W	500	3.7

Further analysis shows that $a/2$ ⟨111⟩ screw dislocations are likely to be even less extended, and consequently the stresses required to constrict the partials cannot be calculated using linear first-order elasticity. However, it is likely that the stacking-fault energy determines the extent of the core asymmetry, and hence affects the stress required to move screw dislocations on the {112} planes. Then, when the sense of the applied stress is unfavorable for twinning, whether dislocations will slip on the {110} planes or the low-stressed {112} planes will be determined primarily by the ratio of the shear strength of these two planes, τ_{112}/τ_{110}, and ultimately this may be determined by the stress required to constrict the partials into the favorable {112} slip plane, and hence by the magnitude of the stacking-fault energy.

It has frequently been observed in iron and iron silicon alloys (Opinsky and Smoluchowski 1951; Vogel and Brick 1953; Steijn and Brick 1954; Erickson 1962) that the ratio $\tau_{112}/\tau_{110} > 1$ and increases with decreasing temperature and increasing alloy content. Thus, for a crystal orientation with the Schmid factor highest for the {112} slip, there may be a transition to {110} slip on lowering the temperature (see, for example, Erickson 1962).

With the deformation axis in the ⟨100⟩ or ⟨110⟩ directions, slip will occur on the {110} planes if the following inequality holds

$$\tau_{112}/0.472 > \tau_{110}/0.408, \tag{1}$$

where τ_{112} and τ_{110} are the critical resolved shear stresses, and 0.472 and 0.408 are the respective Schmid factors on the {112} and {110} planes. This inequality is obviously valid in tantalum and niobium at 77 °K for the sense of stress unfavorable for twinning. However, if one attempts to explain the results for molybdenum in terms of the values of the critical resolved shear stress for the various slip planes, an inconsistency arises. In the temperature

range 293–77 °K, the slip lines observed after tension in ⟨110⟩ suggest that slip took place on the {112} planes with a Schmid factor equal to 0.236. Therefore, since slip on the {110} planes was not observed,

$$\tau_{112}/0.236 < \tau_{110}/0.408. \tag{2}$$

Results in both tension and compression in ⟨100⟩ show that

$$\tau_{110}/0.408 < \tau_{112}/0.472, \tag{3}$$

since the slip lines observed were traces of the {110} type planes. An inconsistency now arises because the inequalities (2) and (3) are incompatible. Slip on the {112} planes has never been observed either in tension or compression in the ⟨100⟩ direction, and this makes it difficult to explain the results in terms of an anisotropy arising only from the direction of slip.

One can further speculate that the slip-line observations did not reveal the true slip planes for the case of deformation in ⟨100⟩. For example, if for ⟨100⟩ in tension {112} planes with a Schmid factor of 0.472 were operative (as Argon and Maloof have observed in tungsten), and {112} planes with a Schmid factor of 0.236 were operative in compression, then the temperature dependence of the resolved shear stress for the ⟨100⟩ and ⟨110⟩ orientations would be as shown in Fig. 9. If stresses are resolved on the observed slip planes, however, the dash–dot curve would result for crystals with ⟨100⟩ orientation in both tension and compression. This would imply that the critical resolved shear stresses in the {112} planes, when the sense of the applied stress is favorable for twinning, are higher than when the sense is unfavorable. However, whichever criterion is used and irrespective of the choice of slip plane, the resolved shear stress for yielding in crystals with ⟨110⟩ orientation is always higher than in crystals with ⟨100⟩ orientation, at least by a factor of 1.5.

In summary, it is concluded from the preceding discussion that the orientation dependence of the yield stress and slip planes in tantalum, niobium, and molybdenum cannot be accounted for simply in terms of an asymmetric core dissociation of screw dislocations on the {112} planes. An additional mechanism, such as the mobility of jogs in screw dislocations, must also be involved.

ACKNOWLEDGMENTS

The authors are indebted to Professor J. G. Ball for providing research facilities in the Department of Metallurgy, and to Mr. D. K. Bowen of the Department of Metallurgy, University of Oxford, who kindly performed the compression tests between 4.2 and 20 °K. They also wish to thank Professor A. S. Argon for permission to quote unpublished work. The present investigation forms part of a program of research on b.c.c. metals, generously financed by the Central Electricity Generating Board and Science Research Council.

REFERENCES

ARGON, A. S. and MALOOF, S. R. 1966. Acta Met. **14**, 1449.
COHEN, J. B., HINTON, R., LAY, K., SASS, S. 1962. Acta Met. **10**, 894.
CRUSSARD, C. 1962. Acta Met. **10**, 749.
DUESBERY, M. S. and FOXALL, R. A. 1965. Conference on Pure Materials, Dresden.
ERICKSON, J. S. 1962. J. Appl. Phys. **33**, 2490.

FRANK, F. C. and NICHOLAS, J. F. 1953. Phil. Mag. **44**, 1213.
GUIU, F. and PRATT, P. L. 1966. Phys. Stat. Sol. **15**, 539.
HARTLEY, C. S. 1966. Acta Met. **14**, 1133.
HIRSCH, P. B. 1960. Fifth Intern. Congr. Crystallography, Cambridge.
KEH, A. S. 1965. Phil. Mag. **12**, 9.
KIM, H. C. and PRATT, P. L. 1966. Phys. Stat. Sol. **14**, K151.
KROUPA, F. and VITEK, V. 1964. Czechoslov. J. Phys. **B14**, 337.
MITCHELL, T. E. and SPITZIG, W. A. 1965. Acta Met. **13**, 1169.
MITCHELL, T. E., FOXALL, R. A., and HIRSCH, P. B. 1963. Phil. Mag. **8**, 1895.
OPINSKY, A. J. and SMOLUCHOWSKI, R. 1951. J. Appl. Phys. **22**, 1488.
REID, C. N., GILBERT, A., and HAHN, G. T. 1966. Acta Met. **14**, 975.
ROSE, R. M., FERRIS, D. M., and WULFF, J. 1962. Trans. AIME, **224**, 981.
SCHOECK, G. 1961. Acta Met. **9**, 382.
ŠESTÁK, B. and ZÁRUBOVÁ, N. 1965. Phys. Stat. Sol. **10**, 239.
SLEESWYK, A. W. 1963. Phil. Mag. **8**, 1467.
STEIJN, R. and BRICK, R. M. 1954. Trans. AIME, **46**, 1406.
TAOKA, T., TAKEUCHI, S., and FURUBAYASHI, E. 1964. J. Phys. Soc. Japan, **19**, 701.
TAYLOR, G. I. 1928. Proc. Roy. Soc. (London), Ser. A, **118**, 1.
VOGEL, F. L. and BRICK, R. M. 1953. Trans. AIME, **197**, 700.
VOTAVA, E. 1964. Phys. Stat. Sol. **5**, 421.

DISCUSSION

U. F. Kocks: Why should compression in ⟨110⟩ be equivalent to tension in ⟨100⟩, since in the latter there are four {211} planes equally stressed, whereas in the former there are only two?

Authors: In ideal orientations the work hardening in the two cases should be different, and this is found experimentally. In most of the experiments, crystals were oriented close to the ⟨110⟩ and ⟨100⟩ and under these circumstances, at least for the initial yield, slip should occur only on one of the {211} planes in each case.

ACKNOWLEDGEMENTS

I am greatly indebted to my supervisor, Professor P.L. Pratt for his guidance and valuable discussions, and to Professor J.G. Ball for providing research facilities during the course of the work.

I would like to express my thanks to Dr. R.L. Segall, School of Physics, University of Warwick for many helpful discussions and critical comments on the manuscript, and Mr. J. Billingham, School of Physics, University of Warwick, and my colleagues in the Crystal Physics group for the many fruitful discussions and encouragement.

I am indebted to the workshop and photographic staff of the Department for their specialized assistance.

Finally, I wish to thank the U.K.A.E.A. and C.E.G.B. for their generous financial assistance.

REFERENCES

Adams, M.A., Roberts, A.C., and Smallman, R.E., (1960)
Acta Met., 8, 328.

Albrecht, W.M., Goode, W.D., and Mallett, M.W. (1959)
J. Electrochem. Soc. 106, 981.

Altshuler, T.L., and Christian, J.W. (1966)
Acta Met. 14, 903.

Amelincks, S. and Dekeyser, W. (1959)
Solid State Physics 8, 327.

Anderson, R.W., and Boronisz, S.E. (1959)
Acta Met. 7, 645.

Andrade, E.N. da C., (1937)
Proc. Roy. Soc. 163A, 16.

Ang, C.Y. (1953)
Acta Met., 1, 123.

Argon, A.S. and Maloof, S.R. (1966)
Acta Met. 14, 1449.

Armstrong, .E., Dickinson, J.M. and Brown, H.L. (1966)
Trans. Met. Soc. A.I.M.E., 236, 1404.

Barrett, C.S. (1943)
"Structure of Metals", McGraw-Hill, N.Y. 402.

Basinski, Z.S., (1957)
Proc. Roy. Soc. 240A, 229.

Basinski, Z.S. and Christian, J.W. (1960)
Aus. J. Phys. 13, 299.

Basinski, Z.S. and Sleeswyk, A., (1967)
Acta Met. 5, 176.

Beardmore, P. and Hull, D., (1965)
J. Less Common Metals 9, 168.

Beardmore, P. and Hull, D. (1966)
J. Inst. Metals 94, 14.

Begley, R.T. (1958)
A.D.C.T.R. 57, 344, (Part II).

Benson, R., Thomas, G. and Washburn, J. (1962)
"Direct observation of imperfection in crystals", Interscience, N.Y. 375.

Berghezan, A. and Fourdeux, A. (1963)
"Symposium on the role of Substructure in the Mechanical Behaviour of Metals", ASD-TDR-63-324, 437.

Bilby, B.A. (1950)
Sheet Metal Industry, 707.

Birbeck, F.E. and Calverley, A.J. (1959)
J. Sci. Inst. 36, 460.

Bowen, D.K., Christian, J.W. and Taylor, G. (1967)
Can. J. Phys. 45, 903.

Brindley, B.J., Cordery, D.J.H. and Honeycombe, R.W.K., (1962)
Acta Met. 10, 1042.

Brittarin, J.C. and Bronisy, S.F. (1958)
A.F.O.S.R. Rept. No. 58-369, A.D. 154, 75.

Brown, N and Ekvoll, R.A. (1962)
Acta Met. 10, 1101.

Buehler, E. (1958)
Trans. Met. Soc. A.I.M.E., 218, 694.

Buehler, B. and Kunzler, J.E. (1961)
Trans. Met. Soc. A.I.M.E. 221, 957.

Bullough, R. and Newman, R.C. (1962)
Proc. Roy. Soc. 266, 198.

Burton, J.A., Prim, R.C. and Slichter, W.P. (1953)
J. Chem. Phys. 21, 1987.

Burris, L., Stockman, C.J. and Dillon, I.G. (1955)
J. Met. 7, 1017.

Carrington, W., Hale, K.F. and McLean, D., (1960)
Proc. Roy. Soc. 259A, 203.

Chalmers, B. (1959)
"Physical Metallurgy", Wiley.

Chaudhuri, A.R., Patel, J.R. and Rubin, L.G. (1962)
J. Appl. Phys. 33, 2736.

Chen, N.K., Maddin, R. and Pond, P.B. (1951)
Trans. Amer. Inst. Min. Met. Eng. 191, 461.

Christian, J.W. (1964)
Acta Met. 12, 99.

Christian, J.W. and Masters, B.C. (1964)
Proc. Roy. Soc. 281A, 223.

Cochardt, A.W., Schoeck, G and Wiedersich, H. (1955)
Acta Met. 3, 533.

Cohen, J.B. Hinton, R., Lay, E. and Sass, (1962)
Acta Met. 10, 894.

Cole, M., Bucklow, I.A., and Grigson, C.W.B., (1961)
British J. Appl. Phys. 12, 296.

Conrad, H. (1961)
J. Iron & Steel Inst. 198, 364.
Conrad, H. (1963)
"The Relation between the Structure and Mechanical Properties of Metals", H.M.S.O., London, 476.
Conrad, H. and Hayes, W. (1963)
Trans. A.S.M., 56, 249.
Conrad, H and Prekel, H.L. (1967)
Acta Met. 15, 955.
Conrad, H. and Schoeck, G. (1960)
Acta Met. 8, 791.
Cottrell, A.H. (1948)
Bristol Conf. Rept. on the Strength of Solids, Phys. Soc., London 30.
Cottrell, A.H. (1950)
Pittsburgh Symp. on the Plastic Deformation of Crystalline Solids.
Cottrell, A.H. (1953)
Dislocations and Plastic Flow in Crystals", London, Oxford Univ. Press.
Cottrell, A.H. (1957)
Conf. on High Rates of Strain, Inst. of Mech. Eng., London, 1.
Cottrell, A.H. (1963)
The Relation between the Structure and Mechanical Properties of Metals," H.M.S.O., London, 456.
Cottrell, A.H. and Bilby, B.A. (1949)
Proc. Phys. Soc. 62A, 49.
Cracknell, A. and Petch, N.J. (1955)
Acta Met. 3, 186.
Crussad, C. (1962)
Acta Met. 10, 749.
Davis, M., Calverley, A. and Lever, R.F. (1956)
J. Appl. Phys. 27, 195.
Dingley, D.J. (1968)
4th European Regional Conf. on Electron Microscopy, Rome, 303.
Dingley, D.J. and Hale, R.F. (1966)
Proc. Roy. Soc. 295A, 55.
Dorn, J.E. and Rajnak, S. (1964)
Trans. Met. Soc. A.I.M.E., 230, 1052.
Drangel, I. and Murray, G. (1964)
Research Rept., Metals Research Coop., N.Y.

Duesbery, M.S. and Foxall, R.A. (1965)
Conf. on Pure Metals, Dresden.

Dyson, B.F., Jones, R.B. and Tegart, W.J.McG., (1958)
J.Inst. Metals, 37, 340.

Erickson, J.S. (1962)
J. Appl. Phys. 33, 2499.

Evans, P.R.V. (1962)
J. Less-Common Metals 4, 78.

Ferris, D.P., Rose, R.M. and Wuff, J. (1962)
Trans. Met. Soc. A.I.M.E., 224, 975.

Ferro, A. (1957)
J. Appl. Phys. 28, 895.

Fisher, J.C. (1955)
Trans. A.S.M., 47, 451.

Fleischer, R.L. (1962)
J. Appl. Phys. 33, 2504.

Fleischer, R.L. (1962)
Acta Met. 10, 835.

Fleischer, R.L. (1964)
"Strengthening of Metals" ed. by D. Peckner, Reinhold.

Fleischer, R.L. (1967)
Acta Met. 15, 1513.

Fleischer, R.L. and Hibbard Jr., W.R. (1963)
"The Relation between the Structure and Mechanical Properties of Metals", H.M.S.O., London.

Formby, C.L. and Owen, W.S. (1965)
J. Less-Common Metals 9, 25.

Fourdeux, A. and Wronski, A. (1964)
J. Less-Common Metals 6, 11.

Foxall, R.A., Duesbery, M.S. and Hirsch P.B. (1967)
Can. J. Phys. 46, 607.

France, L.K. and Loretto, M.H. (1968)
4th European Regional Conf. on Electron Microscopy, Rome, 301.

Frank, F.C. and Nicholas, J.F. (1953)
Phil. Mag. 44, 1213.

Friedel, J. (1955)
Phil. Mag. 46, 1169.

Friedel, J. (1963)
"The Relation between the Structure and Mechanical Properties of Metals," H.M.S.O., London, 410.

Garlick, R.G. and Probst, H.B. (1964)
Trans. Met. Soc. A.I.M.E., 230, 1120.
Gilman, J.J. (1965)
J. Appl. Phys. 36, 3195.
Gilman, J.J. and Johnston, W.G. (1957)
"Dislocation and Mechanical Properties of Crystals", Wiley, 116.
Gregory, D.P. (1963)
Acta Met. 11, 455.
Gregory, D.P., Stroh, A.N. and Rowe, G.H. (1963)
Trans. Met. Soc. A.I.M.E., 227, 678.
Guiu, F. (1965)
Ph.D. Thesis, University of London.
Guiu, F. and Pratt, P.L. (1964)
Phys. Stat. Sol 6, 111.
Guiu, F. and Pratt, P.L. (1966)
Phys. Stat. Sol. 15, 539.
Guyat, P. and Dorn, J.E. (1967)
Can. J. Phys. 45, 983.
Hahn, G.T. (1962)
Acta Met. 10, 727.
Harper, S. (1951)
Phys. Rev. 83, 709.
Harris, B. (1963)
J. Inst. Metals, 92, 89.
Harris, B. and Peacock, D.E. (1965)
J. Less-Common Metals, 8, 78.
Hartley, C.S.
Technical memorandum M.A.M. 65-28, Research and Technology
Division, U.S.A.F.? Wright Patterson, A.F.B., Ohio.
Hartley, C.S. (1966)
Acta Met. 14, 1133.
Hartley, C.S. and Wilson, R.J. (1963)
Acta Met. 11, 835.
Hirsch, P.B. (1960)
5th International Congress on Crystallography, Cambridge.
Ingram, A.G. Bartlet, E.S. and Ogden, H.R. (1963)
Trans. Met. Soc. A.I.M.E., 227, 131.
Jaoul, B. and Gonzalez, D. (1961)
J. Mech. Phys. Sol. 9, 16.

Johnson, A.A. (1960)
Acta Met. 8, 737.
Johnston, W.G. (1962)
J. Appl. Phys. 33, 2716.
Johnston, W.G. and Gilman, J.J. (1957)
J. Appl. Phys. 30, 129.
Keck, P.H. and Golay, J. (1953)
Phys. Rev. 89, 1297.
Keh, A.S. (1965)
Phil. Mag. 12, 9.
Keh, A.S. and Nakada, Y. (1967)
Can. J. Phys. 45, 1101.
Keh, A.S. and Weissman, S. (1963)
"Electron microscopy and strength of crystals", Interscience, 231.
Kim, H.C. and Pratt, P.L. (1966)
Phys. Stat. Sol 14, K151.
Koo, R.C. (1962)
J. Less-Common Metals 4, 138.
Koo, R.C. (1963)
Acta Met. 11, 1083.
Koppenaal, T.J. and Evans, P.R.V. (1965)
J. Less-Common Metals 8, 222.
Kossowsky, R. and Brown, N. (1966)
Acta Met. 14, 131.
Kroupa, F. and Vitek, B. (1964)
Czechoslovak J. Phys. 14B, 337.
Kunzler, J.E. and Wernick, J.H. (1958)
Trans. Met. Soc. A.I.M.E., 212, 856.
Lau, S.S., Ranji, S., Mukherjee, A.K., Thomas, G.,and Dorn, J.E.
(1966), U.C.R.L. - 16778, A.E.C. Contract NIW-7405-Eng-48.
Lawley, A. and Gaigher, H.L. (1963)
Phil. Mag. 8, 1713.
Lawley, A. and Gaigher, H.L. (1964)
Phil. Mag. 10, 15.
Lawley, A. and Meakin, J.D. (1966)
Acta Met. 14, 236.
Lawley, A. and Meaking, J.D. (1966)
Acta Met. 14, 1854.
Lawley, A., van den Sype, and Maddin, R. (1962)
J. Inst. Metals, 91, 23.

Li, J.C.M., (1963
Trans. Met. Soc. A.I.M.E., 227, 239.
Lord, N.W. (1961)
Trans. Met. Soc. A.I.M.E., 221, 957.
Lorreto, M. and Reid, C.N.
(Private communication)
Louat, N. (1956)
Proc. Phys. Soc. 69B, 459
Low, J.R. and Gensamer, M. (1944)
Trans. Met. Soc. A.I.M.E., 158, 207.
Low, J.R. and Turkalo, A.M. (1962)
Acta Met. 10, 215.
Maddin, R. and Chen, N.K. (1953)
Prog. Met. Phys. 5, 53.
McHargue, C.J. and McCoy, H.E. (1963)
Trans. Met. Soc. A.I.M.E., 227, 1170.
McLean, D. (1962)
"Mechanical Properties of Metals", Wiley, 120.
McLennan, J.E. (1965)
Acta Met. 13, 1239.
Mincher, A.L. and Sheeley, W.F. (1961)
Trans. Met. Soc. A.I.M.E., 221, 19.
Mitchell, T.E. (1968)
Phil. Mag. 17, 1169.
Mitchell, T.E., Foxall, R.A. and Hirsch, P.B. (1963)
Phil. Mag. 8, 1895.
Mitchell, T.E. and Spitzig, W.A. (1965)
Acta Met. 13, 1169.
Mordike, B.L. (1962)
Z. Metallkde. 53, 486.
Mordike, B.L. and Hassen, P. (1962)
Phil. Mag. 7, 459.
Mott, N.F. and Nabarro, F.R.N. (1948)
Rept. on Strength of Solids, Phys. Soc. 1.
Nabarro, F.R.N., Basinski, Z.S. and Holt, D.B. (1964)
Advances in Physics, 13, 193.
Nakada, Y. and Keh, A.S. (1967)
Acta Met. 15, 879.

Ohr, S.M. and Beshers, D.N. (1964)
Phil. Mag. 10, 219.
Opinsky, A.J. and Smoluchowski, R. (1951)
J. Appl. Phys. 22, 1488.
Pfann, W.G. (1952)
J. Metals, N.Y. 4, 747.
Pfann, W.G. (1958)
"Zone Melting", Wiley, N.Y., 154.
Powers, R.W. and Doyle, M.V. (1959)
J. Appl. Phys. 20, 514.
Reed, R.E. (1966)
U.C.-25 Metals, Ceramics and Materials, ORNL-3949, Feb.
Reid, C.N. (1966)
Acta Met. 14, 13.
Reid, C.N., Gilbert, A. and Hahn, G.T. (1966)
Acta Met. 14, 975.
Reiss, H. and Halfand, E. (1940)
J. Appl. Phys. 11, 643.
Rose, R.M., Ferris, D.P. and Wulff, J. (1962)
Trans. Met. Soc. A.I.M.E., 224, 981.
Rosen, A., Mote, J.D. and Dorn, J.E. (1966)
Trans. Met. Soc. A.I.M.E., 230, 1070.
Saada, G. (1961)
Acta Met. 9, 166.
Saada, G. (1963)
"Electron Microscopy and Structure of Crystals", Interscience,
N.Y., 651.
Samuels, L.E. (1962)
J. Inst. Metals, 91, 191.
Schadler, H.W. (1960)
Trans. Amer. Inst. Min. Eng. 218, 649.
Schadler, H.W. (1964)
Acta Met. 12, 861.
Schadler, H.W. and Low, J.R. (1962)
General Electric Res. Rept. No. 62-GC-206.
Sargent, G. (1965)
Acta Met. 13, 663.
Sherwood, P.J.
(Private communication)

Sherwood, P.J., Guiu, F., Kim, H.C., and Pratt, P.L. (1967)
Can. J. Phys. 45, 1075.

Schmid, E. and Boas, I.W. (1950)
"Plasticity of Crystals", Hughes, London, 72.

Schoeck, G. (1956)
Phys. Rev. 102, 1458.

Schoeck, G. (1961)
Acta Met. 2, 382.

Schoeck, G. and Seeger, A. (1959)
Acta Met. 7, 469.

Schwartzwart, H. and Low, J.R. (1949)
J. Metals, 1, 637.

Seeger, A. (1956)
Phil. Mag. 1, 651.

Seeger, A. (1958)
Proceedings of the Second International Conf. on the Peaceful Use of Atomic Energy (U.N., Geneva) 6, 250.

Seeger, A., Donth, H. and Pfaff, F. (1957).
Disc. Faraday Soc. 23, 19.

Sestak, B. and Zarubova, N. (1965)
Phys. Stat. Sol. 10, 239.

Simonson, E.B. (1960)
Acta Met. 8, 809.

Sleeswyk, A.W. (1963)
Phil. Mag. 8, 1467.

Smith, H.R. (1958)
"Vacuum Metallurgy", Reinhold, N.Y. 221.

Snoek, J. (1941)
Physica 8, 711.

Snoek, J. (1956)
Phys. Rev. 102, 1458.

Stanley, M.W. and Szkopiaka, Z. (1962)
Proc. Rept. U.K.A.E.A. CON/RIS/18405.

Steele, B.C.H. (1965)
Ph.D. Thesis, University of London.

Steijin, R. and Brick, R.M. (1954)
Trans. Met. Soc. A.I.M.E., 46, 1406.

Stein, D.F. (1966)
Acta Met. 14, 99.

Stein, D.F. (1967)
Can. J. Phys. 45, 1063.
Stein, D.F. and Low, J.R. (1960)
J. Appl. Phys. 31, 362.
Stein, D.F. and Low, J.R. (1966)
Acta Met. 14, 1183.
Stein, D.F., Low, J.R. and Seybolt, A.U. (1963)
Acta Met. 11, 1253.
Stiegler, J.O. and McHargue, C.J. (1964)
"Deformation Twinning", Gordon and Breach Science, N.Y., 209.
Tankins, E.S. and Maddin, R. (1961)
"Columbium Metallurgy," Interscience, N.Y.
Taylor, G.I. (1928)
Proc. Roy. Soc. 118A, 1.
Taylor, G. and Christian, J.W. (1965)
Acta Met. 13, 1216.
Taylor, G. and Christian, J.W. (1967)
Phil. Mag. 15, 873.
Taylor, G. and Christian, J.W. (1967)
Phil. Mag. 15, 893.
Thomas, W.R. and Leak, G.M. (1955)
J. Iron and Steel Inst. 180, 155.
Titchener, A.L. and Davies, G.J. (1963)
J. Sci. Inst. 40, 57.
Tsien, L.C. and Chow, Y.S. (1937)
Proc. Roy. Soc. 168A, 19.
Van Torn, L.I. and Thomas, G. (1963)
Acta Met. 11, 881.
Vogel, F.L. and Brick, R.M. (1953)
Trans. Met. Soc. A.I.M.E., 197, 700.
Votava, E. (1964)
Phys. Stat. Sol. 5, 421.
Wellings, J.F. and Maddin, R. (1962)
University of Pennsylvania Rept.
Wernick, J.H., Doris, D. and Byrnes, J.H. (1959)
Electrochem. Soc. 106, 245.
Wert, C.A. (1950)
Trans. Met. Soc. A.I.M.E., 188, 1242.
Wilcox, B.A. and Huggins, R.A. (1961)
"Columbium Metallurgy", Interscience, N.Y. 257.

Williams, G.R. and Wade, J.B. (1956)
Metallurgia, 54, 263.
Wilson, D.V. and Russel, B. (1960)
Acta Met. 8, 468.
Wilson, D., Russel, B. and Eshelby, J.D. (1956)
Acta Met. 7, 628.
Winkler, C. (1960)
Met. Rev. 5, 1.
Wulff, J. (1957)
"Hochvacuumetechnik M. Auwarter Wissenschaftlich Verlag-Ges MBH
272, Stuttgart.
Yokobori, T. (1952)
Phys. Rev. 88, 1423.